

**Vesicular Stomatitis Virus as a Vector to Deliver Virus-Like Particles of
Human Norovirus: A New Live Vectored Vaccine for Human Norovirus**

DISSERTATION

Presented in Partial Fulfillment of the Requirements for the Degree Doctor of Philosophy in the
Graduate School of The Ohio State University

By

Yuanmei Ma

Graduate Program in Food Science and Nutrition

The Ohio State University

2013

Dissertation Committee:

Dr. Jianrong Li, Advisor

Dr. Hua Wang

Dr. Mark Peeples

Dr. Steven Krakowka

Copyrighted by

Yuanmei Ma

2013

Abstract

Human norovirus (NoV) is the leading cause of acute non-bacterial gastroenteritis worldwide. Currently, noroviruses are classified as Category B biodefense agents because they are highly contagious, extremely stable, resistant to common disinfectants, have a low infectious dose, and are associated with debilitating illness. Despite the significant health, emotional, and economic burden caused by human NoV, there are no vaccines or therapeutic interventions for this virus. This is due in major part to the lack of a cell culture system and an animal model for human NoV infection.

Generally, live attenuated vaccines stimulate strong systemic immunity and provide durable protection due to the continued expression of all of the viral proteins. The development of an attenuated vaccine for human NoV has not been possible because it cannot be grown in cell culture. Thus, a vector-based vaccine may be ideal for controlling this disease. The overall goal of this study is to generate a recombinant vesicular stomatitis virus (VSV)-based live vaccine candidate for human NoV. The major capsid gene (VP1) of a human NoV GII.4 strain was inserted into the VSV genome at gene junction between glycoprotein (G) and large (L) polymerase genes. Recombinant VSV expressing VP1 protein (rVSV-VP1) was recovered from an infectious cDNA clone of VSV. Expression of the capsid protein by VSV resulted in the formation of human NoV virus-like particles (VLPs) that are morphologically and antigenically identical to the

native virions. Recombinant rVSV-VP1 was attenuated in cultured mammalian cells as well as in mice. Mice inoculated with a single dose (10^6 PFU) of rVSV-VP1 through intranasal and oral routes stimulated a significantly stronger humoral and cellular immune response compared to baculovirus-expressed VLP vaccination. In addition, inoculation of mice with rVSV-VP1 also triggered a similar level of fecal and vaginal IgA antibody, compared to VLP vaccination. These results demonstrated that the VSV-based human NoV vaccine induced strong humoral, cellular, and mucosal immunity in a mouse model.

To further improve the safety and efficacy of the VSV-based human NoV vaccine, the gene for the 72kDa heat shock protein (HSP70) was inserted into rVSV and rVSV-VP1 vectors as an adjuvant, which resulted in construction of recombinant VSV expressing HSP70 (rVSV-HSP70) and VSV co-expressing human NoV VP1 protein and HSP70 (rVSV-HSP70-VP1), respectively. The HSP70 insertion resulted in the recombinant virus (rVSV-HSP70-VP1) that form smaller plaques and also demonstrated delayed replication in cell culture compared to rVSV-VP1. In addition, rVSV-HSP70-VP1 reduced the clinical manifestations of VSV infection in BALB/c mice compared to rVSV-VP1, indicating further attenuation caused by the second gene insertion. At the same inoculation dose (1×10^6 PFU), both rVSV-HSP70-VP1 and rVSV-VP1 triggered similar levels of specific humoral, mucosal, and cellular immunity, even though VP1 expression by rVSV-HSP70-VP1 was approximately five-fold less than that of rVSV-VP1. To compensate for the reduced VP1 expression levels, the inoculation dose of rVSV-HSP70-VP1 was increased five-fold to 5×10^6 PFU/mouse or same dosage (1×10^6

PFU/mouse) of rVSV-VP1 and rVSV-HSP70 was combined for vaccination. Mice immunized with 5×10^6 PFU of rVSV-HSP70-VP1 or those receiving combined vaccination generated significantly higher mucosal and/or T cell immunity than those immunized with rVSV-VP1 alone ($P < 0.05$). Therefore, this data indicates that insertion of HSP70 into the VSV vector further attenuates the VSV-based vaccine and HSP70 enhances the human NoV-specific immunities.

To determine whether the VSV-based human NoV vaccine confers protection from human NoV challenge, a gnotobiotic pig NoV challenge model was developed. Newborn gnotobiotic piglets vaccinated intranasally with 2×10^7 PFU of rVSV-based vaccine (rVSV-VP1) produced high levels of human NoV-specific serum IgG and fecal and vaginal IgA antibody levels whereas mock-infected or unvaccinated control groups remained antibody-negative. Three weeks after vaccination, piglets were orally challenged with human NoV GII.4 strain 7I. Protective effects were measured by viral shedding in stools, as well as viral antigen and histologic changes in the small intestine. All three piglets in the unvaccinated challenged group developed histopathologic lesions typical of human NoV infection including villous atrophy, segmented epithelial cell loss, and increased mononuclear inflammatory cell infiltrates including syncytial giant cells in the lamina propria of the duodenum and proximal jejunum by post-challenge day 5. In contrast, only one of five vaccinated piglets exhibited focal epithelium loss and villous atrophy in the duodenum. Similarly, one of five vaccinated piglets had mild edema in the jejunal lamina propria. Immunofluorescent assay showed that a large amount of human NoV antigens were detected in duodenum, jejunum, and ileum of the pigs from the

challenge control group. Piglets vaccinated with rVSV-VP1 had significantly less human NoV antigen in both the duodenum and jejunum sections. These results demonstrate that the rVSV-based human NoV vaccine triggered partially protective immunity in swine and protected gnotobiotic pigs from challenge by human NoV.

In conclusion, the VSV-based human NoV vaccine triggered high levels of humoral, cellular, and mucosal immunity in both the mouse and gnotobiotic pig models, and protected pigs from challenge by human NoV. This study has two important applications for the development of: (i) A highly productive bioreactor to facilitate large scale purification of human NoV VLPs using VSV as a vector; and (ii) A VSV-based vaccine as a novel vaccine candidate against human NoV as well as other non-cultivable viruses.

Dedication

This is dedicated to my family and friends
for their unconditional love and support through this journey

Acknowledgments

I would first like to acknowledge my advisor, Dr. Jianrong Li, for his guidance, support, and patience. During the past four years, his encouragements, inspirations, thoughtful advice to tackle research problems were of immense help for me. His passion, persistence, and devotion to his work make him a role model for everyone in the lab. Without him I could not have finished my dissertation successfully.

I also want to take this opportunity to thank my committee members Dr. Hua Wang, Dr. Mark Peeples, and Dr. Steven Krakowka for their time, constructive comments, and valuable guidance.

I would like to extend my sincere gratitude to Dr. Li's group: Yu Zhang, Dr. Yongwei Wei, Dr. Hui Cai, Dr. Xiaodong Zhang, Yue Duan, Haiwa Wu, Erin Divers, Dr. Junan Li, Kurtis Feng, Ashley Predmore, Elbashir Araud, Jiawei Yeap, Anastasia Purgianto, Dr. Ran Zhao, Dr. Xiangjie Yao, and Yang Zhu. Thank you all for continued support, motivation, and friendship. I am very grateful to Erin Divers, Yu Zhang, Fangfei Lou, and Elbashir Araud for helpful suggestions and grammar corrections of my dissertation. Special thanks to Yu Zhang for generously providing technical helps and sharing knowledge along the way.

I am indebted to my parents for their love, sacrifices and support throughout my life. Without their continuous encouragement, it would not have been possible for me to be who I am today. Last but not least, I owe thanks to my husband Xin for love and motivation, thanks for always being there supporting me.

Vita

June 2004Shenzhen Middle School, China
2008.....B.S. Biotechnology,
Sun Yat-sen University, China
2008 to presentGraduate Research Associate, Department
of Food Science, The Ohio State University

Publications

1. Yuanmei Ma and Jianrong Li. 2011. Vesicular Stomatitis Virus as a Vector To Deliver Virus-Like Particles of Human Norovirus: a New Vaccine Candidate against an Important Noncultivable Virus. *Journal of Virology* **85**(6): 2942.
2. Kurtis Feng, Erin Divers, Yuanmei Ma, Jianrong Li. 2011. Inactivation of a human norovirus surrogate, human norovirus virus-like particles, and vesicular stomatitis virus by gamma irradiation. *Applied and Environmental Microbiology* **77**(10):3507-3517.
3. Erin DiCaprio, Yuanmei Ma, Ana Purgianto, Jianrong Li, John Hughes. 2012. Internalization and dissemination of human norovirus and animal caliciviruses in hydroponically grown romaine lettuce. *Applied and Environmental Microbiology* **78**(17): 6143-6152.

4. Xiaodong Zhang, Yongwei Wei, Yuanmei Ma, Songhua Hu, Jianrong Li. 2010. Identification of aromatic amino acid residues in conserved region VI of the large polymerase of vesicular stomatitis virus is essential for both guanine-N-7 and ribose 2'-O methyltransferases. *Virology* 408(2): 241-252.

Fields of Study

Major Field: Food Science and Nutrition

Table of Contents

Abstract.....	ii
Dedication.....	vi
Acknowledgments.....	vii
Vita.....	viii
Table of Contents.....	x
List of Tables.....	xix
List of Figures.....	xx
Abbreviation.....	xxiv
Chapter 1 : Literature Review.....	1
1.1 Introduction to human norovirus.....	1
1.2 The <i>Caliciviridae</i>	3
1.3 Pathophysiology and epidemiology.....	5
1.4 Viral structure, genome organization and viral protein.....	7
1.4.1 The major capsid protein VP1.....	8
1.4.2 The minor capsid protein VP2.....	11

1.4.3 Non-structural proteins	13
1.5 Human norovirus genogroup and genotype	14
1.6 Cellular receptor and human susceptibility for human norovirus	16
1.7 Challenges in human norovirus research	17
1.7.1 Advances of developing cell culture for human NoV	18
1.7.2 Progress of developing animal models for human NoV	19
1.8 Animal caliciviruses	21
1.8.1 Murine norovirus (MNV)	21
1.8.2 Feline calicivirus	23
1.8.3 Porcine sapovirus	23
1.8.4 Tulane virus	24
1.9 Vaccine candidates against human norovirus	25
1.9.1 VLP-based vaccine candidate	25
1.9.2 Protrusion (P) particle-based vaccine candidate	27
1.9.3 Live-vectored vaccines against human NoV	28
1.10 Introduction to Vesicular Stomatitis Virus	32
1.11 The structure of VSV virions	33
1.12 VSV life cycle	35
1.13 VSV transcription	36

1.14 VSV replication.....	37
1.15 VSV assembly.....	38
1.16 Reverse genetics of VSV.....	38
1.17 VSV as a vector for vaccine development	40
1.18 Advantages of using VSV as a viral vaccine vector.	41
1.19 Introduction to HSP70.....	42
1.20 Function of HSP70 in viral life cycles	43
1.21 HSP70 as a vaccine adjuvant	45
Chapter 2 :Vesicular stomatitis virus as a vector to deliver human norovirus virus-like	
particles: a new vaccine candidate against an important non-cultivable virus	48
2.1 Abstract	48
2.2 Introduction	49
2.3 Materials and methods	53
2.3.1 Plasmid construction.....	53
2.3.2 Recovery and purification of recombinant VSV.	54
2.3.3 Single-cycle growth curves.	54
2.3.4 Analysis of protein synthesis.....	54
2.3.5 Reverse transcription polymerase chain reaction (RT-PCR).	55
2.3.6 Western blotting.	55

2.3.7 Production and purification of VLPs by baculovirus expression system.	56
2.3.8 Production and purification of VLPs by VSV vector.	57
2.3.9 Transmission electron microscopy.	57
2.3.10 Animal experiment.	58
2.3.11 T cell proliferation assay.	59
2.3.12 Serum IgG ELISA.	59
2.3.13 Fecal IgA ELISA.	60
2.3.14 Vaginal Human NoV-specific IgA ELISA.	60
2.3.15 Quantitative and statistical analysis.	61
2.4 Results.	61
2.4.1 Recovery of recombinant VSV expressing human NoV capsid protein.	61
2.4.2 The replication of rVSV-VP1 is delayed in cell culture.	64
2.4.3 High level expression of Human NoV VP1 protein by VSV vector.	66
2.4.4 Characterization of Human NoV VLPs expressed by VSV vector.	70
2.4.5 Recombinant rVSV-VP1 is attenuated in a mouse model.	72
2.4.6 Intranasal and oral administration of rVSV-VP1 induces a strong serum IgG immune response in mice.	74
2.4.7 Immunization of mice with rVSV-VP1 induces a strong cellular immune response in mice.	76

2.4.8 Immunization of mice with rVSV-VP1 induces a mucosal immune response in mice.	77
2.5 Discussion	81
2.5.1 A new approach to generate human NoV VLPs using VSV as the vector.....	82
2.5.2 A new live vaccine candidate against non-cultivable foodborne viruses.	84
Chapter 3 : Heat shock protein 70 (HSP70) enhances safety and immunogenicity of norovirus capsid protein (VP1) when co-expressed from a vesicular stomatitis viral vector.....	88
3.1 Abstract	88
3.2 Introduction	89
3.3 Materials and Methods	92
3.3.1 Recombinant viruses.....	92
3.3.2 Plasmid construction.....	92
3.3.3 Recovery and purification of recombinant VSV.	93
3.3.4 Single-cycle growth curves.	94
3.3.5 Analysis of protein synthesis.....	94
3.3.6 RT-PCR.	95
3.3.7 Western blotting.	95
3.3.8 Production and purification of VLPs by a baculovirus expression system.	96

3.3.9 Animal experiment 1.	97
3.3.10 Animal experiment 2.	97
3.3.11 Animal experiment 3.	98
3.3.12 T cell proliferation assay.	98
3.3.13 Serum IgG ELISA.	99
3.3.14 Fecal IgA ELISA.	99
3.3.15 Vaginal human NoV-specific IgA ELISA.	100
3.3.16 Quantitative and statistical analyses.	101
3.4 Results	101
3.4.1 Recovery of recombinant VSV expressing HSP70 (rVSV-HSP70) and VSV co-expressing human NoV VP1 and HSP70 proteins (rVSV-HSP70-VP1).	101
3.4.2 Single-step growth curves of recombinant VSV in cell culture.	104
3.4.3 Characterization of the expression of VP1 and HSP70 by the VSV vector. ...	106
3.4.4 Recombinant rVSV-HSP70-VP1 is more attenuated than rVSV-VP1 in a mouse model.	111
3.4.5 Recombinants rVSV-HSP70-VP1 and rVSV-VP1 triggered similar levels of humoral, cellular, and mucosal immunities in mice at dose of 10 ⁶ PFU.	114
3.4.6 Recombinant rVSV-HSP70-VP1 stimulated higher T cell and mucosal immune responses than rVSV-VP1 at dose of 5×10 ⁶ PFU.	120

3.4.7 Enhanced mucosal immune responses by combination of rVSV-VP1 and rVSV-HSP70 vaccination.....	127
3.5 Discussion	131
3.5.1 HSP70 enhances the safety of VSV-based human NoV vaccine.	131
3.5.2 HSP70 enhances the immunogenicity of the viral vaccine.	133
3.5.3 VSV as a vector to delivery viral vaccines.	135
Chapter 4 : A vesicular stomatitis virus (VSV)-based human norovirus vaccine provides protection against norovirus challenge in a gnotobiotic pig model	137
4.1 Abstract	137
4.2 Introduction	138
4.3 Materials and Methods	141
4.3.1 Characterization of three human norovirus GII.4 strains.	141
4.3.2 Quantification of viral RNA by real-time RT-PCR.....	143
4.3.3 Delivery of gnotobiotic piglets.	144
4.3.4 Pathogenesis of human NoV in gnotobiotic piglets.	145
4.3.5 Immunogenicity of VSV-based human NoV vaccine (rVSV-VP1) in gnotobiotic piglets.	145
4.3.6 Detection of human NoV in feces, intestinal contents, intestinal tissues by real-time RT-PCR.	147
4.3.7 Indirect immunofluorescence on whole intestinal tissue mounts.	148

4.3.8 Serum IgG ELISA.....	149
4.3.9 Fecal IgA ELISA.....	149
4.3.10 Vaginal and nasal human NoV-specific IgA ELISA.....	150
4.3.11 Histologic examination.....	151
4.3.12 Sequence alignment and analysis.....	151
4.3.13 Statistical analyses.....	151
4.4 Results.....	152
4.4.1 Characterization of three human NoV GII.4 strains from Ohio.....	152
4.4.2 Pathogenesis of human NoV strains 7I and 5M in gnotobiotic piglets.....	156
4.4.3 The safety of rVSV-VP1 in gnotobiotic piglets.....	162
4.4.4 Immunogenicity of rVSV-VP1 in gnotobiotic piglets.....	162
4.5 Discussion.....	171
4.5.1 Pathogenesis of human NoV in animal models.....	171
4.5.2 Protection efficacy of human NoV vaccine candidates.....	174
4.5.3 The need to explore new vaccine candidates against human NoV.....	176
Chapter 5 : Future directions.....	178
5.1 Determine whether the VSV-based human NoV vaccine can provide cross- protection against different human NoV strains.....	178
5.1.1 Improve the adjuvant effect of HSP70.....	180

5.1.2 Facilitate the clinical trials of the VSV-based human NoV vaccine candidate.	
.....	181
References.....	183

List of Tables

Table 1.1. The Caliciviridae genus and representative virus strains (adapted from Farkas et al. 2008).	4
Table 4.1. Primers for cloning and sequencing the genome of human NoV.....	142
Table 4.2. Classification and GenBank accession numbers of norovirus strains used for sequence analysis.....	155
Table 4.3. Histological changes in the small intestines of gnotobiotic pigs infected by human NoV.....	160
Table 4.4. Histological changes in the small intestines of gnotobiotic pigs challenged by human NoV after vaccination.....	169
Table 4.5. Histological changes in the small intestines of gnotobiotic pigs challenged by human NoV after vaccination in detail.....	169

List of Figures

Figure 1.1. Human norovirus visualized by transmission electron microscopy.	2
Figure 1.2. Classification of <i>Caliciviridae</i> , adapted from Rohayem et al. 2010.	5
Figure 1.3. Transmission routes of human caliciviruses, adapted from Lopman et al. 2002.....	7
Figure 1.4. Genome organization of human norovirus.	8
Figure 1.5. Diagram of the human norovirus capsid protein sequence, adapted from Tan and Jiang, 2003.	10
Figure 1.6. Tertiary structure of human norovirus VLPs generated by cryo-electron microscopic reconstruction, adapted from Hutson et al., 2004.....	10
Figure 1.7. Receptor binding region in norovirus P dimer interface, adapted from Tang and Jiang 2010.	11
Figure 1.8. Possible mechanism of VP1/VP2 interaction, adapted from Bertolotti-Ciarlet et al. 2003.....	12
Figure 1.9. Classification of noroviruses into 5 genogroups (GI–V) and 35 genotypes based on sequence diversity in the complete capsid protein VP1 (Hall et al., 2011).	15
Figure 1.10. Diagrams of the synthesis of type 1 and 2 HBGAs.....	17

Figure 1.11. VSV virion structure and genome organization (Adapted from Lichty et al., 2004).	34
Figure 1.12 Overview diagram of VSV life cycle.	35
Figure 1.13. Recovery of infectious VSV from a cDNA clone by reverse genetics.	39
Figure 2.1. Recovery of recombinant VSV expressing human NoV VP1 (rVSV-VP1)..	63
Figure 2.2. Single-step growth curve of recombinant VSV in BSRT7 cells.	65
Figure 2.3. Expression of human NoV VP1 by the VSV vector.	68
Figure 2.4. Kinetics of VP1 expression by VSV vector.	69
Figure 2.5. Electron microscope analysis of purified VLPs.	71
Figure 2.6. Dynamics of mouse body weight after inoculation with recombinant viruses.	73
Figure 2.7. Serum IgG immune responses to human NoV vaccine.....	75
Figure 2.8.T cell proliferative responses to human NoV vaccine.....	77
Figure 2.9. Fecal IgA responses to human NoV vaccine.....	80
Figure 2.10. Vaginal IgA responses to human NoV vaccine.....	81
Figure 3.1. Recovery of recombinant VSV co-expressing human NoV VP1 and HSP70 (rVSV-HSP70-VP1) and VSV expressing HSP70 (rVSV-HSP70).....	103
Figure 3.2. Single-step growth curve of recombinant VSVs in BSRT7 cells.....	105
Figure 3.3. Expression of human NoV VP1 and HSP70 by rVSV-VP1, rVSV-HSP70, and rVSV-HSP70-VP1.	108
Figure 3.4. Kinetics of norovirus VP1 expression by rVSV-VP1 and rVSV-HSP70-VP1.	109

Figure 3.5. Kinetics of HSP70 expression by rVSV-HSP70 and rVSV-HSP70-VP1....	111
Figure 3.6. Dynamics of mouse body weight after inoculation with recombinant viruses.	113
Figure 3.7. Serum IgG immune responses to VSV-based human NoV vaccines.....	115
Figure 3.8. T cell proliferative responses to VSV-based human NoV vaccines.....	116
Figure 3.9. Fecal IgA responses to VSV-based human NoV vaccines.....	118
Figure 3.10. Vaginal IgA responses to VSV-based human NoV vaccines.....	119
Figure 3.11. Dynamics of mouse body weight after inoculation with recombinant viruses.	122
Figure 3.12. Serum IgG immune responses to VSV-based human NoV vaccines.....	123
Figure 3.13. T cell proliferative responses to VSV-based human NoV vaccines.....	124
Figure 3.14. Fecal IgA responses to VSV-based human NoV vaccines.....	125
Figure 3.15. Vaginal IgA responses to VSV-based human NoV vaccines.....	126
Figure 3.16. Dynamics of mouse body weight after inoculation with recombinant viruses for animal study 3.	128
Figure 3.17. Serum IgG immune responses to VSV-based human NoV vaccines.....	129
Figure 3.18. Fecal IgA responses to VSV-based human NoV vaccines.....	130
Figure 3.19. Vaginal IgA responses to VSV-based human NoV vaccines.....	131
Figure 4.1. Primers for cloning and sequencing the genome of human NoV.....	143
Figure 4.2. Flow diagrams of experimental design.....	147
Figure 4.3. Phylogenetic tree of genogroup II NoVs based on the capsid protein VP1 sequences.	154

Figure 4.4. Fecal viral shedding detected by real time RT-PCR after human NoV infection.	157
Figure 4.5. Histological changes in the small intestines of gnotobiotic pigs infected by human NoV.....	159
Figure 4.6. Localization of the human NoV capsid protein in whole-mount small intestinal tissues by an indirect immunofluorescent assay.	161
Figure 4.7. VSV-based human NoV vaccine stimulates a high level of serum IgG immune response in gnotobiotic pigs.	163
Figure 4.8. VSV-based human NoV vaccine stimulates a high level of mucosal IgA immune response in gnotobiotic pigs.	164
Figure 4.9. Fecal viral shedding of human NoV detected by real time RT-PCR after human NoV challenge.....	167
Figure 4.10. Detection of human NoV RNA in intestinal contents by real-time RT-PCR.	168
Figure 4.11. Detection of the human NoV capsid protein in whole-mount small intestinal tissues by an indirect immunofluorescence assay.....	170
Figure 5.1. Strategies to improve the efficacy of VSV-based human NoV vaccine	180

Abbreviation

APCs	Antigen-presenting cells
CAV-9	Coxsackievirus A9
CDC	Centers for Disease Control and Prevention
cDNA	Complementary deoxyribonucleic acid
CDV	Canine distemper virus
CNS	Central nervous system
CPE	Cytopathic effect
CT	Cholera toxin
CTL	Cytotoxic T lymphocyte
CsCl	Cesium chloride
C terminus	Carboxy terminus
°C	Degrees Celsius
DMEM	Dulbecco's modified Eagle medium
DNA	Deoxyribonucleic acid

ELISA	Enzyme-linked immunosorbant assay
EM	Electron microscopy
ER	Endoplasmic reticulum
FBS	Fetal bovine serum
FDA	Food and Drug Administration
Fig	Figure
G	Glycoprotein
GMT	Geometric Mean Titers
HBGA	Histo-blood group antigen
HCV	Hepatitis C virus
HE	Hematoxylin-eosin
HVDDT	HIV Vaccine Design and Development Teams
HIV	Human immunodeficiency virus
HMPV	Human metapneumovirus
HSP	Heat shock protein
IFN	Interferon
Ig	Immunoglobulin
IL	Interleukin

ISCOM	Immunostimulating complexes
JE	Japanese encephalitis
kb	Kilo base
kDa	Kilo Dalton
L	Large polymerase protein
Le	Leader sequence at the 3' end of the VSV genome
LT	<i>E. coli</i> toxin
Luc	Luciferase
M	Matrix protein
MEM	Minimal essential medium
mg	milligram
min	Minute
ml	Milliliter
mm	Millimeter
mM	Millimolar
MHC	Major histocompatibility complex
MNC	Mononuclear cells
MOI	Multiplicity of infection

mRNA	Messenger RNA
MV	Measles virus
N	Nucleoprotein
NaCl	Sodium Chloride
NDV	Newcastle disease virus
NIAID	National Institute of Allergy and Infectious Disease
NNS	Non-segmented negative-sense
NoV	Norovirus
nt	Nucleotide
N terminus	Amino terminus
NV	Norwalk virus
OD	Optical density
ORF	Open reading frame
P	Phosphoprotein
PBS	Phosphate buffered saline
PCR	Polymerase chain reaction
PFU	Plaque forming unit
pH	Decimal cologarithm of hydrogen ion concentration

PPB	Potassium phosphate buffer
PRRSV	Porcine reproductive and respiratory syndrome virus
RdRp	RNA-dependent RNA polymerase
RNA	Ribonucleic acid
RSV	Respiratory syncytial virus
SARS	Severe acute respiratory syndrome
SDS-PAGE	Sodium dodecyl sulfate-polyacrylamide gel electrophoresis
SF9	<i>Spodoptera frugiperda</i> SF9 cells
SI	Stimulation index
T7	T7 bacteriophage
T7 polymerase	Bacteriophage RNA polymerase
TEM	Transmission Electron Microscope
TMB	3, 3',5, 5'-tetramethylbenzidine
TNC	Tris sodium chloride calcium chloride buffer
VEE	Venezuelan Equine Encephalitis
Vero	Immortalized cell line derived from African green monkey kidney cell
VLP	Virus-like particle
VP1	Viral protein 1, major capsid protein of norovirus

VP2	Viral protein 2, minor capsid protein of norovirus
VSV	Vesicular stomatitis virus
vTF7-3	A recombinant vaccinia virus
wt	Wild type
μl	Microliter
μg	Microgram
μm	Micrometer
μM	Micromolar
μCi	Microcurie (unit of radioactivity)

Chapter 1 : Literature Review

1.1 Introduction to human norovirus

Human norovirus (NoV) was discovered following an outbreak of acute gastroenteritis in an elementary school in Norwalk, Ohio in 1968 (Kapikian et al., 1972). Half of the teachers and students developed symptoms of nausea and vomiting, and about one third of their family members also fell ill. Four years later, a 27-33 nm small round structured viral particle was found in stool samples from the outbreak, and it was later confirmed that this viral particle was the causative agent of the outbreak (Fig. 1.1). Consequentially, this virus was named Norwalk-like virus, with other common names including small round-structured virus, and most recently Norovirus (Koopmans and Duizer, 2004; Lopman et al., 2003).

Human NoV is responsible for more than 90% of the nonbacterial foodborne illnesses every year. Human NoV has been estimated to be the second leading cause of hospitalization, and the fourth leading cause of death among foodborne pathogens in the US (Scallan, 2011). The National Institute of Allergy and Infectious Diseases (NIAID) has classified noroviruses as category B biodefense agents because of their high infectivity, high stability, and resistance to common disinfectants. It has been reported

that human NoV is highly contagious and that a few virus particles, usually less than 10, are sufficient to cause an infection (Donaldson et al., 2008; Estes et al., 2006; Koopmans, 2008). Despite the significant economic, social, and health impact and the high morbidity caused by human NoV, no vaccines or antiviral drugs are currently available for this virus. This is due in major part to the lack of a cell culture system or a robust small animal model for human NoV (Duizer et al., 2004b; Estes et al., 2000).

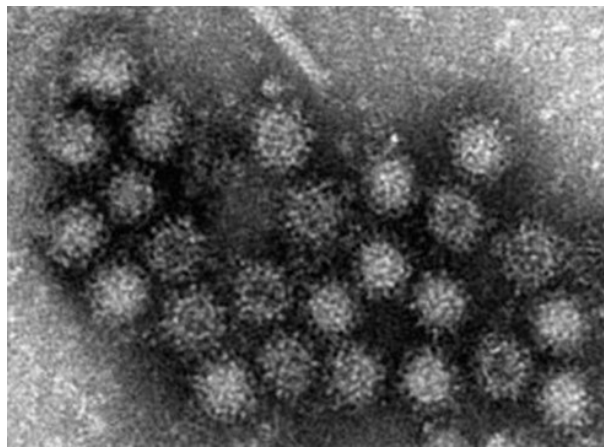


Figure 1.1. Human norovirus visualized by transmission electron microscopy.

1.2 The *Caliciviridae*

Noroviruses belong to the family *Caliciviridae* under the genus *Norovirus*. The *Caliciviridae* is a family of nonenveloped viruses that are about 20-35 nm in diameter. The protein capsid has a molecular weight of about 60 kDa and carries 32 shallow, cup-like circular indentations and exhibits icosahedral symmetry. The genome of *Caliciviridae* is a single-stranded, positive-sense RNA genome of about 8 kbp (Table 1). The family comprises six genera, *Vesivirus* that includes feline calicivirus (FCV), vesicular exanthema of swine virus (VESV), and San Miguel sealion virus (SMSV), *Lagovirus* that includes rabbit hemorrhagic disease virus (RHDV) and European Brown hare syndrome virus (EBHSV), *Norovirus* that includes human NoV, porcine NoV, bovine NoV, and murine NoV, *Sapovirus* which comprises human sapovirus and porcine sapovirus, *Becovirus* or *Nabovirus* which includes bovine enteropathogenic caliciviruses (Newbury agent-1 and Nebraska), and *Recovirus* which includes monkey caliciviruses represented by Tulane virus (Fig. 1.2).

The *Caliciviridae* family includes a large number of viruses that cause acute gastroenteritis in humans and animals. Examples of these viruses include human NoV, human sapovirus, porcine NoV, porcine sapovirus, bovine NoV, and Tulane virus. However, caliciviruses also cause other diseases. For example, murine norovirus in genus *Norovirus* causes systemic infection in mice (Karst et al., 2003). Feline calicivirus within the genus *Vesivirus* causes respiratory tract infections (Doutree et al., 1999). Rabbit haemorrhagic disease virus within genus *Lagovirus* causes haemorrhagic disease

in rabbits (Belz, 2004). Viruses in the *Caliciviridae* can infect a wide range of hosts including humans, primates, cattle, mink, swine, cat, dogs, and rabbits.

Table 1.1. The Caliciviridae genus and representative virus strains (adapted from Farkas et al. 2008).

Calicivirus genus ^a	Virus strain	Accession no.	Complete genome length (nt)	UTR length		ORF length (nt/aa) ^b		
				5' (nt)	3' (nt)	1	2	3
<i>Norovirus</i>	Norwalk	M87661	7,654	4	66	5,370/1,789	1,593/530	639/212
	Southampton	L07418	7,708	4	78	5,367/1,788	1,641/546	636/211
	MD145	AY032605	7,556	4	46	5,100/1,699	1,614/537	807/268
	MNV-1	DQ285629	7,382	5	75	5,058/1,685	1,620/539	627/208
<i>Sapovirus</i>	Manchester	X86560	7,431	12	82	6,843/2,280	498/165	NA
	PEC-Cowden	AF182760	7,320	9	55	6,765/2,254	495/164	NA
<i>Vesivirus</i>	FCV-CF168	U13992	7,677	19	43	5,289/1,762	2,007/668	321/106
	FCV-Urbana	NC_00148	7,683	19	46	5,292/1,763	2,007/668	321/106
	SMSV-1	U15301	8,284	19	182	5,640/1,879	2,109/702	333/110
<i>Lagovirus</i>	RHDV-FRG	M67473	7,437	9	59	7,035/2,344	354/117	NA
	EBHSV-GD	Z69620	7,442	8	92	7,005/2,334	345/114	NA
<i>Becovirus</i>	BEC-NB	AY082891	7,453	74	67	6,633/2,210	678/225	NA
	Newbury-1	DQ013304	7,454	75	67	6,633/2,210	678/225	NA
<i>Recovirus</i>	Tulane	EU391643	6,714	14	74	4,344/1,447	1,605/534	657/218

^a*Becovirus* and *Recovirus* represent two tentative genera

^bThe *Norovirus*, *Vesivirus*, and *Recovirus* genomes are organized into three ORFs; ORF1 encodes the NS polyprotein, ORF2 encodes the capsid protein (VP1), and ORF3 encodes a minor structural protein (VP2). The *Sapovirus*, *Lagovirus*, and *Becovirus* genomes are organized into two ORFs; ORF1 encodes a polyprotein containing the NS proteins and the capsid protein (VP1), and ORF2 encodes the minor structural protein (VP2). NA, not applicable.

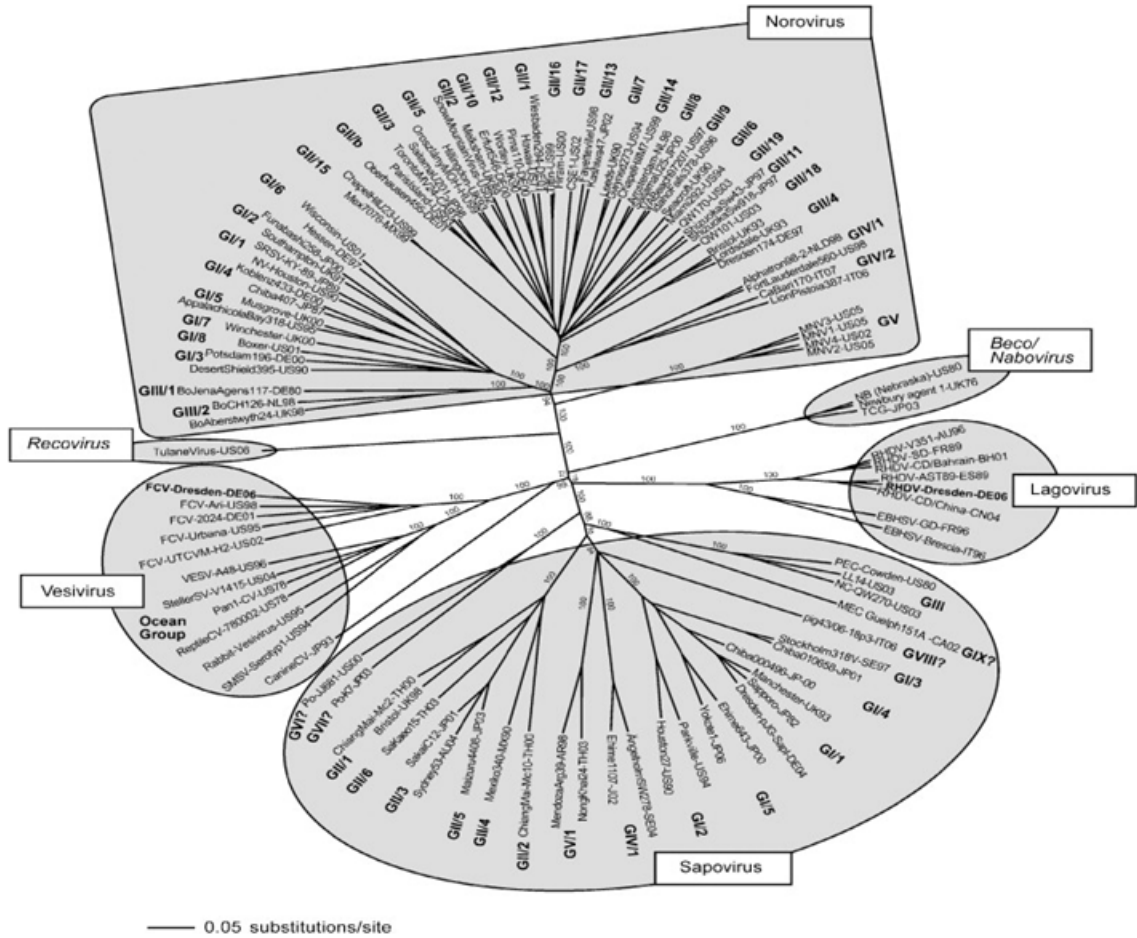


Figure 1.2. Classification of *Caliciviridae*, adapted from Rohayem et al. 2010.

Phylogenetic analysis of strains from *Norovirus*, *Sapovirus*, *Lagovirus*, *Vesivirus*, *Beco/Nabovirus*, and *Recovirus* genera based on capsid sequences.

1.3 Pathophysiology and epidemiology

The illness caused by human NoV has been termed stomach flu or winter vomiting disease. Human NoV causes self-limited disease, with symptoms of diarrhea, vomiting, nausea, abdominal cramping, chills, headache, dehydration, and a high-grade fever. The

incubation period for NoV is about 24 to 72 hours, and symptoms can last for 3-4 days (Koopmans, 2008). Human NoV infection and secondary infection occur in people of all age groups (Johnson et al., 1990; Parrino et al., 1977). People infected by NoV can be symptomatic with relatively mild disease or asymptomatic (Atmar et al., 2008; Rockx et al., 2002). However, disease can be prolonged and even lethal in infants, the elderly, and immunocompromised individuals (Harris et al., 2008; Rockx et al., 2002).

NoV outbreaks usually occur in closed or semi-closed communities, such as cruise ships, restaurants, swimming pools, hospitals, nursing homes, schools, daycare centers, hotels, prisons, military settings, sports stadiums, and disaster relief situations (Becker et al., 2000; Estes et al., 2006; Goodgame, 2006; Rockx et al., 2002). Human NoV is transmitted primarily through infectious vomit or feces via the fecal-oral route, either by direct person-to-person contact or by consumption of contaminated food or water, or by indirect contact with contaminated surfaces (Fig. 1.3). Aerosol transmission of human NoV was also suggested by inhalation of aerosolized vomitus and subsequent ingestion in both a restaurant and emergency room setting (Marks et al., 2000; Marks et al., 2003). Patients have been found to shed NoV for up to 8 weeks after the resolution of clinical symptoms (Atmar et al., 2008), which may help facilitate human NoV transmission.

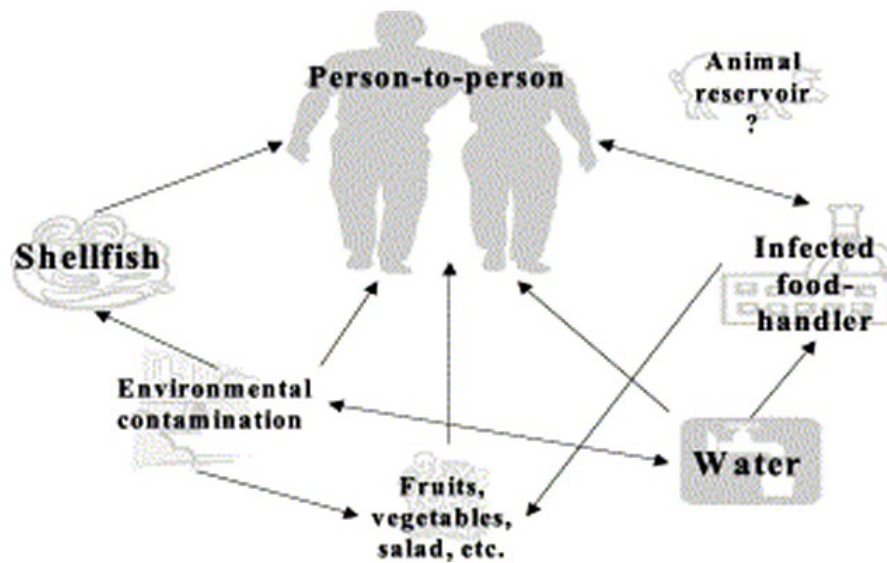


Figure 1.3. Transmission routes of human caliciviruses, adapted from Lopman et al. 2002.

1.4 Viral structure, genome organization and viral protein

Human NoV has a 7.5-7.7kb single-stranded, positive-sense RNA genome, which encodes three open reading frames (ORFs) (Fig. 1.4) (Jiang et al., 1990; Jiang et al., 1993). The first ORF (ORF 1) encodes a nonstructural polyprotein, which is proteolytically cleaved into six nonstructural proteins by 3C-like protease (3C). The proteolytic products are N-terminal protein (designated p48 for Norwalk virus), NTPase, 3A-like protein (designated p22 for Norwalk virus), VPg, viral protease (3CL^{pro}), and RNA-dependent RNA polymerase (RdRp) (Belliot et al., 2003; Fields et al., 2007). The second ORF (ORF2) encodes the major capsid protein VP1, and ORF3 encodes the minor structural capsid protein VP2 (Hardy, 2005; Jiang et al., 1990; Jiang et al., 1993)



Figure 1.4. Genome organization of human norovirus.

The norovirus genome consists of three open reading frames (ORFs). ORF 1 encodes nonstructural proteins. ORF2 and ORF3 encode the major capsid protein VP1 and the minor capsid protein VP2, respectively (Donaldson et al., 2010).

1.4.1 The major capsid protein VP1

The ORF2 is about 1.8kb and encodes the 58-60 kDa major capsid protein (VP1), which normally ranges from 530-555 amino acids in length. VP1 is the major component of the outer shell of the human NoV virion, protecting the genomic RNA from degradation and playing an essential role in the viral life cycle. In 1992, the VP1 gene was cloned into and expressed by a recombinant baculovirus system (Jiang et al., 1992). The VP1 proteins produced by this system were found to form empty non-infectious virus-like particles (VLPs) that are antigenically and morphologically similar to the native human NoV virions. After this discovery, VP1 was expressed in many other protein expression systems such as yeast, insect cells, and mammalian cells. The discovery of VLPs has facilitated the research of structure biology, biochemical properties, immunology, and epidemiology of human NoV. Recently, many breakthroughs in human NoV research has been made using VLPs as a model. For example, cellular receptor of human NoV, the histo-blood group antigen (HBGA), was identified using VLPs in a hemagglutination system for studying human NoV attachment to cells (Hutson et al., 2002; Hutson et al.,

2003). VP1 is vital for the determination of antigenicity and strain specificity and the classification of NoV genogroup and genotype is based on the sequence of the VP1 protein (Ball et al., 1998; Prasad et al., 1999). It was demonstrated that mice inoculated with VLPs generated human NoV-specific humoral, cellular, and mucosal immunities, demonstrating that the VP1 protein is the host protective antigen (Bertolotti-Ciarlet et al., 2003). Using cultivable murine NoV as a model, it was found that VP1 plays many other roles in the virus life cycle such as uncoating, assembly, and exit (Bailey et al., 2008; Taube et al., 2010).

Recently, the three-dimensional structure of human NoV VLPs has been determined using cryo-electron microscopy (cryo-EM) and X-ray crystallography techniques. It was found that human NoV VLPs exhibit a T= 3 icosahedral symmetry with 180 molecules of the VP1 protein organized into 90 dimers (Fig.1.6) (Prasad et al., 1999). There are two principal domains in the VP1 protein, shell (S) and protruding (P), linked by a flexible hinge region (Fig. 1.6). The S domain is involved in the formation of the continuous shell surface, and the P domain forms the prominent protrusion emanating from the shell (Prasad et al., 1999). The P domain is further divided into two sub-domains, P1 and P2. P2 is a 127aa insertion inside the P1 domain, located at the most distal surface of folded VP1 (Fig. 1.5). The P domain is the primary site of antibody recognition and receptor binding, which plays an important role in human NoV infection and determines the host susceptibility (Tan et al., 2003). Furthermore, the sites and specific amino acids involved

in HBGA receptor binding have been identified in the P dimer interface (Fig. 1.7) (Choi et al., 2008; Tan et al., 2003).



Figure 1.5. Diagram of the human norovirus capsid protein sequence, adapted from Tan and Jiang, 2003.

The capsid protein consists of an N-terminal region, a shell (S) domain, and a protruding (P) domain.

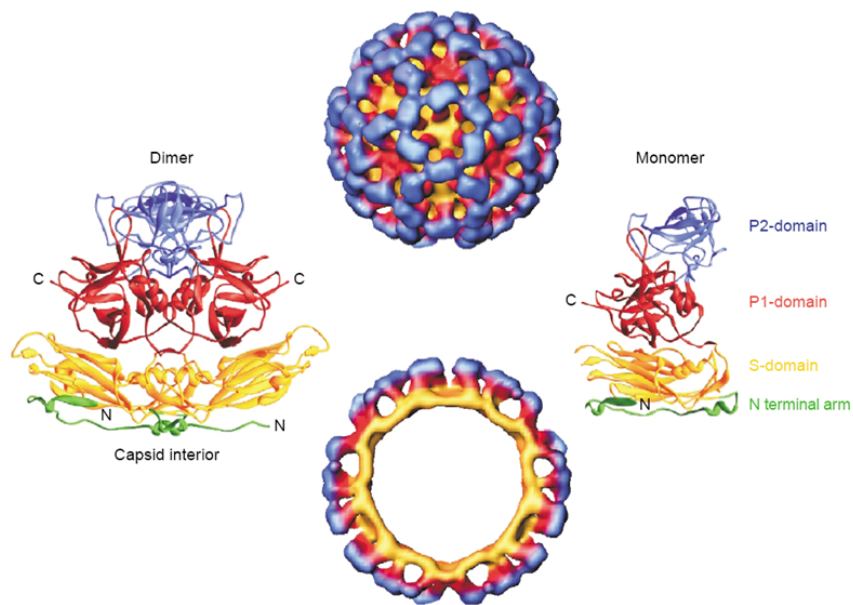


Figure 1.6. Tertiary structure of human norovirus VLPs generated by cryo-electron microscopic reconstruction, adapted from Hutson et al., 2004.

Top figure, surface representation of human norovirus VLPs; Bottom figure, cross-section of human norovirus VLPs; left, ribbon diagram of VP1 dimer; right, ribbon

diagram of monomeric VP1. VP1 contains a P domain, S domain, and N-terminal arm region.

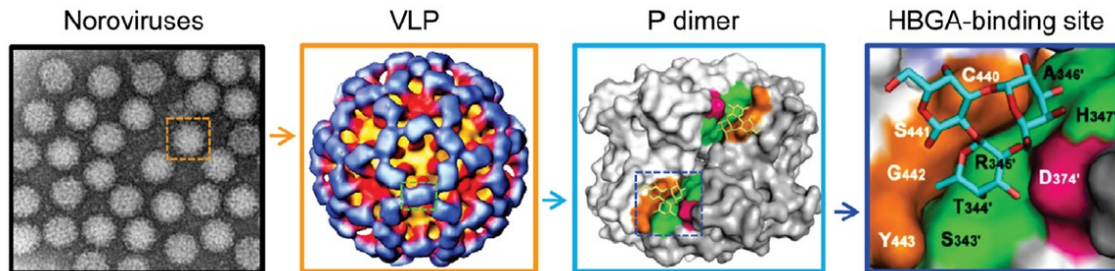


Figure 1.7. Receptor binding region in norovirus P dimer interface, adapted from Tang and Jiang 2010.

Norovirus structure was showed at four different levels. Furthest left, norovirus under electron microscopy; middle left, a single virus-like particle (VLP); middle right, a P dimer with indication of HBGA-binding interface in color; furthest right, crystal structure of the HBGA-binding interface.

1.4.2 The minor capsid protein VP2

The minor capsid protein, VP2, ranges from 208-268 amino acids in length, and has a molecular weight of ~22-29 kDa. VP2 is present in only 1-2 copies in one norovirus virion (Glass et al., 2000). The sequence of VP2 is highly variable among different norovirus strains (Seah et al., 1999). The function of VP2 in viral life cycle is not clearly defined, but there are several roles suggested for this protein. VP2 is a basic protein with an isoelectric point (pI) of more than ten, leading to the speculation that it may be able to bind RNA (Glass et al., 2000). In addition, it has been suggested that VP2 may bind to

RNA and function in encapsidation of the viral genome (Hardy, 2005). Interestingly, it has been shown that co-expression of VP2 and VP1 resulted in increased VP1 expression levels compared to expression of VP1 alone, suggesting that VP2 regulates the synthesis of the VP1 protein (Bertolotti-Ciarlet et al., 2003). In vitro biochemical studies also found that VP2 increased VP1 stability and protected VP1 from disassembly and protease degradation (Bertolotti-Ciarlet et al., 2003). The possible model for the mechanism of the VP2-mediated stabilization of the VP1 capsid protein is shown in Figure 1.8.

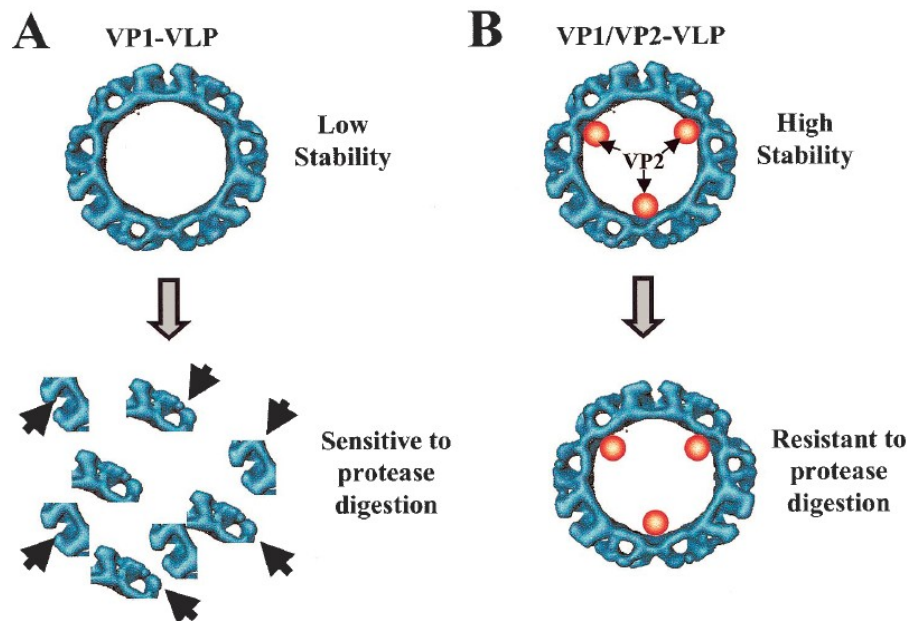


Figure 1.8. Possible mechanism of VP1/VP2 interaction, adapted from Bertolotti-Ciarlet et al. 2003.

Panel A shows VLP composed only of VP1 is more sensitive to proteases. Panel B shows that VP2 stabilizes the VLP structure.

1.4.3 Non-structural proteins

ORF1 encodes a ~200kDa nonstructural polyprotein of approximately 1,800 amino acids. The polyprotein is proteolytically cleaved into six nonstructural proteins: p48, NTPase, p22, VPg, 3CL^{pro}, and RdRp.

The first protein, p48, was found to co-localize with the Golgi complex in transfected cells and induced membrane rearrangement (Fernandez-Vega et al., 2004). It has also been shown to interact with a protein called vesicle associated-membrane protein-associated protein A (VAP-A) which regulates docking and fusion of SNARE-mediated vesicle fusion (Ettayebi and Hardy, 2003). The expression of p48 resulted in the interruption of vesicle transportation and inhibition of cell surface protein expression.

The second protein, p41, has NTPase, but not helicase activity (Pfister and Wimmer, 2001). It can bind and hydrolyzes ATP, but cannot unwind an RNA: DNA heteroduplex.

The possible function of the third protein, p22, is not clear. It was found to be present in a p22-VPg-3CL^{pro} complex, which is a precursor involved in the proteolytic processing pathway (Belliot et al., 2003).

The fourth protein, VPg, covalently links to the 5' end of norovirus genomic and subgenomic RNA (Burroughs and Brown, 1978), based on sequence comparison to other

animal caliciviruses. VPg may be involved in the initiation of translation by recruiting translational machinery, such as eIF3 and 40S subunits (Daughenbaugh et al., 2003).

The fifth nonstructural protein, 3CL^{pro} (representing 3C-like protease), is similar to picornavirus 3C protein. 3CL^{pro} functions as a protease and cleaves the ORF1 polyprotein into mature functional proteins (Belliot et al., 2003). It may also be involved in inhibiting the synthesis of cellular proteins in infected cells, as evidenced by the fact that 3CL^{pro} was able to cleave polymerase A (polyA) binding protein in vitro (Kuyumcu-Martinez et al., 2004).

The sixth protein, the RNA-dependent RNA polymerase (RdRp), is at the C-terminal end of ORF1. The genome replication and transcription of norovirus is dependent on the RdRp. The crystal structure of the human NoV RdRp revealed its RNA polymerase catalytic and structural elements, which are homologous to other positive-stranded RNA viruses (Ng et al., 2002a; Ng et al., 2002b)

1.5 Human norovirus genogroup and genotype

The Norovirus genus is divided into 5 genogroups including GI, GII, GIII, GIV, and GV, based on the phylogenetic analysis of the major capsid sequences (VP1). Each genogroup is further subdivided into genetic clusters termed genotypes (Fig. 1.9). For example, genogroup I contains 8 genotypes, and genogroup II contains 19 genotypes. The majority of human NoVs belong to genogroup I, II, and IV (Zheng et al., 2006). Norwalk virus,

the prototypic norovirus strain, belongs to genogroup I and genotype I (GI.1). GII.4 strains are the most prevalent human NoV strains, and are the most commonly detected and frequently associated with outbreaks worldwide (Hutson et al., 2004). The capsid amino acid sequence within a norovirus genogroup and between genogroups are highly diverse (Zheng et al., 2006). The genomic variations are caused by point mutations and recombination, which can result in the emergence of novel NoV strains. The high genetic variability of GII.4 strains leads to their wide spread and prolonged persistence in the human population. Therefore, GII.4 is the most studied among all norovirus strains (Zakikhany et al., 2012).

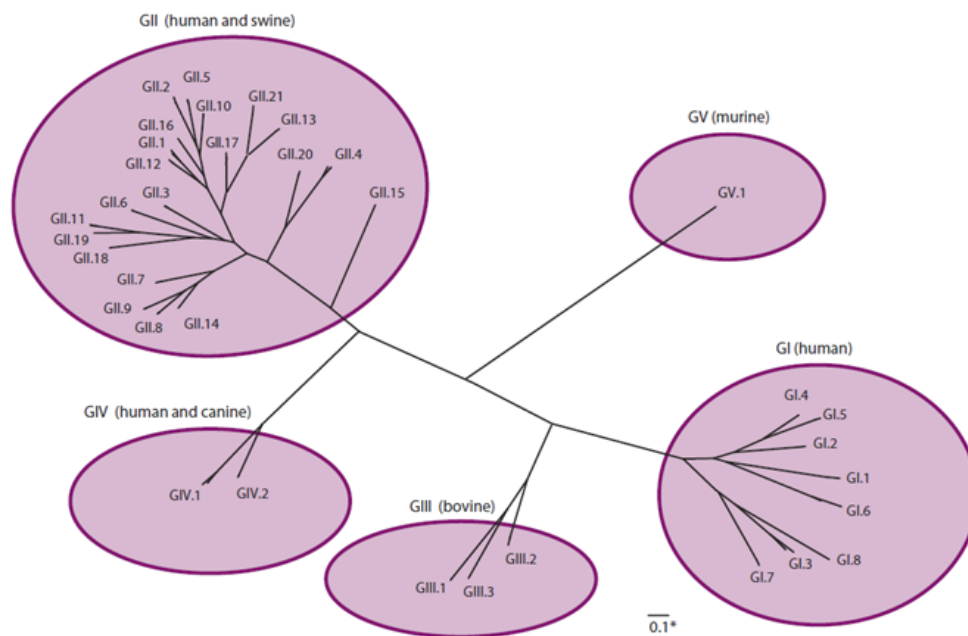


Figure 1.9. Classification of noroviruses into 5 genogroups (GI–V) and 35 genotypes based on sequence diversity in the complete capsid protein VP1 (Hall et al., 2011).

1.6 Cellular receptor and human susceptibility for human norovirus

It has been established that the histo-blood group antigens (HBGAs) on mucosal epithelial cells are the ligands for human NoVs (Hutson et al., 2002; Hutson et al., 2003; Tan et al., 2003). HBGAs are carbohydrates linked to proteins or lipids on the surface of erythrocytes, mucosal epithelial cells, or as free oligosaccharides in saliva, milk, blood, and intestinal contents (Ravn and Dabelsteen, 2000). The ABO, Lewis, and secretor gene families encode for the glycosyltransferase that control the synthesis of different types of HBGAs using precursor oligosaccharides as substrates. There are four types of precursor oligosaccharides: type 1, galactose (Gal) β N-acetylglucosamine β -R; type 2, Gal β 1-4 N-acetylglucosamine β -R; type 3, Gal β 1-3 N-acetylgalactosamine α -R; type 4, Gal β 1-3 N-acetylgalactosamine β -R. The precursors are further fucosylated on the terminal Gal by α 1,2 fucosyltransferase (FUT1 and FUT2), or on the acetylglucosamine by α 1,2 fucosyltransferase (FUT3) (Shirato, 2011). Figure 1.10 shows the synthesis of type 1 and 2 HBGAs. People, who do not express FUT2, are designated non-secretors. They are not able to synthesize ABH type or Lewis antigens on the epithelium. Human NoV shows high variability in the strain-specificity in HBGA binding patterns, with different strains binding to different HBGAs. Norwalk virus (NV) binds to α 1,2-linked fucose residues on carbohydrate antigens, which is synthesized by FUT2. Individuals with functional FUT2 gene, secretors, are susceptible to NV infection, but individuals with recessive FUT2 gene non-secretors, are completely resistant to NV infection (Lindesmith et al., 2003). NV was reported to infect individuals with O blood type easily, but individuals with blood type B were less susceptible to Norwalk virus (Hutson et al., 2005; Hutson et al.,

2002). Nearly all individuals can be infected by noroviruses even if they have different genetic backgrounds, which suggests that noroviruses may be able to co-evolve with human population.

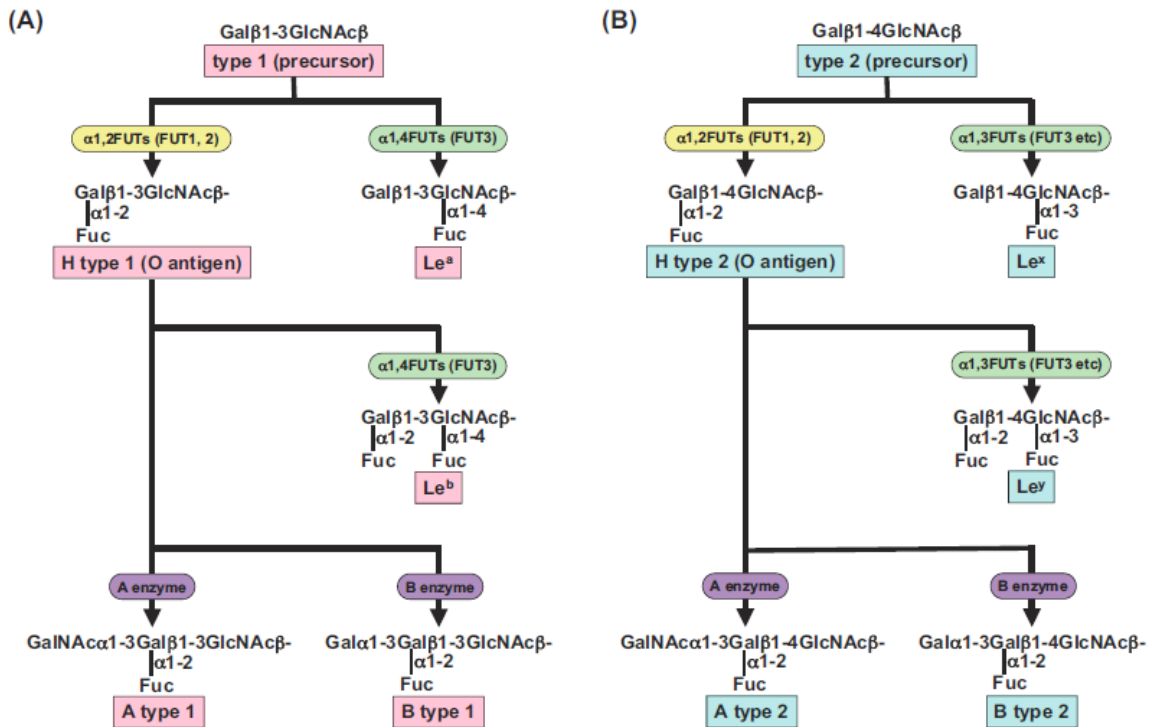


Figure 1.10. Diagrams of the synthesis of type 1 and 2 HBGAs.

(A) synthesis of type 1 HBGAs. (B) synthesis of type 2 HBGAs. Gal, galctose; GlcNAc, N-acetylglucosamine; Fuc, fucose; GalNAc, N-acetylgalactosamine.

1.7 Challenges in human norovirus research

For decades, the progress of human NoV research has been prolonged compared to other viruses, because of two obstacles. First, no cell culture system has been proven to support

human NoV replication *in vitro*. The cell tropism of human NoV is still not known, although numerous efforts have been aimed to the discovery of a cell culture system that will support human NoV propagation (Duizer et al., 2004b). Second, no small animal model is able to support human NoV *in vivo* replication. Hence, pathogenesis and immunology studies, which rely on animal models, have been hampered for human NoV research.

1.7.1 Advances of developing cell culture for human NoV infection

To date many efforts have been made to grow human NoV, but all the attempts have failed to show any convincing evidence. No infectious Norwalk virus was produced in either routine or differentiated gastric cells, duodenal cells, or small intestinal enterocyte-like cells, including A549, AGS, Caco-2, CCD-18, CRFK, CR-PEC, Detroit 551, Detroit 562, FRhK-4, HCT-8, HeLa, HEC, HEp-2, Ht-29, HuTu-80, I-407, IEC-6, IEC-18, Kato-3, L20B, MA104, MDBK, MDCK, RD, TMK, Vero, and 293 (Duizer et al., 2004b). Murine norovirus (MNV) grows in mouse macrophages and dendritic cells *in vitro*, but human NoV cannot replicate in peripheral human macrophages or dendritic cells (Lay et al., 2010). Although the majority of the attempts to culture human NoV have been unsuccessful, there is one report describing the replication of human NoV in small intestinal epithelial cells (Straub et al., 2007). The authors used a highly differentiated 3-dimensional (3-D) organoid model of the human small intestinal epithelium to culture GI and GII human NoV. Viral infection was confirmed by microscopy, PCR, and fluorescent in situ hybridization. However, many other researchers have questioned the validity of

the viral replication level and the evidence of newly synthesized reproducible progenies (Chan et al., 2007). In response to these questions, Straub et al. pointed out that the viral titer did increase, but different virus strains and the multiplicity of infection may affect the magnitude and time course of the viral increase (Chan et al., 2007). Recently, human NoV infection and productive replication was seen in an *ex vivo* culture of human adult duodenal tissues (Leung et al., 2010). Evidence of viral replication was provided by RT-qPCR, in situ hybridisation, and immunohistochemical staining. However, the source of *ex vivo* tissue is limited and relies on tissue donors, therefore large scale production of human NoV by this model is impossible.

1.7.2 Progress of developing animal models for human NoV

For decades, most of the information about human NoV pathogenesis has come from outbreak investigations. Humans are the only known organisms that support efficient human NoV replication, but human volunteer studies are expensive and require complicated *Institutional Review Board* (IRB) protocol and sample collection methods. Due to the difficulties associated with human subject research, it is apparent that animal models need to be developed for human NoV research. Many researchers are trying to develop animal models to study human NoV. Sporadic asymptomatic infections were seen in nonhuman primates, such as rhesus macaques and newborn *Macaca nemestrina*, after Norwalk virus challenge (Rockx et al., 2005; Subekti et al., 2002). Viral RNA was detected in stool samples, however human NoV specific antibody was only detected in a small portion of the challenged group. Chimpanzees have been found to be promising

models to study human NoV pathogenesis and immunology (Bok et al., 2011). Seronegative chimpanzees inoculated intravenously with Norwalk virus showed similar onset and duration of virus shedding in stool and serum antibody responses compared to humans, although clinical signs of gastroenteritis were not observed. In addition, this study also demonstrated that chimpanzees vaccinated intramuscularly with GI NoV VLPs were protected from Norwalk virus infection when challenged 2 and 18 months after vaccination. However, chimpanzee research will probably be prohibited in the future biomedical research according to a report released on December 15, 2011 from National Institute of Health (2011). The use of non-human primates has generated a lot of debates worldwide.

Novel animal models for the study of human NoV replication have been examined using gnotobiotic pigs and gnotobiotic calves as germ-free hosts for human NoV replication (Cheetham et al., 2006; Souza et al., 2008). The pathogenesis of human NoV and the target cells for viral replication were evaluated in a gnotobiotic pig model (Cheetham et al., 2006). Mild diarrhea was seen in 74% (48/65) of pigs after oral inoculation with norovirus GII.4. Viral infection was confirmed using histopathologic examination and an immunofluorescence assay. Seroconversion was detected in 59% (13/22) pigs. Sporadic infection of duodenal and jejuna enterocytes was detected in 58% (18/31) of human NoV-inoculated pigs. Only 1 out of 7 pigs showed mild lesions in the proximal small intestine. Calicivirus-like particles of 25 to 40 nm in diameter were seen in cytoplasmic membrane vesicles in the enterocytes using transmission electron microscopy. This data

demonstrated that the gnotobiotic pig is a viable model to support human NoV replication. Additionally, low levels of antibodies and low numbers of antibody secreting cells were induced systemically and locally in the gut by human NoV in gnotobiotic pigs (Souza et al., 2007a). This pig model was used to test a human NoV VLP-based vaccine adjuvanted with ISCOM or mutant *E. coli* LT toxin (Souza et al., 2007c). High levels of antibody and cytokine responses were induced by the vaccine, leading to homologous protection. Souza et al. attempted to develop gnotobiotic calves as a model to study human NoV infection (Souza et al., 2008). The human NoV GII.4 strain HS66 caused diarrhea and intestinal lesions in the proximal small intestine (duodenum and jejunum) in the gnotobiotic calves, and additionally induced NoV specific antibodies and cytokines. Immunohistochemistry revealed the localization of human NoV viral capsid antigens in the jejunum of infected calves.

1.8 Animal caliciviruses

1.8.1 Murine norovirus (MNV).

MNV, a member of *Norovirus* genus, is the only norovirus that was found to be successfully cultured in cell lines and in small animal model (Wobus et al., 2004). MNV is found to be prevalent in the research mice nowadays, but it was not isolated until 2003 (Hsu et al., 2005). It was first identified from immunocompromised mice deficient in recombination-activating gene 2 (RAG2) and signal transducer and activator of transcription 1 (STAT1) (RAG/STAT1^{-/-}) (Karst et al., 2003). Systemic and even lethal infection is caused by MNV in STAT1^{-/-} mice (Karst et al., 2003). Although MNV dose

not cause diarrhea and vomiting in mice, it replicates and disseminates to lung, spleen, liver, and cause gastroenteritis in normal mice after oral inoculation (Mumphrey et al., 2007). Viruses was also found in stools of infected mice. Additionally, many hematopoietic lineage cell lines, specifically murine macrophage and dendritic cell lines, are found to support MNV proproagations. RAW 264.7 cell line is a typical model used to culture and perform plaque assay for MNV. MNV shares the similar biological and molecular characteristics with human NoV. Genetically, MNV is closely related to human NoV. Both of them are classified into *Norovirus* genus, and share similar genome size and organization. Their biochemical features, including virion size (28-35nm), morphology (round, non-enveloped), structure (icosahedral), and buoyant density ($1.36 \pm 0.04 \text{ g/cm}^3$) are similar (Karst et al., 2003; Wobus et al., 2006). Therefore, MNV has been widely considered as a surrogate for human NoV since its discovery (Wobus et al., 2006). However, the difference, such as viral receptor binding, pathogenesis, and immunity, between MNV and human NoV cannot be ignored (Karst et al., 2003; Wobus et al., 2006). Sialic acid is a cellular receptor for MNV, but HBGAs are the functional receptor for human NoV (Tan and Jiang, 2005a; Wobus et al., 2006). MNV cause systemic infection in mice, but human NoV only induce gastroenteritis in human. Since MNV is the only cultivable norovirus, it has been extensively used as a model to study and gain insight into the viral entry, replication, and gene expression of human NoV.

1.8.2 Feline calicivirus

Feline calicivirus (FCV), which was first discovered in the 1950s, is one of the leading cause of upper respiratory tract infection in cats (Doultree et al., 1999). FCV only cause symptoms, such as sneezing, nasal discharge, fever, running eyes in cats, but not gastroenteritis which is a typical clinical sign of human NoV infection. FCV is classified into the *Vesivirus* genus within the *Caliciviridae* family. FCV is used as a commonly surrogate for human NoV because of its genetic similarity to human NoV. In addition, FCV is cultivable in cell lines. However, the biochemical properties of FCV and human NoV are distinct. FCV is not as stable as human NoV and has lower resistance to environmental stress. Before the discovery of MNV in 2003, FCV was a major surrogate for human NoV inactivation studies and environmental survival (D'Souza et al., 2006; Duizer et al., 2004a).

1.8.3 Porcine sapovirus

Porcine sapovirus is another surrogate for human NoV because of the genetic relatedness. It belongs to the *Sapovirus* genus within the *Caliciviridae* family, and is the only culturable enteropathogenic calicivirus (Wang et al. 2005, Wang et al. 2007). No cell culture system was available for porcine sapovirus until 1980 (Saif et al. 1980). A porcine kidney cell line (LLC-PK) was found to support the replication of Porcine sapovirus Cowden strain (Flynn & Saif 1988). Bile acid or intestinal content fluid filtrate is essential for the growth of this virus (Chang et al. 2004).

Porcine sapovirus resembles human NoV in several aspects. The genome organization, virion structure, and morphology of both viruses are similar. The most important advantage of using porcine sapovirus as a surrogate is that this virus causes gastroenteritis in pigs (Flynn et al. 1988, Guo et al. 2001). Porcine sapovirus also show similar environmental resistance with human NoV (Wang et al. 2012). Based on these two advantages, porcine sapovirus may be an improved model for human NoV compared to MNV and FCV.

1.8.4 Tulane virus

Tulane virus, also known as monkey calicivirus, is a newly isolated virus. It was first identified in feces of rhesus macaques at the Tulane National Primate Research Center (Farkas et al., 2008). The genome of Tulane virus is the shortest among all the know calicivirus, ranging 6,714 nt in length. Based on the sequences alignment, Tulane virus was clustered into a newly created genus, named *Recovirus* (*rhesus enteric Calicivirus*), within the *Caliciviridae* by Farkas et al.. Tulane virus resembles other caliciviruses in size, morphology, and buoyant denstiy. A continuous monkey kidney cell line (LLC-MK2) has been shown to successfully support Tulane virus replication. Although the pathogenesis and immunology of Tulane virus remain to be elucidated, it was found that Tulane virus share the same cellular receptor with human NoV. Of promising note, Type A and B HBGAs were shown to involve in Tulane virus infection (Farkas et al., 2010). Taken together, Tulane virus may serve as a useful surrogate model for studying human NoV pathogenesis.

1.9 Vaccine candidates against human norovirus

1.9.1 VLP-based vaccine candidate

Since human NoV cannot be grown in cell culture, most vaccine studies have been focused on the subunit vaccine. It is known that VP1 is the immunogenic antigen for human NoV. As soon as the genome of human NoV was cloned and sequenced, the VP1 proteins has been expressed many expression system, including yeast, *E. coli*, insect cells, mammalian cell lines, tobacco, and potatoes (Jiang et al. 1992, Mason et al. 1996, Zhang et al. 2006). Jiang et al. (1992) first found that the expression of VP1 alone in cell culture yields self-assembled VLPs that are structurally and antigenically similar to native virions. Baculovirus-insect cell expression system has been shown to be the most efficient expression system for VLPs. Therotically, these VLPs contain optimal epitopes that can trigger human NoV-specific immune responses in hosts. Therefore, VLPs should be a good vaccine candidate for human NoV. Ball et al., (1998) examined oral doses of insect cell-derived VLPs between 5 and 500 µg, either with or without the mucosal adjuvant cholera toxin (CT). Eight out of 11 mice had a detectable serum anti-NoV IgG when mice received 5 µg of VLPs (without CT). Higher titers of serum anti-NoV IgG [geometric mean titers (GMT; 1168)] were observed when mice received 200 µg of VLP (without CT). Interestingly, the GMT of serum IgG was increased to 6400 when CT was used as an adjuvant. Moreover, NoV-specific intestinal IgA were detected in the fecal extracts of mice immunized orally with 200 µg doses. These data suggests that oral vaccination of VLP triggered mucosal and humoral immunities in mice.

Sunsequently, many other researchers showed immunization with VLPs orally or intranasally induced variable humoral, mucosal, and cellular immunities (Guerrero et al. 2001, Souza et al. 2007b, BoK et al. 2011). There are several disadvantages of VLP-based vaccine candidates, in spite that the above studies are very promising. Preparation of VLPs in vitro is expensive, requiring a lot of time and labor. A high dosage of VLPs and even multiple boosters may be required for effective immunization. The efficacy of VLP-based vaccines relies on the addition of mucosal adjuvants such as cholera toxin and *E. coli* toxin, which may have side effects. Additionally, because VLPs are proteins, nonreplicating immunogens, the duration of the antigen stimulation may be limited.

In 1999, Ball and colleagues performed the first clinical study to demonstrate that baculovirus-expressed human NoV VLPs were safe and immunogenic in humans when administered orally (Ball et al. 1999). Tacket et al. (2000) performed a human volunteer study of transgenic potato-based VLP vaccine. Nineteen of 20 (95%) volunteers who ingested transgenic potatoes developed significant increases in the number of specific IgA antibody-secreting cells. Four of 20 (20%) volunteers developed norovirus specific serum IgG, and 6 of 20 (30%) volunteers produced norovirus specific stool IgA. Totally, 19 of 20 volunteers developed immune responses. In the United States, LigoCyte Pharmaceuticals Inc. licensed two VLP-based vaccine candidates, a intranasally delivered dry powder formulation and a intramuscularly delivered liquid formulation. The vaccines contain GSK's MPL® Toll-4 Agonist as an adjuvant for enhancing the efficacy of vaccination. In human clinical trials, volunteers that received the dry powder VLP

vaccine reduced the risk of illness by 47% after exposure to human NoV (LigoCyte Pharmaceuticals Inc. 2010). Individuals who received vaccine had significant reductions in clinical symptom and severity of illness compared with those who received the placebo (LigoCyte Pharmaceuticals Inc. 2010).

1.9.2 Protrusion (P) particle-based vaccine candidate

The two principal domains, shell (S) and protrusion (P), of human NoV capsid protein is linked by a flexible hinge region. Expression of the P domain (without the hinge region) resulted in the formation of ring- or pentagon-shaped structures with a diameter of 5 nm (Tan and Jiang, 2005b). These small particles were named the P particles. Interestingly, Tan also found that the P particles exhibited higher binding ability to HBGAs. The advantages of using the P particle as a human NoV vaccine candidate are that: (1) the P particle can be easily produced by *E. coli* in large scale; (2) it is extremely stable, and (3) it is highly immunogenic (Tan and Jiang, 2005b). Based on structural biology, the P particle is an octahedral nanoparticle consist of 24 copies of the P domain of the norovirus VP1 protein (Tan et al. 2011). Each P domain has three surface loops, resulting in a total of 72 loops per P particle. The P particle can also be used as a platform to deliver other antigens and become a promising vaccine vector. To demonstrate this novel concept, rotavirus VP8 gene was inserted into one of the loops (Tan et al., 2011). The insertion of this foreign gene did not affect the structure of P particle. The resulting VP8 chimeric P particles triggered a strong humoral immune response against rotavirus in mice. Furthermore, the sera from vaccinated mice blocked norovirus VLPs from binding

to HBGAs. Thus, the P particle-VP8 chimeras may serve as a dual vaccine against both rotavirus and norovirus. Similarly, an influenza vaccine was generated by inserting the Matrix protein (M2) of influenza A virus into one of the loops of the P particle, resulting in the formation of M2e-P particles. Mice were fully protected from the influenza virus challenge after the M2e-P particles vaccination (Xia et al. 2011). These findings demonstrated that the P particle is not only an excellent vaccine candidate for human NoV but also a novel vaccine vector for antigen presentation.

1.9.3 Live-vectored vaccines against human NoV

1.9.3.1 Rationales of using a vectored vaccine.

The first live-virus vector vaccine was reported by Smith et al.,(1983). It was found that a recombinant vaccinia virus expressing hepatitis B surface antigen induced hepatitis B-specific antibodies in rabbits. This discovery has inspired the development of many other live-virus vectors, DNA viruses (adenoviruses and herpesviruses); positive-strand RNA viruses (alphaviruses and flaviviruses); negative-sense RNA viruses (vesicular stomatitis virus (VSV) and Newcastle disease virus (NDV)).

Generally, a live attenuated virus vaccine stimulates strong systemic immunity and provides durable protection because of the viral replication *in vivo*. However, developing such kind of vaccine is not realistic for viruses that are not culturable, because viruses cannot be attenuated by passages. Even if an attenuated strain were available, it could not be mass produced. In this situation, a vectored vaccine may be ideal to overcome this

obstacle. Since human NoV cannot be grown in cell culture, several research groups have devoted to develop a vectored vaccine for human NoV.

1.9.3.2 Venezuelan equine encephalitis virus--vectored human NoV vaccine

Venezuelan equine encephalitis virus (VEE) is a member of *Alphavirus* subfamily within *Togaviridae* family. For many years, alphavirus has been used as a vector to deliver antigens. One of important advantages of using VEE as a viral vector is that VEE targets dendritic cells which may improve the efficacy of the vectored vaccine (MacDonald et al., 2000). In fact, VEE is the first viral vector that has been used for delivering human NoV antigen. It is a replicon-based vector that only contains a partial VEE genome encoding nonstructural proteins required for transcription and replication. The vectored vaccine is constructed by cotransfection of a replicon that contains the norovirus capsid gene and helper plasmids that encode VEE structural genes. The efficacy of VEE vectored NoV vaccine has been tested in a mouse model. It was found that mice inoculated with this single-cycle live vectored vaccine triggered a high level of NoV-specific systemic, mucosal, and heterotypic immunity (Harrington et al. 2002). Mice received multivalent norovirus VLP vaccines with alphavirus adjuvant particles induced homotypic and heterotypic humoral and protective immunity to human and murine NoV strains. This multivalent VLP vaccines also triggered robust receptor-blocking antibody responses to heterologous human strains not included in the vaccine composition (LoBue et al. 2009). In addition, inclusion of alphavirus adjuvants in the inoculum significantly augmented VLP-induced systemic and mucosal immunity (LoBue et al. 2009). A VEE-

adjuvanted vaccine was shown to protect mice from the MNV challenge (LoBue et al. 2009). The above results suggested that VEE is a good live vector to deliver NoV vaccine. However, one major concern is that VEE is a biodefense pathogen and the use of functional VEE genes is restricted. The biosafety of VEE needs to be addressed despite the fact that VEE replicon is a single-cycle replicating vector.

1.9.3.3 Adenovirus-vectored human NoV Vaccine

Adenovirus is a double-stranded DNA virus that allows for insertion of exogenous genes without affecting efficient replication or packaging. Replication-defective adenovirus vectors have been explored for use as carriers of vaccines for a variety of pathogens, including human immunodeficiency virus type 1 (HIV-1) (Harro et al., 2009). Recently, adenovirus expressing capsid protein of human NoV has been constructed. Mice vaccinated by the adenovirus-vectored human NoV vaccine produced systemic, mucosal, and cellular Th1/Th2 immune responses (Guo et al. 2008). Interestingly, combination of adenovirus-vectored vaccine and VLP-based subunit vaccine can enhance human NoV-specific immunity. Specifically, mice primed with recombinant adenovirus-vectored vaccine and boosted with traditional VLP-based vaccine produced much stronger humoral, mucosal responses than those immunized with adenovirus-based or VLP vaccine alone (Guo et al. 2009). Although adenovirus-vectored vaccine showed promising in animal models, enthusiasm for clinical trial of this vaccine candidate decreased because a large portion of the global population has preexisting immunities against the adenovirus vector (Sekaly 2008). For example, approximately 40% of humans

residing in the United States and up to 90% of humans residing in some African countries have high levels of preexisting antibodies to this virus (Chen et al., 2010). Thus, in vivo delivery of the adenovirus-vectored vaccine may be hampered.

1.9.3.4 Vesicular stomatitis virus-vectored human NoV vaccine

Vesicular stomatitis virus (VSV) is a nonsegmented negative-sense RNA virus that belongs to the virus family *Rhabdoviridae*. VSV has been shown to be an excellent vector to deliver foreign antigens for live vaccines, oncolytic therapy, and gene therapy (Li et al. 2005, Li et al. 2006). Since the establishment of reverse genetics system, VSV has been used as a vector to deliver many vaccines against viral and bacterial pathogens. However, the use of VSV as a vector to deliver vaccine against noncultivable viruses is understudied. Recently, Ma & Li (2011) generated a recombinant VSV (rVSV-VP1) expressing the major capsid protein of human NoV GII.4 strain. Infection of mammalian cells by rVSV-VP1 resulted in a high level expression of human NoV VLPs. The yield of VLPs by the VSV expression system is approximately ten times higher than that of the baculovirus expression system. It is known that wild type VSV is highly pathogenic to mice. However, recombinant rVSV-VP1 is attenuated in mice. Moreover, mice inoculated with a single dose (10^6 PFU) of rVSV-VP1 through intranasal and oral routes stimulated a significantly stronger humoral and cellular immune response than baculovirus-expressed VLP vaccination. Furthermore, rVSV-VP1 vaccination triggered a high level of fecal and vaginal IgA antibody. In addition, it was found that insertion of heat shock protein 70 (HSP70) into rVSV-VP1 further attenuated the recombinant virus

and enhanced the human NoV specific immunity (Ma and Li, unpublished data). Recombinant rVSV-VP1 also triggered strong human NoV specific immunity in gnotobiotic piglets and protected pigs from the challenge of a human NoV GII.4 strain (Ma and Li, unpublished data). A VSV-based vaccine offers a number of other advantages, such as genetic stability, expression of multiple antigens, simplicity of production, multiple routes of administration, and ease of manipulation. Human infection with VSV is very rare, and the general population is free of preexisting immunity against VSV, unlike the adenovirus. Therefore, these advantages will support the initiation of the clinical trials of a VSV-vectored vaccine in the future. The VSV recombinant system not only provides a new approach to generate human NoV VLPs in vitro but also a new avenue for the development of vectored vaccines against Human NoV.

1.10 Introduction to Vesicular Stomatitis Virus

Vesicular stomatitis virus (VSV) is a non-segmented negative-sense (NNS) RNA virus that belongs to virus genus *Vesiculovirus* in the *Rhabdoviridae* family. Two major serotypes of VSV have been isolated in the U.S.: VSV Indiana strain and VSV New Jersey strain. VSV causes disease symptoms that are indistinguishable from foot-and-mouth disease in horses, cattle, and pigs. Symptoms include lesions in the mucosa around the mouth, nostrils, teats, and coronary bands of the hooves. Vesicles, ulcers, erosions, and crustings are the main manifestations of the lesions associated with VSV infection. Infected animals may develop anorexia, so severe weight loss may also serve as an indicator of VSV infection. VSV infection in livestock is usually not fatal to the animals.

The incubation period of VSV infection varies from 2 to 9 days, and the vesicles typically develop on days 2 to 5 after exposure to the virus. Animals infected with VSV usually recover in approximately 10-14 days unless secondary bacterial infections occur. Insects are the reservoir and carrier for VSV, with livestock as the end host. VSV infection in humans is normally asymptomatic, but in rare cases can result in mild flu-like symptoms. In general, VSV is not regarded as a human pathogen.

1.11 The structure of VSV virions.

VSV is an enveloped virus with a bullet-shaped virion that measures 80×170 nm in size (Fig. 1.11). The genome of VSV is approximately 11 kilobases (kb) in length organized into five VSV genes encoding nucleocapsid (N), phospho- (P), matrix (M), glyco- (G), and large (L) proteins, and leader and trailer regulatory sequences arranged in the order 3'-(leader), N, P, M, G, L, (trailer)-5' (Abraham and Banerjee, 1976; Ball, 1977; Whelan et al., 2004) (Fig. 1.11). Like all other NNS RNA viruses, the genome of VSV is encapsidated with the N protein to form a nuclease-resistant helical N-RNA complex that is the functional template for mRNA synthesis as well as genomic RNA replication. The N-RNA complex is tightly associated with the viral RNA-dependent RNA polymerase (RdRp), which is comprised of the 241-kDa L protein catalytic subunit and the 29-kDa essential P protein cofactor, and results in the assembly of a viral ribonucleoprotein (RNP) complex (Emerson and Wagner, 1972; Emerson and Yu, 1975). The M protein stabilizes the RNP, and the M-RNP complex is tightly surrounded by a lipid envelope. Approximately 400 homotrimers of the glycoprotein (G) protrude from the envelope,

which is essential for viral attachment and entry into cells (Hammond and Helenius, 1994).

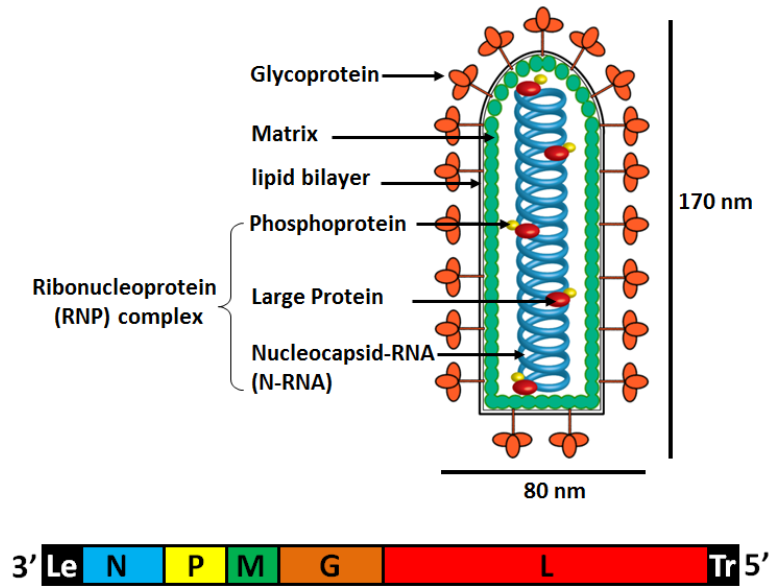


Figure 1.11. VSV virion structure and genome organization (Adapted from Lichty et al., 2004).

VSV encodes five structural proteins: nucleocapsid (N), phospho- (P), matrix (M), glyco- (G), and large (L) proteins. The VSV genome is arranged in the order 3'-(leader), N, P, M, G, L, (trailer)-5'.

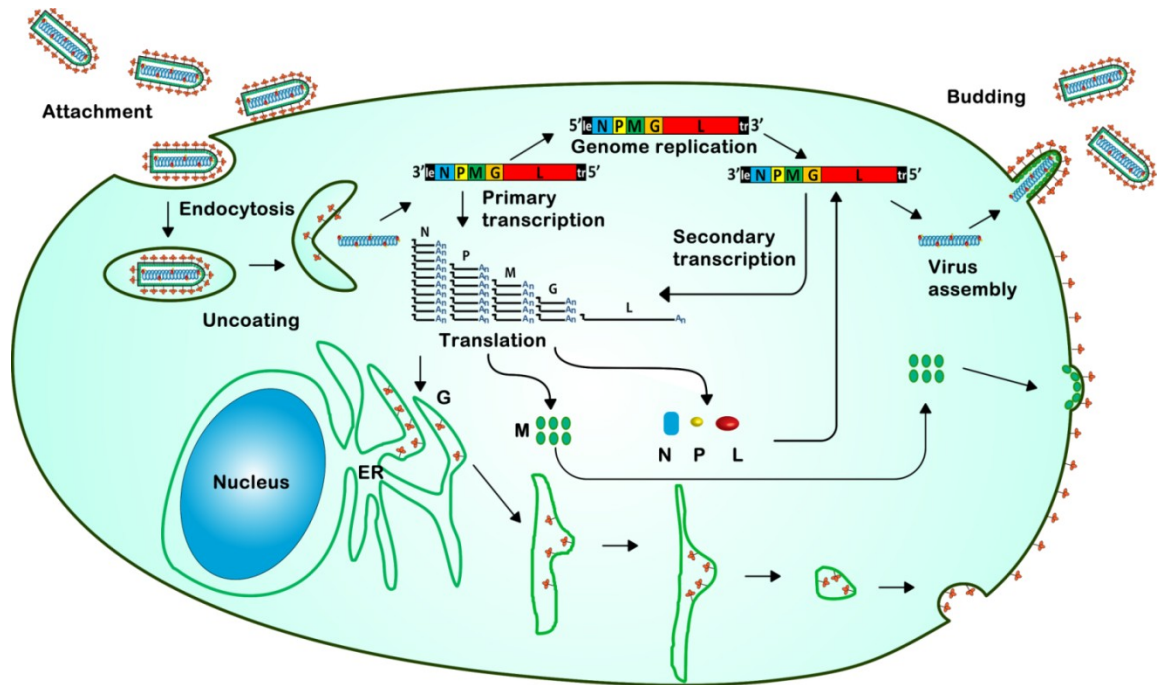


Figure 1.12 Overview diagram of VSV life cycle.

Steps of virus life cycle: attachment, endocytosis, uncoating, genome replication, mRNA transcription, viral protein translation, viral assembly, and budding are shown.

1.12 VSV life cycle.

The overview picture of VSV life cycle is in Fig. 1.12. Upon attaching to an unknown cell receptor(s), VSV enters host cells via receptor mediated endocytosis (Lichy et al., 2004; Matlin et al., 1982). Following low pH-triggered fusion and uncoating, the RNP complex is delivered into the cytoplasm where RNA synthesis and viral replication occur (Follett et al., 1974). During primary transcription, the input RdRp recognizes the specific signals in the N-RNA template to transcribe six discrete RNAs: a 47-nucleotide leader RNA (L⁺), which is neither capped nor polyadenylated, and 5 mRNAs that are capped

and methylated at the 5' end and polyadenylated at the 3' end. These mature mRNAs are then translated by host ribosomes to yield functional viral proteins which are required for viral genome replication. During replication, the RdRP initiates at the extreme 3' end of the genome and synthesizes a full-length complementary antigenome, which is encapsidated by the N protein and subsequently serves as template for synthesis of full-length progeny genomes. These progeny genomes can then be utilized as templates for secondary transcription, or assembled into infectious particles. Finally, viral proteins and genomic RNA are assembled into complete virus particles and the virus exits the cell by budding through the plasma membrane.

1.13 VSV transcription

The VSV genome has leader (Le) sequences at the 3' end, trailer sequences at the 5' end, and intergenic sequences between each gene (Ball, 1977; Whelan and Wertz, 2002). The leader, trailer, and intergenic sequences are essential for viral replication and transcriptional control. The RdRp binds to the initiation site located in the Le sequence and synthesizes mRNA regulated by the first gene-start region. The L protein is also involved in the mRNA cap addition, cap methylation, and polyadenylation. In response to a *cis*-acting element, the cap is added to 5' end of the mRNA through an unconventional mechanism in which the GDP: polyribonucleotidyltransferase (PRNTase) of L transfers a monophosphate RNA onto a GDP acceptor through a covalent protein-RNA intermediate (Li et al., 2008b; Ogino and Banerjee, 2007). The cap is further methylated at the ribose 2'-O and guanine-N-7 by L protein (Li et al., 2009b; Li et al., 2005). When encountering

a gene-end sequence, L polyadenylates and terminates mRNA synthesis. VSV follows a start/stop model of sequential transcription to produce five capped, methylated, and polyadenylated mRNAs, N, P, M, G, and L (Abraham and Banerjee, 1976; Ball and White, 1976). During the start/stop process, the RdRp occasionally detaches from nucleocapsid template at gene junctions, which results in a 30% decline in transcription of downstream genes leading to a gradient of mRNA expression from 3' to 5' end (Abraham et al., 1975; Barr et al., 1997; Hwang et al., 1998).

1.14 VSV replication

One unique feature of VSV gene expression is that a single RdRP controls two distinct RNA syntheses: transcription and replication. Sufficient amounts of N protein is required for the transition from transcription to replication, although the mechanism by which replication is initiated is not fully understood (Blumberg et al., 1983). Viral replication is initiated after the N-RNA template recruits the RdRp at the entry site in Le sequence. The initiation site for transcription is distinct from the initiation site for replication in the genome (Whelan and Wertz, 2002). Transcription initiation occurs at the gene start sequence located between Le and N gene junction, and replication initiation occurs at the beginning of the Le sequence. Viral replication proceeds from the 3' end to the 5' end bypassing the start and stop signals for transcription at the intergenic junctions, resulting in a full-length positive sense antigenomic RNA. The antigenomic RNA subsequently serves as a template for the production of full-length viral genomic RNA.

1.15 VSV assembly

The assembly of VSV requires the involvement of both host cellular components and viral M and G proteins. N proteins bind to genomic RNA to form nucleocapsid core when RNA is being synthesized. Specifically, N proteins associate with the sugarphosphate backbone of RNA in the cytoplasm through an exchange reaction in which P protein is released from N:P dimers. A small amount of cytoplasmic M protein may bind the newly formed RNP, but may not be sufficient to condense it into bullet shaped capsid. At the same time, G proteins are transported to the cellular membrane and form sites for budding. When M proteins accumulate to high levels in the cytoplasm, a portion of the M proteins localize to the inner leaflet of the plasma membrane and the RNPs are transported to the budding site and begin condensation. The interaction of both the cytoplasmic and membrane associated M proteins with the condensing RNPs results in the formation of bullet shape protrusions from the plasma membrane. The release of mature virions may require other cellular machinery such as Nedd-4 or a related ubiquitin ligase (Jayakar et al., 2004).

1.16 Reverse genetics of VSV.

In 1995, an VSV reverse genetics system was established (Lawson et al., 1995; Seán et al., 1995). VSV can be recovered entirely from cloned cDNA by transfecting mammalian cells with plasmids encoding (i) full-length genomic or antigenomic RNA and (ii) the major proteins involved in replication and transcription, namely N, P, and L. As shown in Fig. 1.13, a plasmid encoding the full-length VSV genome [pVSV(+)] was transfected

into Baby Hamster Kidney (BHK) cells, concurrently with three support plasmids carrying VSV L (pL), P (pP), and N (pN) protein genes. The VSV antigenomic RNA and the mRNA of the L, P, and N gene were then transcribed using a T7 RNA polymerase produced by vaccinia virus infection. The newly synthesized L, P and N proteins bound the antigenomic RNA and generated full-length genomic RNA, resulting in the formation of a functional RNP and the production of other viral proteins. After assembly, a complete infectious recombinant VSV was recovered. This is a powerful system that allows for genetic manipulation of viral genome such as mutation, deletion, and insertion of foreign genes.

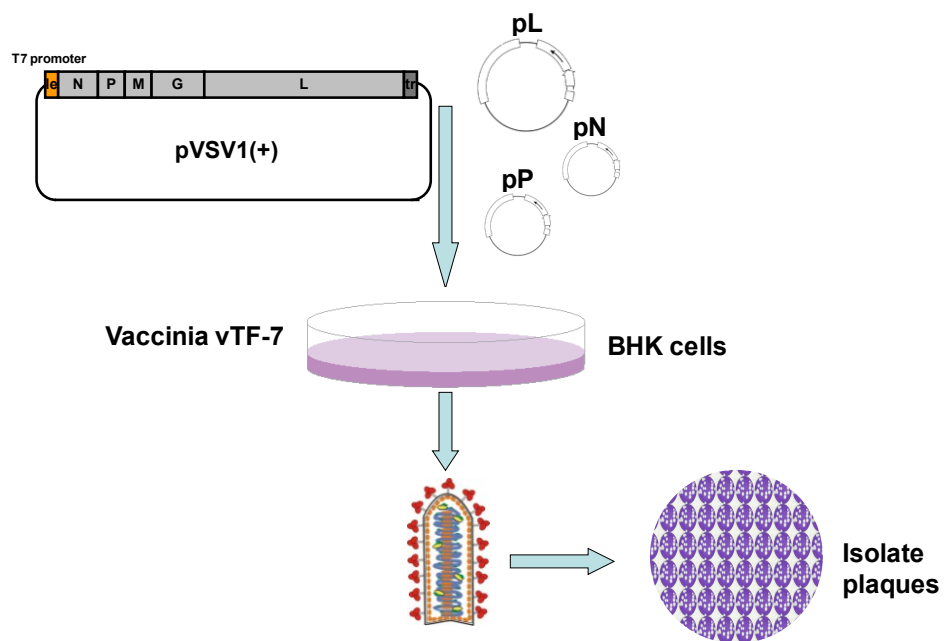


Figure 1.13. Recovery of infectious VSV from a cDNA clone by reverse genetics.

1.17 VSV as a vector for vaccine development

VSV has been shown to be an excellent vector to deliver foreign antigens as live vaccines, oncolytic therapy, and gene delivery. Exogenous genes can be inserted into the VSV genome, resulting in a recombinant VSV expressing these antigens. The inserted foreign genes can be highly expressed in vitro cell culture (Lichty et al., 2004; Whelan et al., 2004). The exogenous antigens are expressed continuously in vivo after the recombinant viruses have been inoculated into animals, and thus trigger specific immune responses. To date, VSV has been successfully examined as a vaccine candidate for a number of pathogens including human immunodeficiency virus (HIV) (Haglund et al., 2002; Johnson et al., 1997; Rose et al., 2001; Schnell et al., 1996; Tan et al., 2005), severe acute respiratory syndrome (SARS) (Faber et al., 2005; Kapadia et al., 2005), hepatitis C virus (Buonocore et al., 2002; Ezelle et al., 2002), influenza virus (Roberts et al., 1999a; Roberts et al., 1998), papillomavirus (Reuter et al., 2002), human respiratory syncytial virus (Kahn et al., 2001), poxvirus (Braxton et al., 2010), arenavirus (Garbutt et al., 2004b), Ebola virus, and Marburg virus (Geisbert et al., 2008b; Jones et al., 2005). These studies have shown that VSV-based vaccines triggered strong immunity in animal models even after a single immunizing dose. The major drawback for VSV is that there is little experience with its administration to humans. Excitingly, at least three independent phase I human clinical trials are currently being carried out to test the safety, immune response, and effectiveness of the VSV-based vaccine and oncolytic therapy in human. Two phase I clinical trials testing VSV-based HIV vaccines (VSV-Indiana HIV gag vaccine, and HIV DNA vaccine followed by VSV-gag vaccine boost) are currently active

according to the online database of NIH. Recombinant VSV expressing interferon beta has been approved for phase I clinical trials to treat patient with cancer. It seems likely that detailed information on safety, replication, pathogenesis, and immunogenicity of VSV-based vaccines in humans will be forthcoming.

1.18 Advantages of using VSV as a viral vaccine vector.

VSV is especially suitable for live vectored vaccine development for the following reasons: (1) VSV has a relatively small genome and simple structure, and is able to grow rapidly and to a high titer in most animal cells; (2) It is impossible for the inserted foreign genes to homologously recombine into the host genome, because the VSV genomes are encapsidated tightly by viral protein and the viral life cycle is restricted to the cytoplasm; (3) Multivalent vaccines are realistic as up to six foreign genes at about 4.5kb in size can be inserted and expressed to high levels by the VSV vector; (4) The recombinant VSV carrying foreign genes is able to grow in many cell lines robustly and the VSV vectored vaccine may not require adjuvants for the expression of high levels of antigen; (5) The transcription level of foreign genes can be control by inserting them at different positions in the genome because of the 3' to 5' gradient of expression as mentioned previously; (6) VSV vectored vaccines have been very effective when administered by the intranasal, intramuscular, intradermal, or oral routes; (7) VSV can be attenuated by a number of approaches including gene rearrangement (Wertz et al., 1998), M gene mutation (Ahmed et al., 2008), G protein cytoplasmic tail truncations (Fang et al., 2012), G protein deletions (Publicover et al., 2005; Schnell et al., 1997); (8) VSV is considered safe to

humans and has been extensively used as vaccine vectors; (9) The human population does not have pre-existing immunity to VSV because they rarely come into contact with VSV, so the virus would be able to replicate efficiently and express the target vaccine antigens at high levels.

1.19 Introduction to HSP70

Heat shock proteins (HSPs) are a family of intracellular proteins that are induced and up-regulated when cells are under stress. These proteins were originally termed HSPs because upon initial discovery they were found to be up-regulated in cells during hyperthermic stress to prevent protein denaturation. HSPs also contribute to maintaining cellular integrity and viability by assisting in protein folding and trafficking functioning as a chaperon, thus preventing the exposure of the hydrophobic domains of the proteins that would cause them to become insoluble and lead to aggregation. HSPs can be classified into either stress-inducible or constitutive families. The HSP70 family is comprised of highly stress-inducible 70-kDa isoforms of HSPs, and is one of the best-characterized HSP families. The HSP70 family consists of four major types of proteins: Hsc70, the constitutively expressed chaperon protein; Hsp70, the major stress-inducible protein; Bip or Grp78, a protein localized in the endoplasmic reticulum (ER) lumen; and mtHsp70, a mitochondrial Hsp70. HSP 70 protein binding is ATP-dependent. When bound to ATP, HSP70 opens its peptide binding pocket and can associate or dissociate with ligands rapidly. When ATP is hydrolyzed into ADP, the pocket closes and locks the

ligand in the binding site. This interchange of ATP and ADP facilitates ligand binding-release cycles by HSP70.

1.20 Function of HSP70 in viral life cycles

HSP70 is involved in all stages of the viral life cycle. A typical cellular response to many viral infections is an increase in the HSP70 expression. In addition, HSP70 is found associated within virion particles of many NNS RNA viruses, including rabies virus, VSV, Influenza A (Sagara and Kawai, 1992), and HIV (Gurer et al., 2002), suggesting that HSP70 plays an important role during life cycles of these viruses. HSP70 has also been found to participate in viral entry into host cells. Hsc70 assists attachment of rotavirus to the host cell surface and facilitates the uptake of virus by the endosomes (Arias et al., 2002). The interaction of BiP, an HSP 70 homolog, with Coxsackievirus A9 is required for viral attachment and entry (Triantafilou et al., 2002).

HSP70 also participates in viral uncoating and genome release. The viral genome is packaged and condensed within its capsid proteins to form the nucleocapsid structure, which serves to protect the genome from the host immune defenses. The partial unwinding of the nucleocapsid coat is required to release the viral genome and allow for the polymerase to initiate viral transcription and replications, and facilitate viral protein translation by cellular ribosomes. HSP70 is found attached to the adenovirus hexon protein, penton protein, and fiber structure after the virions are released from endocytic vesicles into the cytoplasm. The DNA genome of adenovirus is transferred into the

nucleus through nuclear pores in a HSP70-dependent manner, allowing for viral DNA replication (Saphire et al., 2000).

HSP70 chaperon machinery is essential for viral replication and gene expression. HSP70 enhances the replication of the DNA genome of human papillomavirus-11 (Lin et al., 2002; Liu et al., 1998), simian virus 40 (Wright et al., 2009), and herpes simplex virus (Burch and Weller, 2004). Measles virus (MV) and canine distemper virus (CDV) are both single-stranded negative-sense RNA viruses with genomes encapsidated by nucleocapsid (N) protein. The interaction of HSP70 and N protein enhances viral replication by facilitating the successive movement of polymerase along nucleocapsid-RNA genome templates (Oglesbee et al., 1996). It has been postulated that HSP70 assists in viral gene expression within host cells. It has been demonstrated that the transcription and viral protein expression of CDV is enhanced by HSP70 in an unknown mechanism. The transcription of HIV has been shown to be inhibited by pharmacological inactivation of the HSP70-HSP90 chaperons, indicating that these proteins serve an important function in HIV transcription (O'Keefe et al., 2000).

HSP70 has also been shown to regulate the correct folding and maturation of viral proteins. In the ER, the resident HSP70, Bip, is essential for the proper folding of the envelope proteins of VSV (de Silva et al., 1990; Hammond and Helenius, 1994), Sindbis virus (Carleton and Brown, 1996), influenza A virus (Singh et al., 1990), and HIV (Earl

et al., 1991). By binding the viral proteins tightly, Bip prevents immature protein glycosylation, disulfide bond generation, and misfolding.

1.21 HSP70 as a vaccine adjuvant

HSP70 can be used as a vaccine adjuvant because it potentially enhances both innate and adaptive immunity (Millar et al., 2003; Srivastava, 2002; Vabulas et al., 2002). HSP70 activates dendritic cells through toll-like receptors (TLR), activates natural killer cells, and increases presentation of antigens to effector cells, and enhances T-cell and humoral immune responses against their associated antigens (Asea et al., 2002; Multhoff, 2002). Cell surface HSP70 is capable of recruiting Natural Killer (NK) cells to lyse the infected cells, which is an innate immune response (Multhoff, 2002; Oglesbee et al., 2002). Upon cell necrosis, HSP70-viral protein complex is released and binds to antigen-presenting cells (APCs). In this process, HSP70 functions as an adjuvant and stimulates APC maturation, cytokine secretion, and activation of cytotoxic T cells (CTL), which is a crucial component of adaptive immunity (Oglesbee et al., 2002; Todryk et al., 2003). It also has been proposed that HSP-chaperoned peptides enter APCs through specific receptors, such as TLRs, scavenger receptors (LOX-1) and/or CD91, and prime T cells by increasing antigen display by major histocompatibility complex (MHC) class I and II molecules (de Jong et al., 2009). HSPs also induce maturation of DCs and secretion of the proinflammatory cytokines interleukin (IL)-12 and tumor necrosis factor (TNF)- α , and chemokines (Newport, 1991; Suzue and Young, 1996). The roles of HSP70 in priming multiple host defense pathways are being exploited in vaccine development for

cancer and infectious diseases. HSP70 has been shown to be a strong adjuvant for a number of viral vaccines including porcine reproductive and respiratory syndrome virus (PRRSV) (Li et al., 2009a), Japanese encephalitis (JE) virus (Fei-fei et al., 2008; Ge et al., 2007), Hantaan virus (Li et al., 2008a), respiratory syncytial virus (RSV) (Zeng et al., 2008), measles virus (MV) (Oglesbee et al., 2002), and canine distemper virus (CDV) (Oglesbee et al., 1996).

The role of HSP70 in immunity to MV is best characterized among all the single-stranded negative-sense RNA viruses. HSP70 may involve in the facilitating of MV replication in host cells and the limitation of viral replication by innate and adaptive immunity (Srivastava, 2002). The RNA genome of MV is packaged by nucleocapsid (N) protein, forming a stable nucleocapsid-RNA complex. HSP70 enhances MV transcription and genome replication by binding to the C-terminus of MV N protein, which is the polymerase binding site (Zhang et al., 2005). An in vitro study has shown that HSP70 forms stable complexes with N protein in MV infected cells (Oglesbee et al., 1990). The viral gene expression and cytopathic effect of MV increases as the levels of HSP70 elevates in the cytoplasm, and decreases as a result of HSP70 reduction (Carsillo et al., 2006b; Vasconcelos et al., 1998). It has been proposed that HSP70 facilitates the progression of the polymerase along template by altering the interaction between the polymerase and the genome (Bourhis et al., 2006). The virulence of MV in mice is affected by the mouse immune system. MV susceptible mice have deficiencies in their antiviral response, so they are receptive to MV infection. MV resistant mice have robust

antiviral immunity, so they are resistant to MV infection. In vivo studies have shown that constitutive human HSP70 expression in MV susceptible neonatal mice enhances MV virulence (Carsillo et al., 2006a). MV caused higher mortality, increased brain viral RNA burden, viral protein expression, and cytopathic effect, in the susceptible mice receiving human HSP70. However, HSP70 also boosts both innate and adaptive immunity after virus infection. Compared to non-transgenic mice, constitutive expression of HSP70 in MV resistant mice increased the survival rate from 65% to 100% (Carsillo et al., 2009). It has been proposed that HSP70 enhances the innate immune response against MV through Toll-like receptor (TLR) 2 and 4 signaling pathways (Vabulas et al., 2002). The excess extracellular HSP70 may act as a signal and interact with TLRs on macrophages to signal antigen presentation, type I IFN production, and release of proinflammatory cytokines. The mechanism of viral clearance after MV infection can be summarized as follows: HSP70 increases viral replication and virulence in the initially infected cells, leading to the release of HSP70, which in turn activates macrophages through TLR2 and TLR4. The activated macrophages signal IFN- β expression and increase viral antigen presentation to T cells to activate adaptive immunity. Both extracellular HSP70 and HSP70-viral protein complex released from infected cells can activate macrophages. In this process, HSP70 functions as an adjuvant to enhance antiviral innate and adaptive immunity (Oglesbee and Niewiesk, 2011). Based on the elucidation of the mechanism of HSP70 to activate the immune system post viral infection, HSP70 is proposed to be a potential adjuvant for viral vectored vaccines.

Chapter 2 : Vesicular stomatitis virus as a vector to deliver human norovirus virus-like particles: a new vaccine candidate against an important non-cultivable virus

2.1 Abstract

Human norovirus (NoV) is a major causative agent of foodborne gastroenteritis worldwide. Currently, there are no vaccines or effective therapeutic interventions for this virus. Development of an attenuated vaccine for human NoV has been hampered by the inability to grow the virus in cell culture. Thus, a vector-based vaccine may be ideal. In this study, we constructed a recombinant vesicular stomatitis virus (rVSV-VP1) expressing VP1, the major capsid protein of human NoV. Expression of the capsid protein by VSV resulted in the formation of human NoV virus-like particles (VLPs) that are morphologically and antigenically identical to native virions. Recombinant rVSV-VP1 was attenuated in cultured mammalian cells as well as in mice. Mice inoculated with a single dose of rVSV-VP1 through intranasal and oral routes stimulated a significantly stronger humoral and cellular immune response compared to baculovirus-expressed VLP vaccination. Moreover, we demonstrated that mice inoculated with rVSV-VP1 triggered a

comparable level of fecal and vaginal IgA antibody. Taken together, the VSV recombinant system not only provides a new approach to generate human NoV VLPs in vitro, but also a new avenue for the development of vectored vaccines against norovirus and other non-cultivable viruses.

2.2 Introduction

Human norovirus (NoV), formerly called Norwalk-like virus, was initially isolated in the outbreak of gastroenteritis in an elementary school in Norwalk, Ohio, in 1968 (Kapikian et al., 1972). Human NoV, a member of the *Caliciviridae* family, is a major causative agent of foodborne gastroenteritis in both developed and developing countries. It has been estimated that over 90% of outbreaks of acute nonbacterial gastroenteritis are caused by noroviruses (Estes et al., 2000; Estes et al., 2006; Koopmans, 2008; Mead et al., 1999). Human NoV are transmitted primarily through the fecal-oral route, either by direct person-to-person contact or by fecally contaminated food or water. Human NoV is highly contagious, and only a few virus particles are thought to be sufficient to cause an infection (Donaldson et al., 2008; Estes et al., 2006; Koopmans, 2008). Outbreaks frequently occur in restaurants, hotels, daycare centers, schools, nursing homes, cruise ships, swimming pools, hospitals, and military installations (Estes et al., 2000; Estes et al., 2006; Harris et al., 2008; Koopmans, 2008; Mead et al., 1999). For these reasons, human NoV and other Caliciviruses have been classified as NIAID Category B priority bio-defense pathogens. Despite the significant economic impact and high morbidity caused by human NoV, no vaccines or anti-viral drugs are currently available for

this virus. This is due in major part to the lack of a cell culture system and an animal model for human NoV (Duizer et al., 2004b; Estes et al., 2000).

Human NoV is a non-enveloped, positive-sense RNA virus. The genome of human NoV is 7.3-7.7 kb in length and encodes three open reading frames (ORFs) (Jiang et al., 1990). ORF1 encodes a polyprotein that is cleaved to produce 6 nonstructural proteins, including the RNA-dependent RNA polymerase (RdRp) (Bertolotti-Ciarlet et al., 2003; Jiang et al., 1990). ORF2 encodes the major capsid protein (VP1) that contains the antigenic and receptor binding sites (Bertolotti-Ciarlet et al., 2003; Chen et al., 2006; Jiang et al., 1990; Jiang et al., 1992; Tan et al., 2009; Tan et al., 2004) and plays an essential role in viral attachment and entry (Tan et al., 2009; Tan et al., 2004; White et al., 1996). ORF3 encodes a minor capsid protein (VP2) that may play a role in stabilizing virus particles (Bertolotti-Ciarlet et al., 2003). It is known that the expression of VP1 alone in cell culture yields self-assembled virus-like particles (VLPs) that are structurally and antigenically similar to native virions (Chen et al., 2006; Jiang et al., 1992; Prasad and Hardy, 1999). Consequently, most human NoV vaccine studies have focused on VLPs. To date, human NoV VLPs have been expressed in *E. coli* (Tan et al., 2004), yeast (Xia et al., 2007), insect cells (Ball et al., 1998; Bertolotti-Ciarlet et al., 2002; Hardy et al., 1995; Jiang et al., 1992), mammalian cell lines (Taube et al., 2005) and plants (such as tobacco and potatoes) (Xia et al., 2007). Immunization of mice with VLPs orally or intranasally induced variable humoral, mucosal, and cellular immunities (Ball et al., 1998; Estes et al., 2000; Guerrero et al., 2001; Kitamoto et al., 2002; Xia et al., 2007). It was reported that human volunteers who received 250-2000 μg of VLPs developed significant

increases in IgA anti-VLP antibody-secreting cells and 30-40% of volunteers developed mucosal anti-VLP IgA (Tacket et al., 2003). Although these studies are very promising, there are several limitations to the development in vitro-expressed VLPs into a vaccine candidate. Preparation of VLPs in vitro is time consuming and expensive. Immunization usually requires high dosage of VLPs (usually more than 100 µg) and multiple booster immunizations (Estes et al., 2000; Souza et al., 2007b). The efficacy of VLP-based vaccines relies on the addition of mucosal adjuvants such as cholera toxin (CT) and *E. coli* toxin (LT), which may have side effects such as neurotoxicity and induction of immune tolerance (Clements et al., 1988; Petrovsky and Aguilar, 2004). Also, the duration of the antigen stimulation may be limited because VLPs are actually proteins, a non-replicating immunogen.

Generally, a live attenuated virus vaccine stimulates strong systemic immunity and provides durable protection because replication in vivo results in high level intracellular synthesis of the full complement of viral antigens over a prolonged period. However, such a vaccine is not realistic for viruses that cannot be grown in cell culture. Given this limitation, the virus cannot be attenuated, and even if attenuated strains were available, they could not be mass produced. In this situation, a vectored vaccine may be ideal to overcome this obstacle. Vesicular stomatitis virus (VSV) has been shown to be an excellent vector to deliver foreign antigens (Lichty et al., 2004; Whelan et al., 2004). VSV is a non-segmented negative-sense (NNS) RNA virus that belongs to virus family *Rhabdoviridae*. Recombinant VSV can be recovered entirely from an infectious cDNA clone by a reverse genetics system (Lawson et al., 1995; Whelan et al., 1995). With this technique, an exogenous gene can be inserted into

the VSV genome and recombinant VSV expressing this antigen can be recovered. The exogenous antigen is expressed continuously in vivo once the recombinant viruses are inoculated into animals, and thus trigger specific immune responses. To date, VSV has been successfully examined as a vaccine candidate for a number of pathogens including human immunodeficiency virus (HIV) (Haglund et al., 2002; Johnson et al., 1997; Rose et al., 2001; Tan et al., 2005), severe acute respiratory syndrome (SARS) (Faber et al., 2005; Kapadia et al., 2005), hepatitis C virus (Buonocore et al., 2002; Ezelle et al., 2002), influenza virus (Roberts et al., 1999b; Roberts et al., 1998), papillomavirus (Reuter et al., 2002), human respiratory syncytial virus (Kahn et al., 2001), poxvirus (Braxton et al., 2010), arenavirus (Garbutt et al., 2004a), Ebola virus and Marburg virus (Geisbert et al., 2008a; Jones et al., 2005). These studies have shown that VSV-based vaccines triggered strong immunity in animal models even after a single immunizing dose. Particularly, the VSV-based HIV vaccine has been applied for clinical study through HIV Vaccine Design and Development Teams (HVDDT) program at NIAID in partnership with Wyeth Pharmaceuticals (Spearman, 2003). However, the exploration of VSV as a vector to deliver vaccines against noncultivable viruses has not been reported.

In this study, we have successfully recovered a recombinant VSV expressing human NoV capsid protein (rVSV-VP1) which was attenuated in cell culture. Infection of mammalian cells with recombinant rVSV-VP1 resulted in high level production of human NoV VLPs. Importantly, we further demonstrated that rVSV-VP1 was attenuated in mice and elicited a high level of human NoV specific humoral, cellular, and mucosal immune responses

in a mouse model. Thus, the VSV recombinant system not only provided a new approach to generate human NoV VLPs, but also resulted in a novel live vectored vaccine candidate for human NoV, and perhaps for other non-cultivable foodborne viruses as well.

2.3 Materials and methods

2.3.1 Plasmid construction.

Plasmids encoding VSV N (pN), P (pP), and L (pL) genes; and an infectious cDNA clone of the viral genome, pVSV1(+), were generous gifts from Dr. Gail Wertz (61). Plasmid pVSV1(+) GxxL, which contains *Sma* I and *Xho* I at the G and L gene junction, was kindly provided by Dr. Sean Whelan. The capsid VP1 gene of human NoV genogroup II.4 strain HS66 (kindly provided by Dr. Linda Saif) was amplified by high fidelity PCR with the upstream and downstream primers containing VSV gene start and gene end sequences. The resulting DNA fragment was digested with *Sma* I and *Xho* I, and cloned into pVSV(+)-GxxL at the same sites. The resulting plasmid was designated as pVSV1(+)-VP1, in which human NoV VP1 gene was inserted into G and L gene junction. The firefly luciferase gene was amplified from pGL2 Luciferase Reporter Vector (Promega, Madison, WI) by PCR and cloned into pVSV1(+) at gene junction between leader and N, resulted in construction of pVSV1(+)-Luc. The human NoV VP1 gene was also cloned into a pFastBac-Dual expression vector (Invitrogen, Carlsbad, CA) at *Sma* I and *Xho* I sites under the control of the p10 promoter, which resulted in construction of pFastBac-Dual-VP1. All constructs were confirmed by sequencing.

2.3.2 Recovery and purification of recombinant VSV.

Recovery of recombinant VSV from the infectious clone was carried out as described previously (61). Briefly, recombinant VSV was recovered by co-transfection of pVSV1(+)-VP1, pN, pP, and pL into BSRT7 cells infected with a recombinant vaccinia virus (vTF7-3) expressing T7 RNA polymerase. At 96 h post-transfection, cell culture fluids were collected, filtered through 0.2 μ M filter, and the recombinant virus was further amplified in BSRT7 cells. Subsequently, the viruses were plaque purified as described previously (Li et al., 2006; Li et al., 2005). Individual plaques were isolated, and seed stocks were amplified in BSRT7 cells. Viral titer was determined by plaque assay performed in Vero cells.

2.3.3 Single-cycle growth curves.

Confluent BSRT-7 cells were infected with individual viruses at a multiplicity of infection (MOI) of 10. After 1 h of absorption, the inoculum was removed, the cells were washed twice with DMEM, fresh DMEM (supplemented with 2% fetal bovine serum) was added, and the infected cells were incubated at 37°C. Aliquots of the cell culture fluid were removed at the indicated intervals, and virus titers were determined by plaque assay in Vero cells.

2.3.4 Analysis of protein synthesis.

Confluent BSRT7 cells were infected with either rVSV or rVSV-VP1 as described above. At the indicated time post-infection, cells were washed with methionine- and cysteine-

free (M^-C^-) media and incubated with fresh M^-C^- medium supplemented with actinomycin D (15 μ g/ml). After a 1h incubation, the medium was replaced with M^-C^- medium supplemented with EasyTag [35 S]-Express (4 μ Ci/ml) (Perkin-Elmer, Wellesley, MA). After a 4h incubation, cytoplasmic extracts were prepared and analyzed by sodium dodecyl sulfate-polyacrylamide gel electrophoresis (SDS-PAGE) as described previously (Li et al., 2006; Li et al., 2005). Labeled proteins were detected either by autoradiography or by using a phosphorimager.

2.3.5 Reverse transcription polymerase chain reaction (RT-PCR).

Viral RNA was extracted from either rVSV or rVSV-VP1 using an RNeasy Mini Kit (Qiagen, Valencia, CA) according to the manufacturer's instructions. Two primers (5'-CGAGTTGGTATTTATCTTTGC-3' and 5'-GTACGTCATGCGCTCATCG-3') were designed to target VSV G gene at position 4524 and L gene at position 4831 (numbering refers to the complete VSV Indiana genome sequence), respectively. RT-PCR was performed using a One Step RT-PCR kit (Qiagen). The amplified products were analyzed on 1% agarose gel electrophoresis.

2.3.6 Western blotting.

BSRT7 cells were infected either with rVSV or VSV-VP1 as described above. At the indicated time post-infection, cell culture medium was harvested and clarified at 3,000 rpm for 15 min, and further concentrated at 30,000 rpm for 1.5h. In the mean time, cells were lysed in lysis buffer containing 5% β -mercaptoethanol, 0.01% NP-40, and 2%

sodium dodecyl sulfate (SDS). Proteins were separated by 12% SDS-PAGE and transferred to a Hybond ECL nitrocellulose membrane (Amersham) in a Mini Trans-Blot electrophoretic transfer cell (Bio-Rad). The blot was probed with guinea pig anti-human NoV VP1 antiserum (a generous gift from Dr. Xi Jiang) at a dilution of 1:5000, followed by horseradish peroxidase-conjugated goat anti-guinea pig IgG secondary antibody (Santa Cruz) at a dilution of 1:20,000. The blot was developed with SuperSignal West Pico Chemiluminescent Substrate (Thermo Scientific) and exposed to Kodak BioMax MR film (Kodak).

2.3.7 Production and purification of VLPs by baculovirus expression system.

Baculovirus expression plasmid encoding the human NoV VP1 gene (pFastBac-VP1) was transformed into DH10Bac. Baculovirus expressing the VP1 protein was generated by transfection of bacmids into *Spodoptera frugiperda* (Sf9) cells with a Cell-fectin Transfection kit (Invitrogen), according to the instructions of the manufacturer. Purification of VLPs from insect cells was described as previously with some minor modifications (Ball et al., 1998; Jiang et al., 1992; Souza et al., 2007b). Sf9 cells were infected with baculovirus at an MOI of 10, the infected Sf9 cells and cell culture supernatants were harvested at 6 days post-inoculation. The VLPs were purified from cell culture supernatants and cell lysates by ultracentrifugation through a 40% (w/v) sucrose cushion, followed by CsCl isopycnic gradient (0.39 g/cm³) ultracentrifugation. Purified VLPs were analyzed by SDS-PAGE, Western blotting, and electron microscope (EM).

The protein concentration of the VLPs was measured by Bradford reagent (Sigma Chemical Co., St. Louis, MO).

2.3.8 Production and purification of VLPs by VSV vector.

Recombinant rVSV-VP1 was inoculated into 10 confluent T150 flasks of BSRT7 cells at a MOI of 0.01 in a volume of 2 ml of Dulbecco modified Eagle medium (DMEM). At 1 h post-absorption, 15 ml of DMEM supplemented with 2% fetal bovine serum was added to the cultures, and infected cells were incubated at 37°C for 24 to 48 h. Cell culture fluids were harvested when extensive cytopathic effect (CPE) was observed. Cell culture fluids were clarified by centrifugation at 3,000 rpm for 30 min. Virus was concentrated through 40% (w/v) sucrose cushion by centrifugation at 30,000 rpm for 2 h at 4°C in a Ty 50.2 rotor (Beckman). The pellet was resuspended in TNC buffer (0.05 M Tris-HCl, 0.15 M NaCl, 15mM CaCl₂ [pH 6.5]) and further purified through CsCl isopycnic gradient by centrifugation at 35,000 rpm for 18h at 4°C in a SW55 rotor (Beckman). The final pellet was resuspended in 0.3 ml of TNC buffer. Purified VLPs were analyzed by SDS-PAGE, Western blotting and EM. The protein concentration of the VLPs was measured by Bradford reagent (Sigma Chemical Co., St. Louis, MO).

2.3.9 Transmission electron microscopy.

Negative staining electron microscopy of purified VLPs was performed as described previously (Kapikian et al., 1972). Briefly, 20 µl of VLP suspension was fixed in copper grids (Electron Microscopy Sciences, Inc.) and negatively stained with 1% ammonium

molybdate. Virus particles were visualized by FEI Tecnai G2 Spirit Transmission Electron Microscope (TEM) at 80 kV at the Microscopy and Imaging Facility at The Ohio State University. Images were captured on a MegaView III side-mounted CCD camera (Soft Imaging System, Lakewood, CO) and figures were processed using Adobe Photoshop software (Adobe Systems, San Jose, CA).

2.3.10 Animal experiment.

Twenty five four-week-old specific-pathogen-free female BALB/c mice (Charles River laboratories, Wilmington, MA) were randomly divided into five groups (5 mice per group). Mice in groups 1-3 were inoculated with 10^6 PFU of rVSV, rVSV expressing luciferase (rVSV-Luc), and rVSV-VP1, respectively. Mice in group 4 were inoculated with 100 μ g of VLPs (purified from baculovirus expression system). Mice in group 5 were inoculated with 200 μ l of DMEM and serve as unimmunized control. All mice were inoculated through the combination of intranasal and oral routes. Half of the antigens were inoculated intranasally, and the other half was administrated orally. After inoculation, the animals were evaluated on a daily basis for mortality, weight loss, and the presence of any symptoms of VSV infection. Blood samples were collected from each mouse weekly by facial vein bleed, and serums were isolated for IgG antibody detection. Fecal and vaginal homogenate samples were isolated weekly for the detection of norovirus specific IgA. At 5 weeks post-inoculation, all mice were sacrificed. The spleens were isolated from each mouse and mononuclear cells (MNC) suspensions were prepared for a T cell proliferation assay.

2.3.11 T cell proliferation assay.

96-well plates were coated with 50 μ l of highly purified HoNoV VLPs (10 μ g/ml) in 200 mM NaCO₃ buffer (pH 9.6) at 4°C overnight. After homogenization, spleen cells were washed twice with PBS and plated in triplicate at 5×10^5 cells/well in a 96-well-plate in RPMI 1640 medium with 2 % naive mouse serum . After 48 h incubation at 37 °C, 0.5 μ Ci of [³H] thymidine was added to each well, and 16 h later cells were harvested onto glass filters and counted with a Betaplate Counter (Wallac, Turku, Finland). The stimulation index (SI) was calculated as the mean of the following ratio: proliferation (cpm) of human NoV VLP-stimulated cells/proliferation of cells in medium.

2.3.12 Serum IgG ELISA.

96-well plates were coated with 50 μ l of highly purified HoNoV VLPs (7.5 μ g/ml) in 50 mM NaCO₃ buffer (pH 9.6) at 4°C overnight. Individual serum samples were tested for human NoV-specific IgG on VLP-coated plates. Briefly, Serum samples were two-fold serially diluted and added to VLP-coated wells. After incubation at room temperature for 1 h, the plates were washed five times with PBS-Tween (0.05%), followed by incubation with 50 μ l of goat anti-mouse IgG horseradish peroxidase-conjugated secondary antibodies (Sigma) at a dilution of 1:80,000 for 1 h. Plates were washed and developed with 75 μ l of 3, 3',5, 5'-tetramethylbenzidine (TMB), and the optical density (OD) at 450 nm was determined using an ELISA plate reader. End point titer values were determined

as the reciprocal of the highest dilution that had an absorbance value greater than background level (DMEM control).

2.3.13 Fecal IgA ELISA.

For each stool sample, human NoV-specific and total fecal IgA were determined as described previously. Fecal pellets were diluted 1:2 (w/v) in PBS containing 0.1% Tween and Complete EDTA-free proteinase inhibitor cocktail tablet (Roche). Samples were vortexed twice for 30 s, and clarified twice by centrifugation at $10,000 \times g$ for 10 min. 96-well plates were coated with 50 μ l of highly purified human NoV VLPs (1 μ g/ml) in 50 mM NaCO₃ buffer (pH 9.6) at 4°C overnight for detection of human NoV-specific IgA, while total fecal IgA was determined by capturing all fecal extract IgA molecules with 1 μ g/ml sheep anti-mouse IgA. To block nonspecific protein binding, the plates were incubated for 4 h at 4°C with 10% (w/v) dry milk in PBS (10% BLOTTO). The level of IgA was calculated from a standard curve that was determined by the absorbance values of the mouse IgA standard (Sigma). Human NoV-specific IgA levels were expressed in nanograms per milliliter, and each corresponding total IgA level was expressed in micrograms per milliliter.

2.3.14 Vaginal Human NoV-specific IgA ELISA.

96-well plates were coated with human NoV VLPs in selected columns as described above. After an overnight blocking at 4°C with 5% BLOTTO, 75 μ l of an undiluted vaginal sample per well or a 1:5 dilution of the sample was added, and the sample was serially diluted twofold down the plate and incubated for 2 h at 37°C. The remaining

protocol was identical as described above for the human NoV-specific fecal IgA ELISA or the serum IgG ELISA.

2.3.15 Quantitative and statistical analysis.

Quantitative analysis was performed by either densitometric scanning of autoradiographs or by using a phosphorimager (GE Healthcare, Typhoon) and ImageQuant TL software (GE Healthcare, Piscataway, NJ). Each experiment was performed three to six times. Statistical analysis was performed by a paired Student's *t* test. A value of $p < 0.05$ was considered statistically significant.

2.4 Results

2.4.1 Recovery of recombinant VSV expressing human NoV capsid protein.

The feasibility of VLP delivery using VSV as a vector has not been tested although many other antigens have been successfully expressed by VSV. Since the abundance of gene expression decreases with distance from the 3' end to 5' end of VSV genome (Iverson and Rose, 1981), we attempted to recover recombinant VSV harboring the VP1 gene in the 3'-proximal position in the genome. Unfortunately, after multiple attempts, we failed to recover recombinant viruses with the VP1 gene inserted in any of the following gene junctions, leader-N, N-P, P-M or M-G. However, recombinant VSV expressing human NoV VP1 (designated as rVSV-VP1) was successfully recovered when the VP1 gene was inserted at the G-L gene junction in the VSV genome (Fig. 2.1A). Recombinant rVSV-VP1 formed much smaller plaques as compared to rVSV (Fig. 2.1B). After 24 h of

incubation, rVSV formed plaques that were 4.3 ± 0.8 mm in diameter. However, the average plaque size for rVSV-VP1 was 1.7 ± 0.6 mm even after 48 h of incubation, suggesting that rVSV-VP1 may have a defect in viral growth. To confirm that the recovered virus indeed containing the VP1 gene, viral genomic RNA was extracted followed by RT-PCR using two primers annealing to VSV G and L genes, respectively. As shown in Fig. 2.1C, a 2.0 kb cDNA band containing the VP1 gene was amplified from genomic RNA extracted from rVSV-VP1 while a 300 bp cDNA lacking an inserted gene was amplified from rVSV. The cDNA was purified and sequenced, confirming that VP1 of human NoV was indeed inserted into the VSV genome. Using similar strategy, we also recovered rVSV expressing firefly luciferase (rVSV-Luc), in which luciferase was inserted between leader and N gene junction (data not shown).

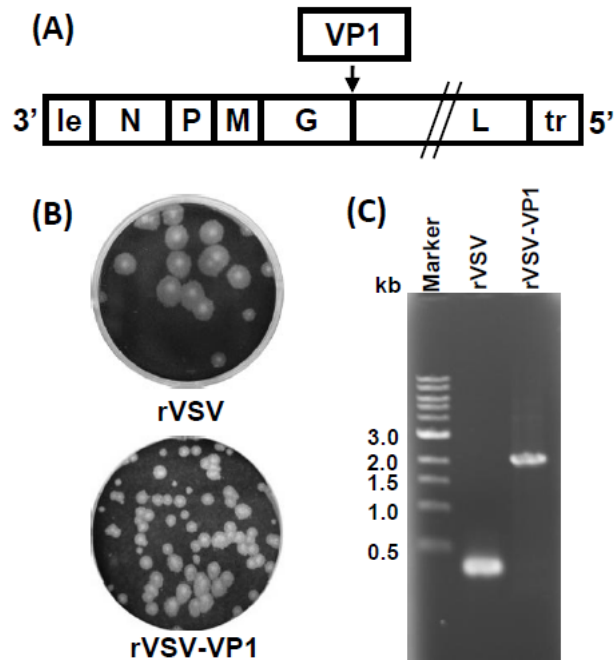


Figure 2.1. Recovery of recombinant VSV expressing human NoV VP1 (rVSV-VP1).

(A) Insertion of VP1 into the VSV genome at the gene junction between G and L. Le, VSV leader sequence; N, nucleocapsid gene; P, phosphoprotein gene; M, matrix protein gene; G, glycoprotein gene; L, large polymerase gene; Tr, VSV trailer sequence. (B) The plaque morphology of recombinant viruses is shown compared to rVSV. Plaques of rVSV-VP1 were developed after 48 h of incubation compared to rVSV, which was developed after 24 h incubation. (C) Amplification of VP1 gene from recombinant rVSV-VP1 by RT-PCR. Genomic RNA was extracted from each viruses and VP1 gene was amplified by RT-PCR using two primers annealing to G and L genes.

2.4.2 The replication of rVSV-VP1 is delayed in cell culture.

To further characterize recombinant rVSV-VP1, we monitored the kinetics of release of infectious virus by a single-step growth assay in BSRT7 cells. Briefly, BSRT7 cells were infected with each of the recombinant viruses at an MOI of 10 and viral replication was determined at time points from 0-48 h post-infection. As shown in Fig. 2.2, rVSV-VP1 had significant delay in viral replication as compared to that of rVSV. Wild-type rVSV reached peak titer (4.6×10^9 pfu/ml) at 12 h post-infection. However, rVSV-VP1 reached its peak titer of 4.0×10^9 pfu/ml at approximately 30 h post-infection. At an MOI of 10, recombinant rVSV exhibited significant cytopathic effect (CPE) by 6 h post-infection (data not shown) and cells were completely killed by 14 h post-infection. However, rVSV-VP1 first showed CPE after 12 h post-infection and most cells were killed by 36 h post-infection. These results suggested that rVSV-VP1 had delayed replication and was attenuated in cell culture.

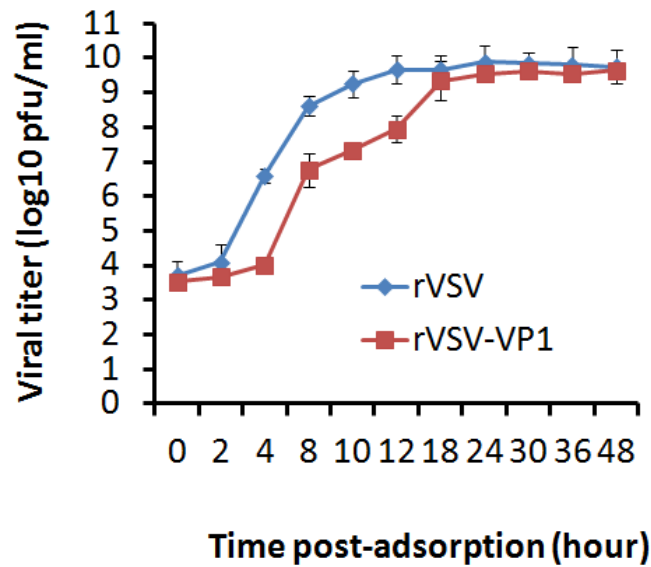


Figure 2.2. Single-step growth curve of recombinant VSV in BSRT7 cells.

Confluent BSRT7 cells were infected with individual viruses at an MOI of 10. After 1 h incubation, the inoculum was removed, the cells were washed with DMEM, and fresh medium (containing 2% fetal bovine serum) was added, followed by incubation at 37°C. Samples of supernatant were harvested at the indicated intervals over a 48-h time period, and the virus titer was determined by plaque assay. Titers are expressed as the mean ± the standard deviation of three independent single-step growth experiments.

2.4.3 High level expression of Human NoV VP1 protein by VSV vector.

To examine the expression of human NoV VP1 by VSV, we first determined protein synthesis in virus-infected cells by metabolic labeling as described in Materials and Methods. Briefly, BSRT7 cells were infected with either rVSV or rVSV-VP1 and, at the indicated time post-infection, the cells were incubated with [³⁵S] methionine-cysteine for 4 h. After incubation, cytoplasmic extracts were prepared, and total protein was analyzed by SDS-PAGE. As shown in Fig. 2.3A, rVSV synthesized five viral proteins, L, G, P, N and M. In rVSV-VP1 infected cells, an additional protein band with molecular weight of approximately 58 kDa was detected. This protein is the correct size for the human NoV capsid protein VP1. The abundance of this protein increased when cells were infected with a higher MOI of rVSV-VP1 (data not shown). Significantly less VSV proteins were synthesized from rVSV-VP1 infected cells compared to that of rVSV (Fig.2.3A, compare lane 1 and 2). Quantitative analysis of three independent experiments showed that there is approximately 25-50% as much of the VSV proteins synthesized by rVSV-VP1 relative to wt (Fig.2.3B). The combination of decreased viral plaque size, delayed single step viral replication and reduced protein synthesis suggest that rVSV-VP1 is attenuated in cell culture. To further characterize the expression of the VP1 protein, we performed a Western blot analysis using a polyclonal antibody against the VP1 protein. Briefly, BSRT7 cells were infected with rVSV, rVSV-VP1, or rVSV-Luc at an MOI of 10, and cell lysates were harvested at 8 h post-infection. The cell lysates were analyzed by SDS-PAGE, followed by Western blot. As shown in Fig.3D, a 58 kDa protein band was visualized in rVSV-VP1, but not in rVSV or rVSV-Luc lysates. For comparison, cell

culture medium was harvested at 54 h post-infection. After 30,000 rpm ultracentrifugation, the pellets were analyzed by Western blot. Interestingly, two protein bands with molecular weights of 58 and 52 kDa were detected from the supernatant by Western blot (Fig. 2.3E). If the 58 kDa protein is the native full-length VP1 protein, the 52 kDa protein must be a cleaved form of VP1 (cVP1) protein. However, in the cell lysate, the majority of VP1 remained uncleaved. This was consistent with the earlier observation that human NoV VP1 can be cleaved when expressed in mammalian and insect cells (Bertolotti-Ciarlet et al., 2002; Hardy et al., 1995). Taken together, these results demonstrated that (i) expression of VP1 by VSV resulted in two forms of VP1 protein, and (ii) the expressed VP1 protein was antigenic and reacted with anti-human NoV VP1 antibody.

We also monitored the kinetics of VP1 expression in BSRT7 cells. Briefly, BSRT7 cells were infected with rVSV-VP1 at an MOI of 10 and cell culture medium and cell lysates were harvested separately at the indicated times. The expression of VP1 was determined by Western blot. In the cell lysate, VP1 expression was detected at 4 h post-infection, gradually increased, and reached a peak at 30 h post-infection (Fig.2.4A, C). VP1 protein was secreted into cell culture medium, but was not detectable until at 24 h post-infection (Fig. 2.4B, C). A high level of VP1 protein was released to the supernatant after 24-48 h post-infection. Thus, VP1 protein was not only expressed in the cytoplasm but also released into cell culture medium.

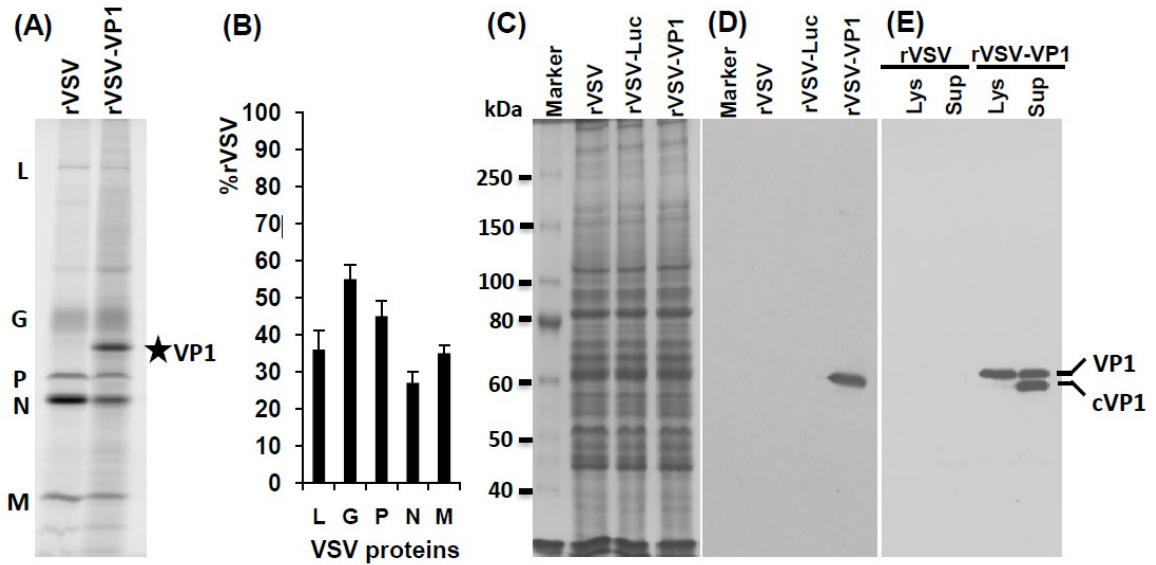


Figure 2.3. Expression of human NoV VP1 by the VSV vector.

(A) Viral protein synthesis in BSRT-7 cells. BSRT-7 cells were infected with rVSV or rVSV-VP1 at MOI of 10. Proteins were metabolically labeled by incorporation of [³⁵S]methionine-cysteine in the presence of actinomycin D. Cytoplasmic extracts were harvested at 5 h post-infection, and proteins were analyzed by SDS-PAGE and detected by using a phosphorimager. The identity of the proteins is shown on the left. (B) Quantitative analysis of VSV structural proteins between rVSV and rVSV-VP1. Data was generated using three independent experiments. For each protein the mean \pm the standard deviation was expressed as a percentage of that observed for rVSV. (C) SDS-PAGE analysis of total cell lysate from virus-infected cells. BSRT-7 cells were infected with rVSV, rVSV-VP1 or rVSV-Luc at MOI of 10, cells were lysed in 500 μ l of lysis buffer, and 10 μ l of lysate were analyzed by SDS-PAGE. (D) Analysis of VP1 expression in cell lysate by Western blot. Identical samples from

panel C were blotted with guinea pig anti-human NoV VP1 antiserum. (E) Analysis of VP1 protein in cell culture medium by Western blot. BSRT-7 cells were infected with rVSV or rVSV-VP1, cell culture medium was harvested at 54 h post-infection. After 29,000 rpm ultracentrifugation, the pellets were subjected to Western blot. Lys = cell lysate; Sup = cell culture supernatant; cVP1= cleaved VP1 protein.

(B)

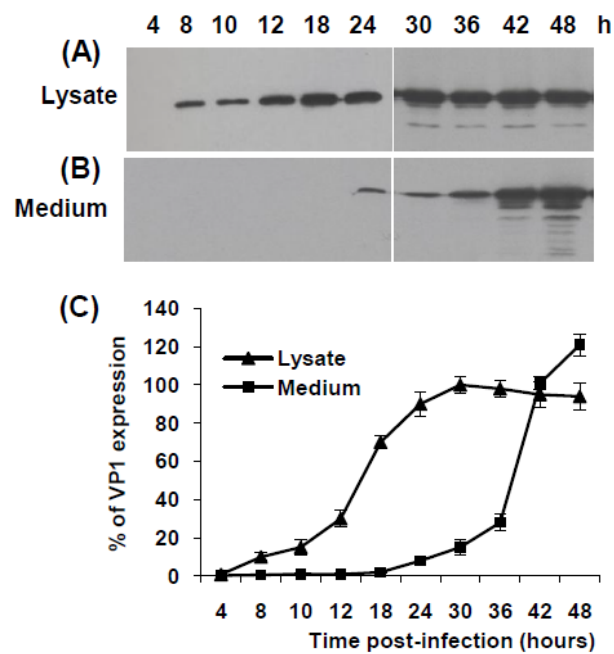


Figure 2.4. Kinetics of VP1 expression by VSV vector.

(A) Dynamics of VP1 expression in cell lysate by Western blot. BSRT-7 cells were infected with rVSV and rVSV-VP1 at an MOI of 10. Cytoplasmic extracts were harvested at indicated time points. Equal amounts of total cytoplasmic lysate were analyzed by SDS-PAGE, followed by Western blot analysis using guinea pig anti-human NoV VP1 antiserum. (B) Dynamics of VP1 expression in cell culture medium by

Western blot. Cell culture supernatants were harvested at indicated time points. VP1 proteins were pelleted from cell culture supernatants through 29,000 rpm of ultracentrifugation, and resuspended in 200 μ l of NTE. Equal amounts of suspension were subjected to Western blot. (C) Quantitative analysis of VP1 expression in cytoplasmic lysate and cell culture supernatants. Three independent experiments were used to generate the quantitative analysis shown. Data was expressed as the mean \pm the standard deviation.

2.4.4 Characterization of Human NoV VLPs expressed by VSV vector.

To determine whether expression of VP1 from VSV leads to the assembly of VLPs, BSRT7 cells were infected with rVSV-VP1 and the cell culture media were harvested at 48 h post-infection. The expressed VP1 protein was purified as described in Materials and Methods. Crude cell culture medium (unpurified) and purified VP1 proteins were subjected to negative stain EM. Human NoV VLPs purified from insect cells by baculovirus were used as a control. As shown in Fig. 2.5A, particles of two sizes (35-38 and 18-20 nm) were observed in baculovirus-expressed VLPs. In unpurified cell culture medium, two types of virus particles, VSV and human NoV VLPs, were found (Fig.2.5B). VSV is a bullet-shaped particle around 120 nm in length and 70 nm in diameter, while human NoV VLPs are small round structured particles, 38 nm in diameter. After CsCl isopycnic gradient purification, a large number of human NoV VLPs were obtained. The majority of the VLPs expressed by VSV had a diameter of approximately 38 nm although 20 nm-particles were also found (Fig. 2.5B and C).

Therefore, these results confirm that expression of VP1 protein by the VSV vector resulted in the assembly of VLPs that are structurally similar to native virions.

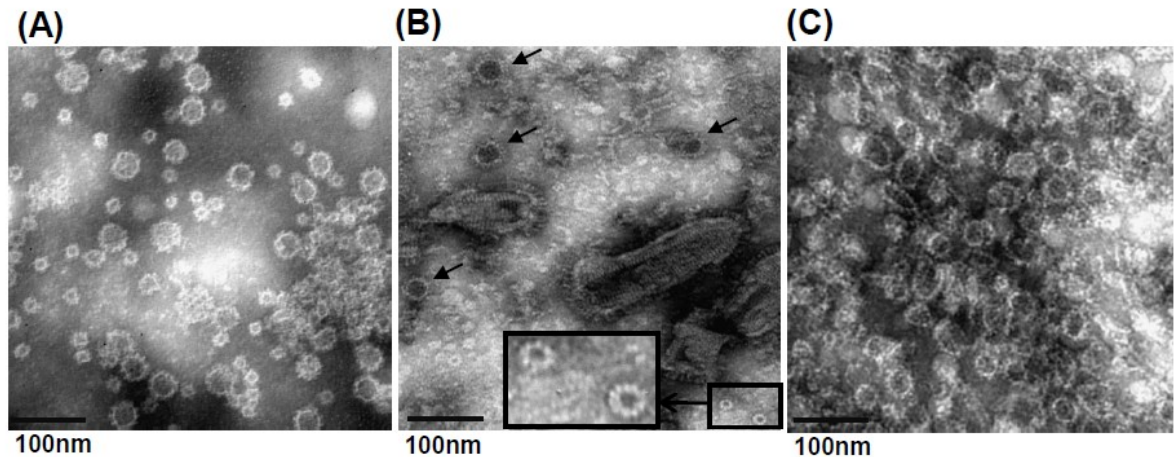


Figure 2.5. Electron microscope analysis of purified VLPs.

20 μ l of VLP suspension was added to copper grids and negatively stained with 1% ammonium molybdate. Virus-like particles were visualized by FEI Tecnai G2 Spirit Transmission Electron Microscope. (A) VLPs purified from insect cells by baculovirus infected with baculovirus expressing human NoV VLPs. (B) Cell culture supernatant. BSRT7 cells were infected with rVSV-VP1 and cell culture supernatants were harvested at 48 h post-infection. The larger VLPs with 38 nm in diameter are indicated with an arrow. The smaller, 19 nm, diameter VLPs are highlighted in a box in the lower right corner and magnified in the connected box. (C) VLPs purified from BSRT7 cells infected by rVSV-VP1.

2.4.5 Recombinant rVSV-VP1 is attenuated in a mouse model.

It has been well documented that the wild-type rVSV Indiana strain is highly virulent for mice (Ball et al., 1999b; Lichty et al., 2004). To test the safety of rVSV-VP1, mice were inoculated with 10^6 PFU of either rVSV or rVSV-VP1 through a combination of intranasal and oral routes. After inoculation, animals were evaluated daily for weight loss, and the presence of any clinical signs. Consistent with previous reports (Ball et al., 1999b), mice infected with rVSV had severe weight loss (Fig.2.6) and exhibited typical clinical signs including ataxia, hyperexcitability, tremors, circling, and paralysis. At 10 days post-inoculation, two of the five mice were dead in the rVSV group. At day 16, we euthanized the remaining three mice in the rVSV group since they were extremely sick. Mice inoculated with rVSV-VP1 also showed a significant weight loss ($P < 0.05$) during the first week post-inoculation, but started to gain weight after 10 days post-inoculation (Fig.2.6). After 3 weeks post-inoculation, there was no significant difference in weight as compared to DMEM control ($P > 0.05$). In addition, mice inoculated with rVSV-VP1 showed no significant clinical signs of VSV infection. Mice inoculated with DMEM did not have any weight loss or clinical signs. This experiment suggests that rVSV-VP1 was attenuated in mice.

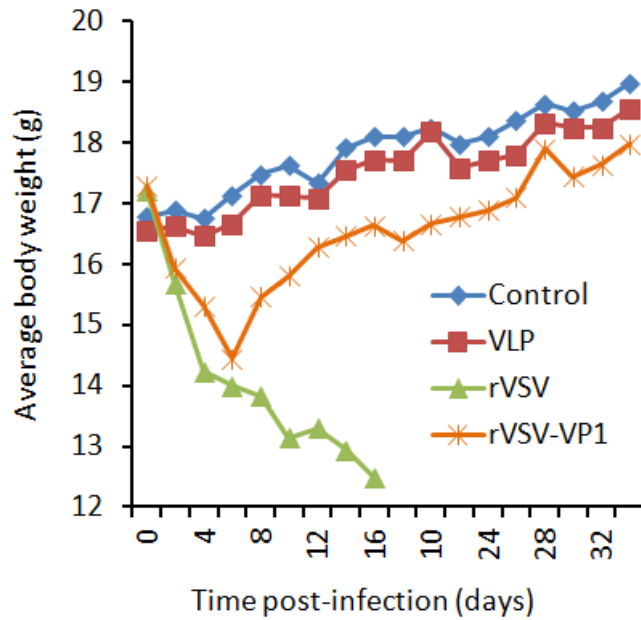


Figure 2.6. Dynamics of mouse body weight after inoculation with recombinant viruses.

Five BALB/c mice in each group were inoculated with 10^6 PFU of rVSV, 10^6 PFU of rVSV-VP1 or 100 μ g of VLPs (purified from insect cells by baculovirus) through a combination of intranasal and oral routes. Body weight for each mouse was evaluated every other day. The average body weight of five mice was shown. At day 10, two out of five mice were dead in rVSV group. The remaining three mice were euthanized at day 16 because of severe illnesses.

2.4.6 Intranasal and oral administration of rVSV-VP1 induces a strong serum IgG immune response in mice.

To evaluate whether rVSV-VP1 induces antibodies against human NoV, blood samples were isolated from each mouse and the serum IgG antibody response was determined by ELISA as described in Materials and Methods. The Geometric Mean Titers (GMT) were calculated for each group of mice and compared. Prior to inoculation, all mice were negative (titer, <10) for human NoV-specific IgG (data not shown). As shown in Fig.2.7, mice inoculated with rVSV-VP1 generated a much higher serum IgG response than the mice that received baculovirus-produced VLPs during the five week experimental period ($P < 0.05$). At one week post-inoculation, all mice inoculated with rVSV-VP1 had a high level of serum IgG with a GMT of 10,809. The IgG antibody gradually increased at week 2 post-inoculation with a GMT of 32,768 and remained at a high level through week 5. Mice inoculated with 100 μg of baculovirus-produced VLPs had a similar level of human NoV-specific IgG antibodies at week 1 post-inoculation. However, the IgG antibody in the VLP group had decreased by week 2 post-inoculation. Moreover, from weeks 2 to 5, the GMT in rVSV-VP1 group was significantly higher than that of VLP group ($P < 0.05$). As controls, mice inoculated with rVSV-Luc and DMEM lacked human NoV-specific serum IgG antibody responses during the experiment period. Thus, this experiment demonstrates that (i) a single dose inoculation of mice with recombinant rVSV-VP1 stimulated a high level of serum IgG antibody response; and, (ii) IgG antibody response induced by rVSV-VP1 was significantly stronger than that of the baculovirus-produced VLP-based vaccine candidate.

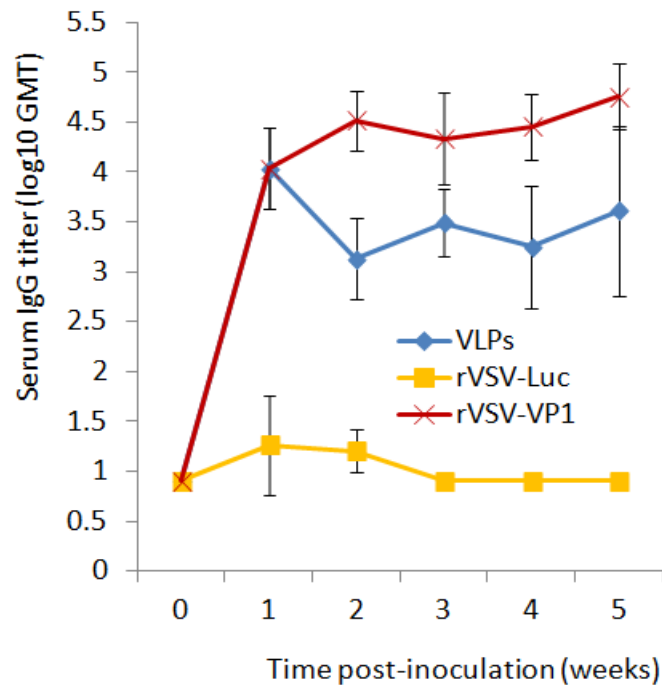


Figure 2.7. Serum IgG immune responses to human NoV vaccine.

Groups of five BALB/c mice were inoculated with 10^6 PFU of rVSV-VP1 or 10^6 PFU of rVSV-Luc or 100 μ g of VLPs through the combination of intranasal and oral routes.

Serum samples were collected weekly and analyzed by ELISA for human NoV-specific serum IgG antibody. Data was expressed by Geometric Mean Titers (GMT) of five mice.

Error bars at each time point represent the standard deviation between mice.

2.4.7 Immunization of mice with rVSV-VP1 induces a strong cellular immune response in mice.

To determine the cellular immune response of the VSV-based human NoV vaccine, spleens were isolated from each mouse at week 5 post-inoculation, and the cellular immune responses were measured by a T cell proliferation assay. As shown in Fig.2.8, mice inoculated with rVSV-VP1 stimulated a much higher human NoV-specific T cell proliferation response than that of traditional VLPs-based vaccine ($P < 0.05$). All mice in the rVSV-VP1 group had strong human NoV-specific T cell responses with an average stimulation index of 9.7. However, only 3 out of the 5 mice in the VLP group had a T cell immune response with an average stimulation index of 4.8. Mice inoculated with rVSV-Luc and DMEM had no human NoV-specific T cell immune response. Therefore, this data demonstrates that rVSV-VP1 stimulated a significantly stronger T cell immune response than that of the VLP-based vaccine candidate.

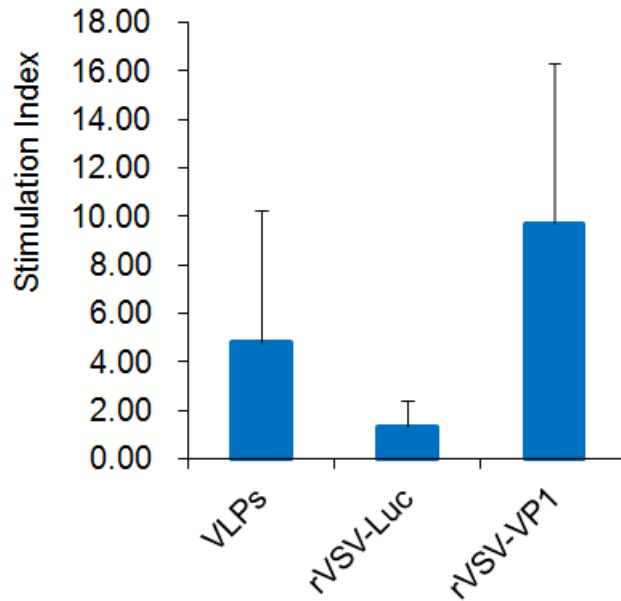


Figure 2.8. T cell proliferative responses to human NoV vaccine.

Spleen cells were harvested from all mice in each group at week 5 post-inoculation, and stimulated with human NoV VLPs. T cell proliferation was measured by [³H]thymidine incorporation. The stimulation index (SI) was calculated as the mean of the following ratio: proliferation of human NoV VLP-stimulated cells/proliferation of cells in medium in cpm. Data was expressed as the mean of five mice ± the standard deviation.

2.4.8 Immunization of mice with rVSV-VP1 induces a mucosal immune response in mice.

Norovirus causes gastroenteritis; it is likely that mucosal antibodies play an important role in protection from infection. To measure the mucosal immune response, human NoV-specific and total IgA in fecal and vaginal swab extracts were assayed by ELISA. The level of IgA response was expressed as the ratio between human NoV-specific IgA

and total IgA. Prior to inoculation, there was no human NoV-specific IgA in either fecal or vaginal samples in any mice. Fig.2.9 shows the fecal IgA antibody response from week 1 to 5. In week 1, only one and two out of five mice had an IgA response in rVSV-VP1 group and VLP group, respectively. At week 2, all mice in the VLP group developed human NoV specific IgA, while four out of five mice in rVSV-VP1 group exhibited an IgA response. At week 3, the IgA antibody started to decrease in both rVSV-VP1 and VLP groups. There was no significant difference in IgA responses between these two groups at weeks 2 and 3 ($P>0.05$). At weeks 4 and 5, the VLP group had a higher IgA antibody than that of rVSV-VP1 group. However, the number of mice that had detectable IgA in the VLP group (2-3 mice) was less than that of the rVSV-VP1 group (4-5 mice). Overall, these results demonstrated that rVSV-VP1 was able to trigger a human NoV-specific mucosal IgA immune response in the intestine. Recombinant rVSV-VP1 had a comparable level of IgA at weeks 1-3, but had a lower IgA at weeks 4 and 5 as compared to VLP group. None of mice in rVSV-Luc and DMEM groups showed human NoV-specific IgA antibody in the entire experiment period.

Using an identical approach, the vaginal IgA antibody responses were also determined. Interestingly, the ratio between human NoV-specific IgA and total IgA in vaginal sample was much higher than that of fecal samples. Thus, the level of IgA response was expressed as \log_{10} (ratio between human NoV-specific IgA and total IgA). As shown in Fig.2.10, both rVSV-VP1 and VLP groups triggered a high level of vaginal IgA antibody. At week 1 post-inoculation, all mice in the VLP group had vaginal IgA

antibody. However, four out of five mice in rVSV-VP1 group had an IgA response. In the following 4 weeks, all mice developed an IgA response in both rVSV-VP1 and VLP groups. In weeks 1-2, average IgA titer in the VLP group was higher than the rVSV-VP1 group ($P < 0.05$). In weeks 3-5, however, there was no significant difference in vaginal IgA response between these two groups ($P > 0.05$). Mice inoculated with rVSV-Luc and DMEM did not have any human NoV-specific IgA antibody in vaginal samples during the five week experiment period. Overall, these results demonstrated that mice inoculated with rVSV-VP1 and VLPs stimulated a comparable vaginal IgA antibody response. We conclude that VSV-based human NoV vaccine is capable of inducing a high level of mucosal immunity in mice, in both the intestinal and vaginal extracts.

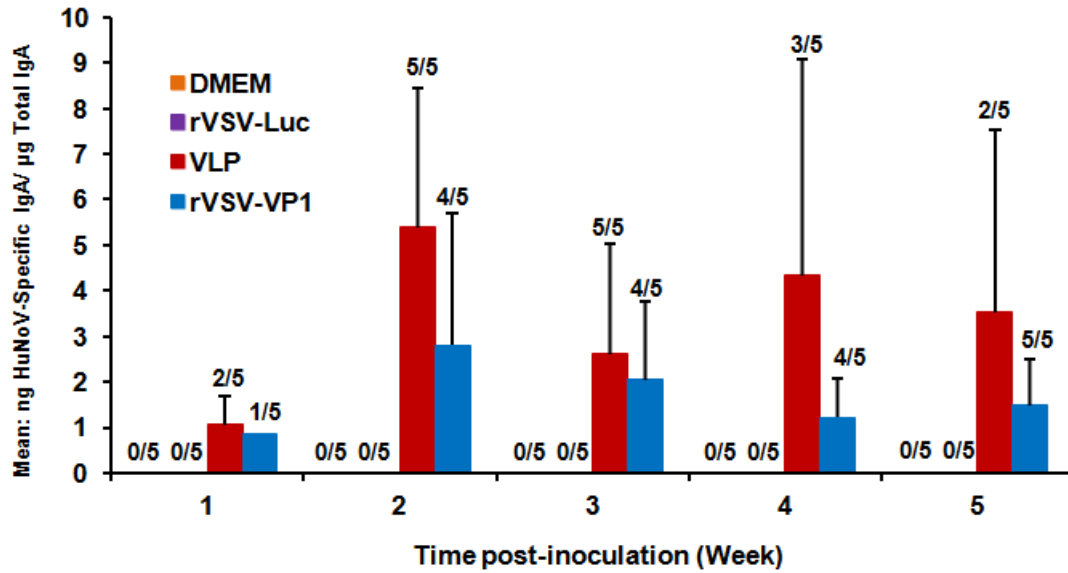


Figure 2.9. Fecal IgA responses to human NoV vaccine.

Fecal samples were collected from all mice in each group weekly. Samples were diluted in PBS, vortexed, clarified by centrifugation, and human NoV-specific and total IgA antibody were determined by ELISA. The ratio between human NoV-specific IgA and total IgA was calculated for each mouse. Data were expressed as average titer of IgA-positive mice \pm the standard deviation.

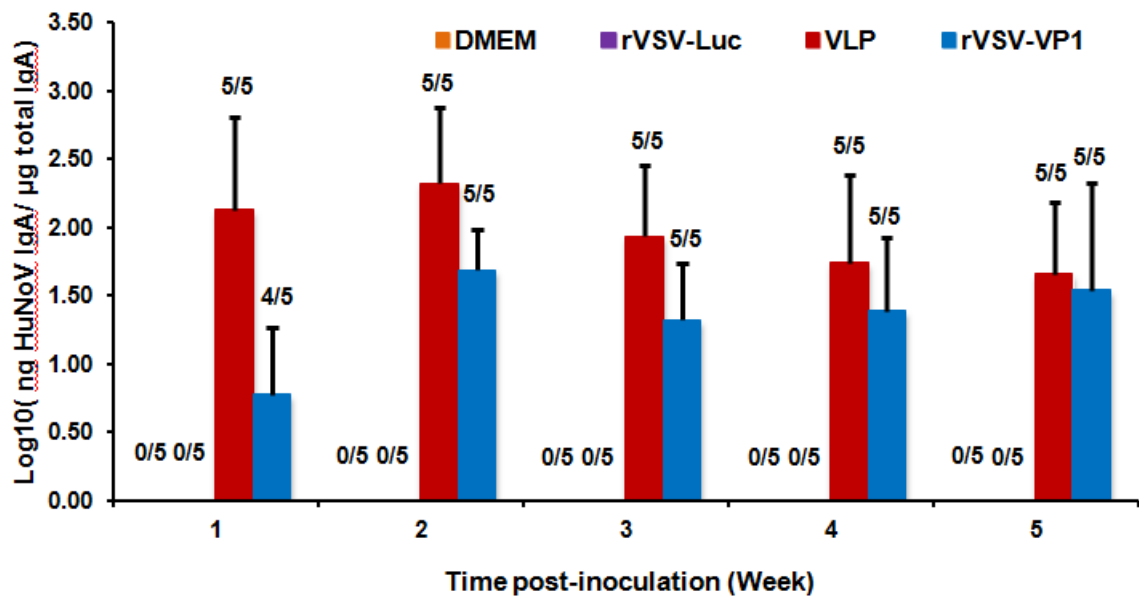


Figure 2.10. Vaginal IgA responses to human NoV vaccine.

Vaginal samples were collected weekly from each mouse, and human NoV-specific and total IgA antibody were determined by ELISA. The level of vaginal IgA was shown as log 10 (ratio between human NoV-specific IgA and total IgA). Data were expressed as Geometric Mean Titer (GMT) of IgA-positive mice \pm the standard deviation.

2.5 Discussion

In this study, we recovered a recombinant rVSV expressing human NoV VP1 protein. We demonstrated that VP1 protein was not only highly expressed by the VSV vector, but also self-assembled into VLPs that were morphologically and antigenically similar to the native virions. Recombinant rVSV-VP1 was attenuated in cell culture as well as in mice. We further demonstrated that mice inoculated with VSV-based human

NoV vaccine responded with a high level of human NoV specific humoral, cellular, and mucosal immunity. These results showed that VSV can be an excellent vector to deliver human NoV VLPs, and that it is a novel vaccine candidate against human NoV. To our knowledge, this is the first demonstration using VSV as the vector to deliver VLPs of non-cultivable viruses in vitro as well as in vivo.

2.5.1 A new approach to generate human NoV VLPs using VSV as the vector.

VSV is one of the most attractive viral vectors for vaccines, oncolytic therapy, and gene delivery (Lichty et al., 2004; Whelan et al., 2004). Since the establishment of the reverse genetics system for VSV in 1995, hundreds of exogenous genes have been expressed by VSV as a vector. However, the feasibility of using VSV as the vector to express and deliver VLPs has not been well studied. To date, there has only been one report which demonstrated using VSV to generate VLPs. Specifically, it demonstrated that the expression of the hepatitis C virus (HCV) core, E1, and E2 proteins by VSV assembled to form HCV-like particles in BHK-21 cells which were similar to the ultrastructural properties of HCV virions (Ezelle et al., 2002). However, Blanchard et al., (2003) argued that these particles may be the endogenous viruses of BHK-21 cells such as intracisternal R-type particles, not the complete budded HCV-like particles (Blanchard et al., 2003). Later, it was shown that expression of HCV E1 and E2 by propagating and non-propagating (G protein deleted) VSV vector resulted in correctly folded E1/E2 heterodimers (Majid et al., 2006a). However, detailed characterization of these HCV-like particles was lacking in their study.

In contrast to HCV, expression of human NoV VP1 alone led to the formation of VLPs (Jiang et al., 1992). We initially inserted the VP1 gene into the 3' proximal end of the VSV genome. However, recombinant VSV expressing VP1 was recovered only when the VP1 gene was inserted between the gene junction of G and L, which is located at the 5' proximal end of the VSV genome. It was likely that the high expression level of VP1 at the 3' proximal end of the VSV genome inhibited the recovery of the virus. Indeed, recovery of rVSV was inhibited when a plasmid encoding VP1 gene was co-transfected with VSV infectious clone (data not shown). We found that recombinant rVSV-VP1 showed diminished plaque size in Vero cells and delayed replication in BSRT7 cells. In addition, there was significantly less VSV proteins synthesized in rVSV-VP1 infected cells as compared to rVSV ($P < 0.05$). However, a high level of VP1 protein was found in cell lysates at early time points in rVSV-VP1 infected cells. At later times, a high level of VP1 was also found in cell culture supernatants. The expressed VP1 was antigenic as shown by Western blot using a polyclonal antibody against VP1. While the expression of VP1 occurs in the cytoplasm, it is likely that some VP1 protein was secreted into the medium across the cell membrane since most cells were healthy at 30 h post-infection. Another possibility is that some cells were lysed resulting in the release of VP1 into the medium. EM analysis confirmed that the expressed VP1 protein assembled into VLPs. These results demonstrated that VSV-expressed VLPs are structurally and antigenically similar to native virions. In addition, there are a number of advantages of using VSV as the vector to express human NoV VLPs. First, VSV grows to a high titer in a wide range of mammalian cells, facilitating the large scale production of VLPs. Second, it is a time-

saving approach. It only took 2 days to generate VLPs using VSV as the vector. However, it took 6 days when a baculovirus system was used. Third, it is a highly productive system. A large number of VLPs can be found by EM analysis using cell culture supernatants (without purification). Therefore, a VSV vector is a novel and efficient approach to generate human NoV VLPs.

2.5.2 A new live vaccine candidate against non-cultivable foodborne viruses.

Noroviruses are responsible for more than 90% of nonbacterial gastroenteritis worldwide and cause up to 200,000 deaths in children of less than 5 years of age in developing countries (Estes et al., 2000; Estes et al., 2006; Harris et al., 2008; Koopmans, 2008). Many attempts have been made to develop an effective vaccine against this biodefense agent. To date, most studies have focused on the VLPs purified from the baculovirus expression system. It has been shown that human NoV VLP vaccination induced humoral and cellular immune in both humans and mice (Ball et al., 1998; Estes et al., 2000; Guerrero et al., 2001; Kitamoto et al., 2002; Xia et al., 2007; Zhang et al., 2006). Since human NoV is non-cultivable, live vectored vaccines may provide a novel and effective vaccine strategy. Two live viral vectors, Venezuelan Equine Encephalitis (VEE) and adenovirus, have been studied to deliver human NoV VLPs in vivo. It was shown that the VEE replicon expressing human NoV VLPs induced human NoV specific systemic, mucosal, and heterotypic immunity in mice (Baric et al., 2002; Harrington et al., 2002). Using cultivable murine norovirus (MNV) as a model, it was shown that VEE-based vaccine induced homotypic and heterotypic humoral and cellular immunity, and protected

mice from MNV challenge (LoBue et al., 2010; LoBue et al., 2009). Recently, it was reported that a recombinant adenovirus expressing human NoV capsid protein stimulated a specific immune response in mice (Guo et al., 2009). These studies demonstrated the feasibility of using a vectored vaccine against human NoV. However, there are some potential disadvantages using VEE and adenovirus as vectors. Although the VEE replicon is a single cycle replicating vector, the biosafety of VEE has been questioned since VEE is a biodefense pathogen and the use of functional VEE genes is restricted. For adenovirus, in vivo delivery of the vectored vaccine may be hampered by the host immune response since a large portion of the global population has pre-existing immunities against the adenovirus vector. In fact, recent clinical trials suggest that adenovirus performs poorly as a vaccine vector (Sekaly, 2008).

In this study, we developed a VSV-based vaccine candidate against human NoV. This VSV-based human NoV vaccine stimulated approximately ten times higher serum IgG than that of traditional VLP-based vaccine. High levels of serum antibody lasted at least five weeks post-inoculation. However, antibody induced by traditional VLP-based vaccines began to decline at only two weeks post-inoculation. VSV-based human NoV vaccine stimulated a strong T-cell proliferation response in vitro with an average stimulation index of 9.7, which is more than 2 times higher than that of VLP groups. Since human NoV causes acute gastroenteritis, it is likely that mucosal immunity plays an important role in protecting humans from disease. Thus, we used a combination of intranasal and oral routes for vaccination. Consistent with earlier observations, we also

found that not all of the mice developed IgA responses in fecal extracts despite the high dose of VLPs used. There were 5 mice that had a fecal IgA response at weeks 2 and 3 but only two to three mice had a detectable fecal IgA response at weeks 4 and 5. However, 4-5 mice from the rVSV-VP1 group had a fecal IgA response from weeks 2-5. Mice inoculated with rVSV-VP1 and VLPs stimulated a comparable fecal IgA antibody at weeks 1-3 although rVSV-VP1 group had a lower level of fecal IgA antibody at weeks 4 and 5. Interestingly, all mice in both VLP and rVSV-VP1 groups had vaginal IgA antibody. Moreover, the rVSV-VP1 group had an equivalent level of vaginal IgA response as compared to VLP vaccination at weeks 4 and 5. Taken together, these results suggest that the VSV-based human NoV vaccine induced significantly stronger humoral and cellular immunity than the traditional VLP-based vaccine. In addition, rVSV-VP1 was able to trigger a comparable level of mucosal immunity. Thus, our data demonstrated that mice inoculated by a single dose of rVSV expressing human NoV VLPs triggered a high level of humoral, cellular, and mucosal immunity. This is likely related to the extremely high level of intracellular synthesis of VLPs in the infected cells of mice. Furthermore, VLPs may be continuously expressed *in vivo* by the VSV vector, which in turn stimulated long-lasting immune responses. In contrast, conventional purified VLPs are non-replicating antigens, and thus the duration of the immune response may be limited. A VSV-based vaccine offers a number of other distinctive advantages including genetic stability, expression of multiple antigens, simplicity of production, multiple routes of administration, and ease of manipulation. Unlike adenovirus vector, human infection with VSV is very rare (Fellowes et al., 1955; Hanson et al., 1950), and the

general population is free of pre-existing immunity against VSV (Lichty et al., 2004). Therefore, these advantages support the initiation of clinical trials of VSV vectored vaccine in the future.

Unfortunately, there is no robust small animal model for human NoV infection. Recently, it was shown that gnotobiotic pigs infected with human NoV genogroup II.4 strain HS66 developed diarrhea, viral shedding, and histopathological lesions in their intestines (Cheetham et al., 2006). Subsequently, vaccination of gnotobiotic pigs with baculovirus-expressed VLPs generated systemic immune responses and provided partial protection against viral shedding and diarrhea (Souza et al., 2007b). It will be of great interest to determine whether a VSV-based human NoV vaccine can protect swine from virulent challenge.

In summary, our study highlights the potential of using VSV as a vaccine vector to deliver human NoV VLPs in vitro and in vivo. Our study has two important applications for the development of: (i) a highly productive bioreactor to facilitate large scale production of human NoV VLPs using VSV as a vector; and (ii) a VSV-based vaccine as a novel vaccine candidate against human NoV as well as other non-cultivable viruses.

Chapter 3 : Heat shock protein 70 (HSP70) enhances safety and immunogenicity of norovirus capsid protein (VP1) when co-expressed from a vesicular stomatitis viral vector

3.1 Abstract

Human norovirus (NoV) accounts for more than 90% of non-bacterial gastroenteritis worldwide (Mead et al., 1999; Scallan, 2011). Research efforts on human NoV are hampered as it is not cultivable in vitro and lacks a small animal model. Currently, there is no vaccine available to combat human NoV. In Chapter 2, it was demonstrated that recombinant vesicular stomatitis virus (VSV) expressing human NoV capsid protein (rVSV-VP1) induced strong humoral, mucosal, and cellular immune responses in mice. The objective of this Chapter is to further improve the safety and efficacy of the vaccine candidate by inserting heat shock protein 70 (HSP70) as an adjuvant into the rVSV-VP1 vector. The HSP70 insertion caused the recombinant virus (rVSV-HSP70-VP1) to form smaller plaques and also delayed replication in cell culture compared to rVSV-VP1. In addition, rVSV-HSP70-VP1 caused less clinical manifestations of VSV infection in BALB/c mice compared to rVSV-VP1, further implicating enhanced attenuation due to the double insertion. At the same inoculation dose (1×10^6 PFU), both rVSV-HSP70-VP1 and rVSV-VP1 triggered similar levels of

specific humoral, mucosal, and cellular immunity, even though VP1 expression by rVSV-HSP70-VP1 was approximately five-fold less than that of rVSV-VP1. To compensate for the reduced VP1 expression levels, we increased the inoculation dose of rVSV-HSP70-VP1 five-fold to 5×10^6 PFU/mouse or combined vaccination of rVSV-VP1 and rVSV-HSP70. Mice immunized with 5×10^6 PFU of rVSV-HSP70-VP1 or those receiving combined vaccination generated significantly higher mucosal and/or T cell immunity than those immunized with rVSV-VP1 alone ($P < 0.05$). Collectively, these data indicate that: (i) Insertion of HSP70 into VSV vector further attenuates the VSV-based vaccine in cell culture and in the mice model, thus improving the safety of the vaccine candidate and (ii) HSP70 enhances the human NoV-specific immunity triggered by VSV-based human NoV vaccine.

3.2 Introduction

The *Caliciviridae* family includes a number of significant enteric viruses that cause gastroenteritis in humans and animals. Examples of these viruses include human norovirus (NoV), bovine NoV, porcine NoV, human sapovirus, and the newly discovered monkey calicivirus (Tulane virus, TV). Currently, human NoV and other caliciviruses are classified as Category B biodefense agents by the National Institute of Allergy and Infectious Diseases (NIAID) because they are highly contagious, extremely stable, resistant to common disinfectants, require a low infectious dose, and are associated with debilitating illness. Despite the fact that human NoV causes significant health, emotional,

social and economical burdens worldwide, there are no vaccines or anti-viral drugs available to combat this infectious agent.

The only human NoV vaccine candidate currently in human clinical trial is the virus like particle (VLP)-based subunit vaccine (Atmar et al., 2011). Volunteers that received the dry powder VLP vaccine reduced their risk of illness by 47% after exposure to human NoV (LigoCyte Pharmaceuticals Inc. 2010). There were significant reductions in clinical norovirus illness, infection, and severity of illness in individuals who received vaccine compared with those who received the placebo (LigoCyte Pharmaceuticals Inc. 2010). Although these studies are promising, the efficacy of this vaccine needs to further be improved. It is not known whether a VLP-based vaccine can completely protect human from re-infection. In addition, the duration of the protection is a concern because VLPs are nonreplicating immunogens. Therefore, there is critical need to explore other vaccine candidates such as a live vectored vaccine candidate for human NoV.

In Chapter 2, a recombinant VSV (rVSV-VP1) that expresses the major capsid protein of human NoV was generated. The yield of VLPs by the VSV expression system is approximately ten times higher than that of the baculovirus expression system. Recombinant rVSV-VP1 was attenuated in cell culture as well as in mice compared to parental VSV. Mice inoculated with a single dose of rVSV-VP1 through intranasal and oral routes stimulated a significantly stronger humoral and cellular immune response than baculovirus-expressed VLP vaccination. In addition, mice inoculated with rVSV-VP1 triggered a comparable level of fecal and vaginal IgA antibodies. These findings demonstrated that the VSV expression system is not only a highly productive system to

generate VLPs in vitro, but also a promising vectored vaccine candidate for human NoV. However, recombinant rVSV-VP1 still causes significant body weight loss in mice even though it is attenuated compared to rVSV. In addition, whether the efficacy of this vaccine candidate can be enhanced by insertion of an adjuvant gene is not known.

The objective of this Chapter is to further improve the VSV-based human NoV vaccine by co-expression of an adjuvant gene and human NoV VP1 from the VSV vector. Heat shock protein 70 (HSP70) was chosen as a vaccine adjuvant because it has been shown to modulate both innate and adaptive immune responses (Chen et al., 2000; Ciupitu et al., 1998; Kumaraguru et al., 2002; Oglesbee et al., 2002; Todryk et al., 2003). HSPs are a family of intracellular proteins, which act as molecular chaperones with essential functions in folding and intracellular translocation of other proteins. The major inducible HSP70 is one of best-characterized HSPs. In addition to serving as molecular chaperone, it has been demonstrated that HSP70-peptide complexes or peptide-HSP70 fusion proteins act as a chaperon of peptides and enhance the T- and B-mediated adaptive immunity by binding to antigen-presenting cells (APCs), and stimulating the APC maturation and cytokine secretion and up-regulates the molecules involved in antigen presentation (MHC class I/II and costimulatory markers) and in adhesion (Milani et al., 2002; Millar et al., 2003). It is also hypothesized that HSP70 may enhance the safety of the VSV-based human NoV vaccine based on the rationale that insertion of an additional gene into VSV vector will result in further transcription attenuation. In addition, it has been shown that HSP70 enhanced clearance of other non-segmented negative-sense RNA viruses such as measles virus and canine distemper virus in mice (Carsillo et al., 2004).

To test these hypotheses, recombinant VSVs expressing HSP70 (rVSV-HSP70) and co-expressing HSP70 and VP1 (rVSV-HSP70-VP1) were constructed. Subsequently, the safety and efficacy of recombinants rVSV-VP1, rVSV-HSP70-VP1 or co-administration of rVSV-VP1 and rVSV-HSP70 were compared in a mouse model. It is found that insertion of HSP70 into VSV vector not only improved the safety of vaccine candidate, but also enhanced the human NoV-specific immunities triggered by VSV-based human NoV vaccine.

3.3 Materials and Methods

3.3.1 Recombinant viruses.

Wild type rVSV, and the recombinant viruses rVSV-VP1 and rVSV-Luc were described in Chapter 2. Recombinant rVSV-VP1 harbors the VP1 gene of human NoV at the VSV gene junction between G and L gene sequences; whereas rVSV-Luc contains the firefly luciferase gene at the VSV gene junction between the leader sequence and the N gene.

3.3.2 Plasmid construction.

Plasmids encoding VSV N (pN), P (pP), and L (pL) genes, and an infectious cDNA clone of the viral genome, pVSV1(+), were generous gifts from Dr. Gail Wertz. Plasmids pVSV1(+) GxxL and pVSV1(+) LexxN were kindly provided by Dr. Sean Whelan. Plasmid pVSV1(+) GxxL contains SmaI and XhoI at the G and L gene junction. Plasmid pVSV1(+) LexxN contains SmaI and XhoI at the leader sequence and N gene junction. The capsid VP1 gene of human NoV genogroup II.4 strain HS66 was kindly provided by

Dr. Linda Saif. The HSP70 gene was provided by Dr. Michael Oglesbee. The VP1 and HSP70 genes were amplified by high-fidelity PCR, and cloned into pVSV(+)_{GxxL} at *Sma*I and *Xho*I sites, which resulted in the construction of plasmids pVSV1(+)-VP1 and pVSV1(+)-HSP70, respectively. A third plasmid [pVSV1(+)_{Le}-HSP70-N] was constructed by insertion of HSP70 gene into pVSV1(+)_{LexxN} at the leader and N gene junction. To construct a plasmid encoding both HSP70 and VP1 genes, a DNA fragment containing VP1 gene was recovered by digestion of pVSV1(+)-VP1 with *Hpa*I and *Kpn*I enzymes, and cloned into the same sites in pVSV1(+)_{Le}-HSP70-N. The HSP70 gene was inserted into the leader and N gene junction and the human NoV VP1 gene was inserted into the G and L gene junction; the resulting plasmid was designated pVSV1(+)-HSP70-VP1. All inserted genes contained the VSV gene start and gene end sequences. Finally, all plasmid constructs were confirmed by sequencing.

3.3.3 Recovery and purification of recombinant VSV.

The recovery of recombinant VSV from the infectious clone was carried out as described previously in Chapter 1. Briefly, BSRT7 cells were infected with a recombinant vaccinia virus (vTF7-3) expressing T7 RNA polymerase, followed by cotransfection with a plasmid encoding the VSV genome [pVSV1(+)-HSP70 or pVSV1(+)-HSP70-VP1] and plasmids pN, pP, and pL. At 96 h posttransfection, cell culture fluids were collected and filtered through a 0.2- μ m filter, and the recombinant VSV was further amplified in BSRT7 cells. Subsequently, the recovered viruses were plaque purified as described

previously. Individual plaques were isolated, and seed stocks were amplified in BSRT7 cells. The viral titer was determined by a plaque assay performed in Vero cells.

3.3.4 Single-cycle growth curves.

Confluent BSRT7 cells were infected with individual viruses at a multiplicity of infection (MOI) of 10. After 1 h of absorption, the inoculum was removed, the cells were washed twice with Dulbecco's modified Eagle's medium (DMEM), fresh DMEM (supplemented with 2% fetal bovine serum) was added, and the infected cells were incubated at 37°C. Aliquots of the cell culture fluid were removed at specific timepoints and the virus titer at each timepoint was determined by plaque assay in Vero cells.

3.3.5 Analysis of protein synthesis.

Confluent BSRT7 cells were infected with rVSV, rVSV-VP1, rVSV-HSP70, or rVSV-HSP70-VP1 at MOI of 10 as described above. At 3 h postinfection, cells were washed with methionine- and cysteine-free (M^-C^-) medium and incubated with fresh M^-C^- medium supplemented with actinomycin D (15 μ g/ml). After 1 h of incubation, the medium was replaced with M^-C^- medium supplemented with EasyTag 35 S-Express (4 μ Ci/ml; Perkin-Elmer, Wellesley, MA). After 4 h of incubation, cytoplasmic extracts were prepared and analyzed by sodium dodecyl sulfate-polyacrylamide gel electrophoresis (SDS-PAGE) as described previously. Labeled proteins were detected either by autoradiography or by using a phosphorimager.

3.3.6 RT-PCR.

Viral RNA was extracted from rVSV, rVSV-VP1, rVSV-HSP70, or rVSV-HSP70-VP1 using an RNeasy mini kit (Qiagen, Valencia, CA) according to the manufacturer's instructions. Two primers (5'-CGAGTTGGTATTTATCTTTGC-3' and 5'-GTACGTCATGCGCTCATCG-3') were designed to target the VSV G gene at position 4524 and the L gene at position 4831 (numbering refers to the complete VSV Indiana genome sequence), respectively. These two primers were used to detect the insertion of VP1 or HSP70 genes at the G and L gene junction. Another two primers [VSV(+)-1-17, 5'-ACGAAGACAAACAAACC-3' and VSV(-), 5'-CCTCATTTGCAGGAAG-3'] were designed to target VSV leader sequence at position 1 and the N gene at position 115. These two primers were used to detect the HSP70 gene which was inserted between the VSV leader and N gene junction. Reverse transcription-PCR (RT-PCR) was performed using a One Step RT-PCR kit (Qiagen, Germany). The amplified products were analyzed by 1% agarose gel electrophoresis.

3.3.7 Western blotting.

BSRT7 cells were infected with rVSV, VSV-VP1, rVSV-HSP70, or rVSV-HSP70-VP1 at MOI of 10 as described above. At specific timepoints postinfection, cells were lysed in lysis buffer containing 5% β -mercaptoethanol, 0.01% NP-40, and 2% SDS. Proteins were separated by 12% SDS-PAGE and transferred to a Hybond enhanced chemiluminescence nitrocellulose membrane (Amersham/ GE Healthcare, Piscataway, NJ) in a Mini Trans-Blot electrophoretic transfer cell (Bio-Rad, Hercules, CA). The blot was probed with

guinea pig anti-human NoV VP1 antiserum (a generous gift from Dr. Xi Jiang) at a dilution of 1:5,000, followed by horseradish peroxidase-conjugated goat anti-guinea pig IgG secondary antibody (Santa Cruz Biotechnology, CA) at a dilution of 1:20,000. The HSP70 protein was detected with mouse anti-HSP70 antibody (a generous gift from Dr. Michael Oglesbee) at 1:2000, followed by horseradish peroxidase-conjugated goat anti-mouse IgG secondary antibody (Thermo Scientific, USA). The blot was developed with SuperSignal West Pico chemiluminescent substrate (Thermo Scientific, USA) and exposed by Kodak BioMax MR film.

3.3.8 Production and purification of VLPs by a baculovirus expression system.

Purification of human NoV VLPs from insect cells by baculovirus expression system was as described previously in Chapter 1. Briefly, *Spodoptera frugiperda* (Sf9) cells were infected with baculovirus expressing the human NoV VP1 protein at an MOI of 10, and the infected Sf9 cells and cell culture supernatant were harvested at 6 days postinoculation. The VLPs were purified from cell culture supernatant and cell lysate by ultracentrifugation through a 40% (wt/vol) sucrose cushion, followed by CsCl isopycnic gradient (0.39 g/cm³) ultracentrifugation. Purified VLPs were analyzed by SDS-PAGE, Western blotting, and electron microscopy (EM). The protein concentrations of the VLPs were measured by using Bradford reagent (Sigma Chemical Co., St. Louis, MO).

3.3.9 Animal experiment 1.

Thirty-five 4-week-old specific-pathogen-free female BALB/c mice (Charles River Laboratories, Wilmington, MA) were randomly divided into seven groups (five mice per group). Mice in groups 1 to 5 were inoculated with 10^6 PFU of rVSV, rVSV-Luc, rVSV-VP1, rVSV-HSP70, or rVSV-HSP70-VP1, respectively. Mice in group 6 were inoculated with 100 μ g of VLPs (purified from the baculovirus expression system). Mice in group 7 were inoculated with 200 μ l of DMEM and served as unimmunized controls. All mice were inoculated through the combination of intranasal and oral routes. Half of the antigens were inoculated intranasally, and the other half were administered orally. After inoculation, the animals were evaluated on a daily basis for mortality, weight loss, and the presence of any symptoms of VSV infection. Blood samples were collected from each mouse weekly by facial vein bleed, and serum was isolated for IgG antibody detection. Fecal and vaginal swab homogenate samples were isolated weekly for the detection of norovirus specific IgA. At 5 weeks postinoculation, all mice were sacrificed. Spleens were isolated from each mouse, and mononuclear cell (MNC) suspensions were prepared for T cell proliferation assay.

3.3.10 Animal experiment 2.

Twenty five 4-week-old specific-pathogen-free female BALB/c mice (Charles River laboratories) were randomly divided into five groups (five mice per group). Mice in groups 1-2 were inoculated with 10^6 PFU of rVSV-VP1 or rVSV-HSP70-VP1. Mice in

groups 3-4 were inoculated with 5×10^6 PFU of rVSV-VP1 or rVSV-HSP70-VP1. Mice in group 5 were inoculated with 200 μ l of DMEM and served as unimmunized controls. The remaining procedure was identical to animal experiment 1.

3.3.11 Animal experiment 3.

Fifteen 4-week-old specific-pathogen-free female BALB/c mice (Charles River Laboratories) were randomly divided into three groups (five mice per group). Mice in group 1 were inoculated with 10^6 PFU of rVSV-VP1. Mice in group 2 were inoculated with 10^6 PFU of rVSV-VP1 and 10^6 PFU of rVSV-HSP70. Mice in group 3 were inoculated with 200 μ l of DMEM and served as unimmunized controls. The remaining procedure was identical to animal experiment 1.

3.3.12 T cell proliferation assay.

Ninety-six-well plates were coated with 50 μ l of highly purified human NoV VLPs (10 μ g/ml) in 200 mM NaCO₃ buffer (pH 9.6) at 4°C overnight. After homogenization, spleen cells were washed twice with phosphate-buffered saline (PBS) and plated in triplicate at 5×10^5 cells/well in a 96-well-plate in RPMI 1640 medium with 2% naive mouse serum. After 48 h of incubation at 37°C, 0.5 μ Ci of [³H]thymidine was added to each well and incubated for 16 h. Following incubation, cells were transferred onto glass filters and counted with a Betaplate counter (Wallac, Turku, Finland). The stimulation

index (SI) was calculated as the mean of the following ratio: proliferation of human NoV VLP-stimulated cells/proliferation of cells in medium (in cpm).

3.3.13 Serum IgG ELISA.

Ninety-six-well plates were coated with 50 µl of highly purified human NoV VLPs (7.5 µg/ml) in 50 mM NaCO₃ buffer (pH 9.6) at 4°C overnight. Individual serum samples were tested for human NoV-specific IgG on VLP-coated plates. Briefly, serum samples were 2-fold-serially diluted and added to VLP-coated wells. After incubation at room temperature for 1 h, the plates were washed five times with PBS-Tween (0.05%), followed by incubation with 50 µl of goat anti-mouse IgG horseradish peroxidase-conjugated secondary antibody (Sigma) at a dilution of 1:80,000 for 1 h. Plates were washed and developed with 75 µl of 3,3',5,5'-tetramethylbenzidine (TMB), and the optical density (OD) at 450 nm was determined using an enzyme-linked immunosorbent assay (ELISA) plate reader. End point titer values were determined as the reciprocal of the highest dilution that had an absorbance value greater than background level (DMEM control).

3.3.14 Fecal IgA ELISA.

For each stool sample, human NoV-specific and total fecal IgA were determined as described previously. Fecal pellets were diluted 1:2 (wt/vol) in PBS containing 0.1%

Tween and a Complete EDTA-free proteinase inhibitor cocktail tablet (Roche, Mannheim, Germany). Samples were vortexed twice for 30 s and clarified twice by centrifugation at $10,000 \times g$ for 10 min. Ninety-six-well plates were coated with 50 μ l of highly purified human NoV VLPs (1 μ g/ml) in 50 mM NaCO₃ buffer (pH 9.6) at 4°C overnight for detection of human NoV-specific IgA, while total fecal IgA was determined by capturing all fecal extract IgA molecules with 1 μ g/ml sheep anti-mouse IgA (Sigma). To block nonspecific protein binding, the plates were incubated for 4 h at 4°C with 10% (wt/vol) dry milk in PBS (10% BLOTTO). The level of IgA was calculated from a standard curve that was determined by the absorbance values of the mouse IgA standard (Sigma). The human NoV-specific IgA level was expressed in nanograms per milliliter, and each corresponding total IgA level was expressed in micrograms per milliliter.

3.3.15 Vaginal human NoV-specific IgA ELISA.

Ninety-six-well plates were coated with human NoV VLPs in selected columns as described above. After an overnight blocking at 4°C with 5% BLOTTO, 75 μ l of an undiluted vaginal sample per well or a 1:5 dilution of the sample was added, the sample was serially diluted 2-fold down the plate and incubated for 2 h at 37°C. The remaining protocol was identical as described above for the human NoV-specific fecal IgA ELISA or the serum IgG ELISA.

3.3.16 Quantitative and statistical analyses.

Quantitative analysis was performed by either densitometric scanning of autoradiographs or by using a Typhoon PhosphorImager (GE Healthcare) and ImageQuant TL software (GE Healthcare, Piscataway, NJ). Each experiment was performed three to six times. Statistical analysis was performed by one-way multiple comparisons using Minitab 16 statistical analysis software (Minitab Inc., State College, PA). A *P* value of <0.05 was considered statistically significant.

3.4 Results

3.4.1 Recovery of recombinant VSV expressing HSP70 (rVSV-HSP70) and VSV co-expressing human NoV VP1 and HSP70 proteins (rVSV-HSP70-VP1).

Previously, we recovered recombinant rVSV-VP1 and rVSV-Luc, in which human NoV VP1 or firefly luciferase (Luc) genes were inserted at the G-L gene junction and the leader-N gene junction, respectively. Using a similar approach, we successfully recovered two additional recombinant viruses, rVSV-HSP70, and rVSV-HSP70-VP1 (Fig. 3.1A). Recombinant rVSV-HSP70 harbors HSP70 gene at the G-L gene junction whereas rVSV-HSP70-VP1 contains double insertions with HSP70 inserted at the leader-N gene junction and VP1 inserted at the G- L gene junction. As shown in Fig.3.1B, the plaque morphology of these recombinant viruses in Vero cells differed, depending on the site of the insertion. Recombinants rVSV-VP1, rVSV-Luc, and rVSV-HSP70 formed plaques of similar size, but these plaques were smaller than those of wild type rVSV. Interestingly, the double inserted recombinant virus, rVSV-HSP70-VP1, formed much

smaller plaques than rVSV-VP1 (Fig. 3.1B). After 24 h of incubation, rVSV formed plaques that were 4.1 ± 0.4 mm (mean \pm standard deviation) in diameter. The average plaque size for rVSV-VP1, rVSV-Luc, and rVSV-HSP70 was 1.7 ± 0.6 mm, 1.2 ± 0.4 mm, and 1.6 ± 0.3 mm, respectively, after 48 h of incubation. However, the plaque size for rVSV-HSP70-VP1 was 1.2 ± 0.2 mm, suggesting that rVSV-HSP70-VP1 viral growth is further impaired compared to rVSV-VP1. To confirm that the recovered virus indeed contained the target genes, viral genomic RNA was extracted from each recombinant virus followed by RT-PCR using primers annealing to either the VSV leader sequence and N gene or G and L genes. As shown in Fig. 3.1C, a 2.0-kb cDNA band containing the VP1 or a 2.3-kb band containing the HSP70 gene was amplified from genomic RNA extracted from rVSV-VP1, rVSV-HSP70, and rVSV-HSP70-VP1 while a 300-bp cDNA was amplified from parental rVSV lacking either insert, demonstrating that the VP1 or HSP70 was inserted at G and L gene junction. In addition, a 2.0-kb cDNA band containing HSP70 gene was amplified from rVSV-HSP70-VP1 using primers annealing to VSV leader and N gene, demonstrating that HSP70 was inserted at gene junction between leader and N gene. Subsequently, the amplified cDNA was purified and sequenced, confirming that VP1 or HSP70 was indeed inserted into the targeted position in VSV genome. Finally, the entire genome of each recombinant was sequenced to confirm that no additional mutation was introduced.

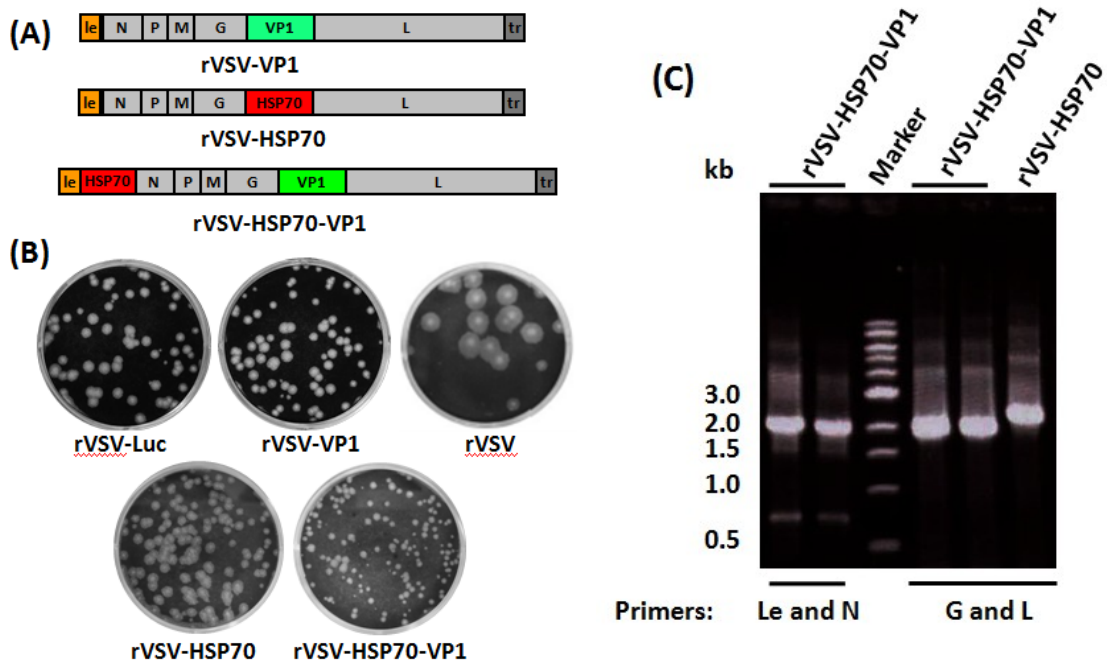


Figure 3.1. Recovery of recombinant VSV co-expressing human NoV VP1 and HSP70 (rVSV-HSP70-VP1) and VSV expressing HSP70 (rVSV-HSP70).

(A) Construction of plasmids. For rVSV-VP1, the VP1 was inserted at the G-L gene junction in VSV genome. For rVSV-HSP70, the HSP70 was inserted into VSV genome at gene junction between leader and N. For rVSV-HSP70-VP1, the HSP70 and VP1 genes were inserted at gene junctions between leader and N, and G and L, respectively. Le, VSV leader sequence; N, nucleocapsid gene; P, phosphoprotein gene; M, matrix protein gene; G, glycoprotein gene; L, large polymerase gene; Tr, VSV trailer sequence.

(B) The plaque morphology of recombinant viruses is shown compared to rVSV. Plaques of rVSV-VP1, rVSV-HSP70 and rVSV-HSP70-VP1 were developed after 48 h of incubation compared to rVSV, which was developed after 24 h incubation. (C)

Amplification of VP1 and HSP70 genes from recombinant rVSV-VP1, rVSV-HSP70 and rVSV-HSP70-VP1 by RT-PCR. Genomic RNA was extracted from each virus. The VP1

gene was amplified by RT-PCR using two primers annealing to G and L genes. The HSP70 gene was amplified using the same two primers annealing to G and L genes and the other two primers annealing to leader and N.

3.4.2 Single-step growth curves of recombinant VSV in cell culture.

The kinetics of release of infectious virus for each recombinant VSV was compared by using a single-step growth assay in BSRT7 cells. As shown in Fig. 3.2, recombinant rVSV-VP1, rVSV-HSP70, and rVSV-HSP70-VP1 had a significant delay in viral replication compared to that of rVSV. Wild-type rVSV reached a peak titer (4.6×10^9 PFU/ml) at 12 h postinfection. Recombinant rVSV-VP1 reached a peak titer of 4.0×10^9 PFU/ml at approximately 24 h postinfection. However, recombinant rVSV-HSP70 and rVSV-HSP70-VP1 reached a peak titer of 2.5×10^9 and 7.2×10^8 PFU/ml, respectively at approximately 30 h postinfection. Overall, rVSV-HSP70-VP1 had more delayed replication compared to rVSV-VP1, and the peak titer of rVSV-HSP70-VP1 was 0.8 logs lower than that of rVSV-VP1. These results indicate that all recombinants had delayed replication in cell culture and rVSV-HSP70-VP1 was more attenuated than rVSV-VP1.

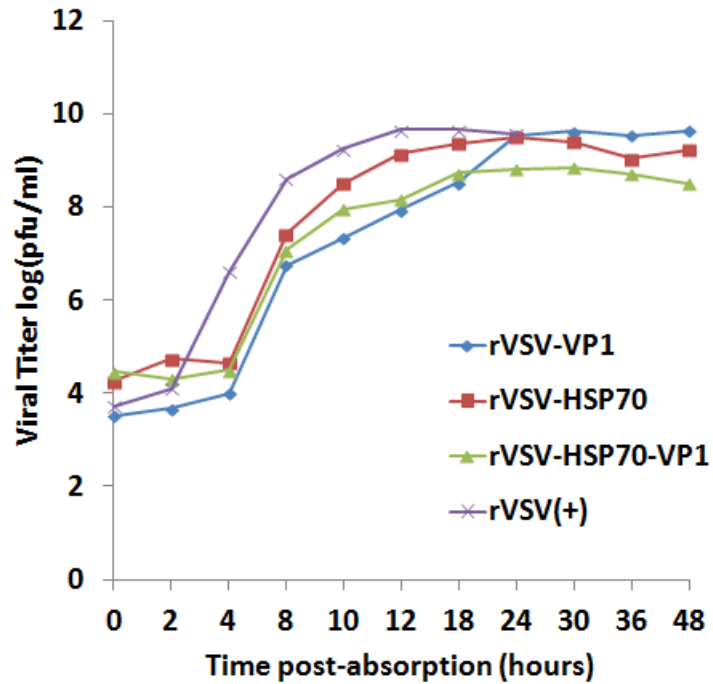


Figure 3.2. Single-step growth curve of recombinant VSVs in BSRT7 cells.

Confluent BSRT7 cells were infected with individual virus at an MOI of 10. After 1 h incubation, the inoculum was removed, the cells were washed with DMEM, and fresh medium (containing 2% fetal bovine serum) was added, followed by incubation at 37°C. Samples of supernatant were harvested at the indicated intervals over a 48-h time period, and the virus titer was determined by plaque assay. Titers are expressed as mean \pm standard deviation of three independent single-step growth experiments.

3.4.3 Characterization of the expression of VP1 and HSP70 by the VSV vector.

The expression of VP1 and HSP70 by the VSV vector was determined by [³⁵S] metabolic labeling in virus-infected cells. Briefly, BSRT7 cells were infected with each recombinant at MOI of 10 and, at 3 h postinfection the cells were metabolically labeled with [³⁵S]methionine-cysteine for 4 h. After incubation, cytoplasmic extracts were prepared, and total protein was analyzed by SDS-PAGE. As shown in Fig. 3.3, rVSV synthesized five viral proteins, L, G, P, N, and M. In rVSV-VP1-infected cells, an additional protein band with a molecular mass of approximately 58 kDa was detected, which correlates to the size of the VP1 protein of human NoV. In rVSV-HSP70-infected cells, an additional 70 kDa protein band was detected and this is the correct size for HSP70. In rVSV-HSP70-VP1-infected cells, two additional protein bands with molecular weights of 70 kDa and 58 kDa were detected, which are consistent with the size of VP1 and HSP70, respectively. The protein bands were quantitated by Quantity One Software (Bio-Rad). As shown in Fig. 3.3, all recombinants synthesized significantly less native VSV proteins compared to rVSV. In addition, rVSV-HSP70-VP1 expressed much lower levels of VSV proteins than rVSV-VP1 and rVSV-HSP70, suggesting again that rVSV-HSP70-VP1 was more attenuated in cell culture. Quantitative analysis showed approximately 25-50%, 30-50%, and 5-25% relative expression of VSV proteins by rVSV-VP1, rVSV-HSP70, and rVSV-HSP70-VP1 compared to the wild type rVSV (Fig. 3.3). We also quantified the VP1 synthesized by rVSV-VP1 and rVSV-HSP70-VP1 and the HSP70 synthesized by rVSV-HSP70 and rVSV-HSP70-VP1. As shown in Fig. 3.3, rVSV-HSP70-VP1 synthesized approximately 5 times more HSP70 protein than rVSV-

HSP70, which is due to the fact that rVSV-HSP70-VP1 harbors HSP70 gene at leader and N gene junction whereas rVSV-HSP70 contains HSP70 at G and L gene junction. This is also consistent with VSV protein synthesis strategy in which the abundance of gene expression decreases with distance from the 3' end to the 5' end of the VSV genome. Similarly, VP1 synthesized by rVSV-VP1 was approximately 5 times more than rVSV-HSP70-VP1. This is because insertion of additional HSP70 gene in rVSV-HSP70-VP1 resulted in further transcription attenuation of the downstream genes.

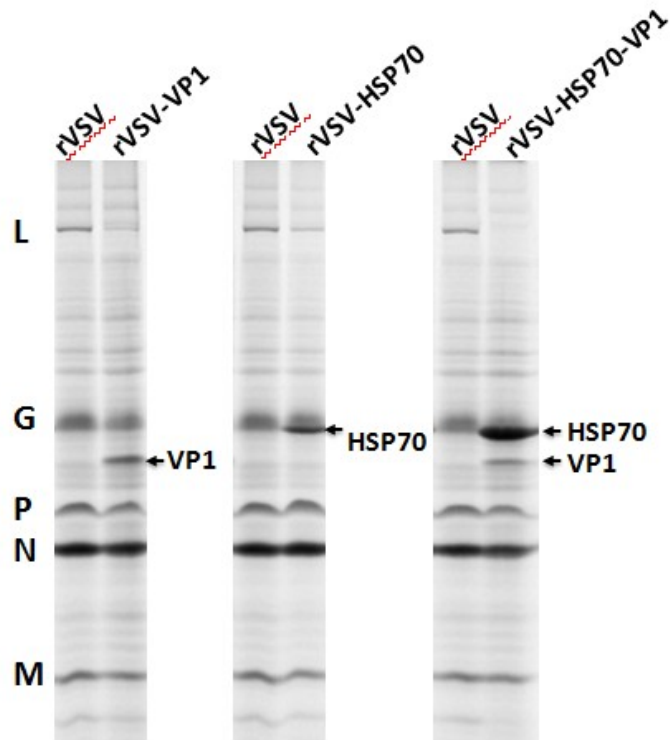


Figure 3.3. Expression of human NoV VP1 and HSP70 by rVSV-VP1, rVSV-HSP70, and rVSV-HSP70-VP1.

BSRT-7 cells were infected with rVSV or rVSV-VP1 or rVSV-HSP70 or rVSV-HSP70-VP1 at MOI of 10. Proteins were metabolically labeled by incorporation of [³⁵S]methionine-cysteine in the presence of actinomycin D. Cytoplasmic extracts were harvested at 5 h post-infection, and proteins were analyzed by SDS-PAGE and detected using a phosphorimager. The identity of the proteins is shown on the left.

The kinetics of VP1 expression by rVSV-VP1 and rVSV-HSP70-VP1 were monitored by Western blot. Briefly, BSRT7 cells were infected with rVSV-VP1, or rVSV-HSP70-VP1 at an MOI of 10, and cell lysates were harvested at various time points. The cell lysates

were analyzed by SDS-PAGE, followed by Western blotting using a polyclonal antibody against the VP1 protein. As shown in Fig.3.4, high levels of VP1 protein were detected in cells infected by rVSV-VP1 at 8 h postinfection. The VP1 expression gradually increased at 30 h postinfection. In contrast, VP1 expression in rVSV-HSP70-VP1 was significantly delayed and the level of VP1 in rVSV-HSP70-VP1 was significantly less than rVSV-VP1. VP1 was not detectable in rVSV-HSP70-VP1 at 8 h postinfection and only low levels of VP1 were detected at 12 h postinfection. Quantitative analysis showed that the VP1 level of rVSV-HSP70-VP1 was approximately 5 times less than rVSV-VP1 at 30 h postinfection, which is consistent with the [³⁵S] metabolic labeling experiment (Fig.3.3).

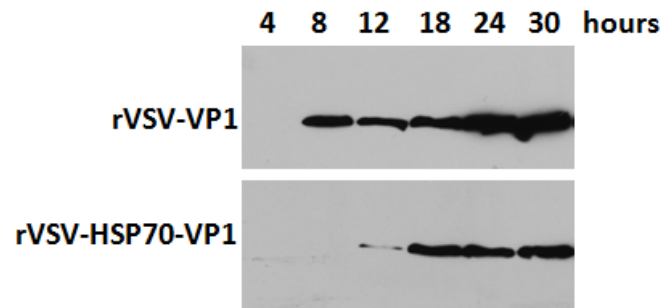


Figure 3.4. Kinetics of norovirus VP1 expression by rVSV-VP1 and rVSV-HSP70-VP1.

BSRT-7 cells were infected with rVSV-VP1 or rVSV-HSP70-VP1 at an MOI of 10. Cytoplasmic extracts were harvested at indicated time points. Equal amounts of total cytoplasmic lysate were analyzed by SDS-PAGE, followed by Western blot analysis using guinea pig anti-human NoV VP1 antiserum.

The kinetics of HSP70 expression by rVSV-HSP70 and rVSV-HSP70-VP1 were monitored by a Western blot analysis. Briefly, BSRT7 cells were infected with rVSV-HSP70, or rVSV-HSP70-VP1 at an MOI of 10, and cell lysates were harvested at various time points. The cell lysates were analyzed by SDS-PAGE, followed by Western blotting using an antibody against the HSP70 protein. As shown in Fig.3.5, HSP70 protein was detectable in cells infected by both viruses at 8 h postinfection. The HSP70 expression gradually increased for 24 h postinfection. However, the HSP70 level in rVSV-HSP70-VP1 infected cells was approximately 5 times more than rVSV-HSP70 infected cells at the three time points (8, 16, and 24 h postinfection), which is consistent with [³⁵S] metabolic labeling experiment (Fig.3.3).

Therefore, these results demonstrated that (i) both VP1 and HSP70 proteins were highly expressed by the VSV vector; (ii) the VP1 protein level expressed by rVSV-HSP70-VP1 was approximately 5 times less than rVSV-VP1; and (iii) the HSP70 protein expression level of rVSV-HSP70-VP1 was approximately 5 times more than rVSV-HSP70.

Collectively, the combination of decreased viral plaque size, delayed single step viral replication, and reduced VSV protein synthesis suggests that rVSV-HSP70-VP1 is more attenuated than rVSV-HSP70 and rVSV-VP1 in cell culture.

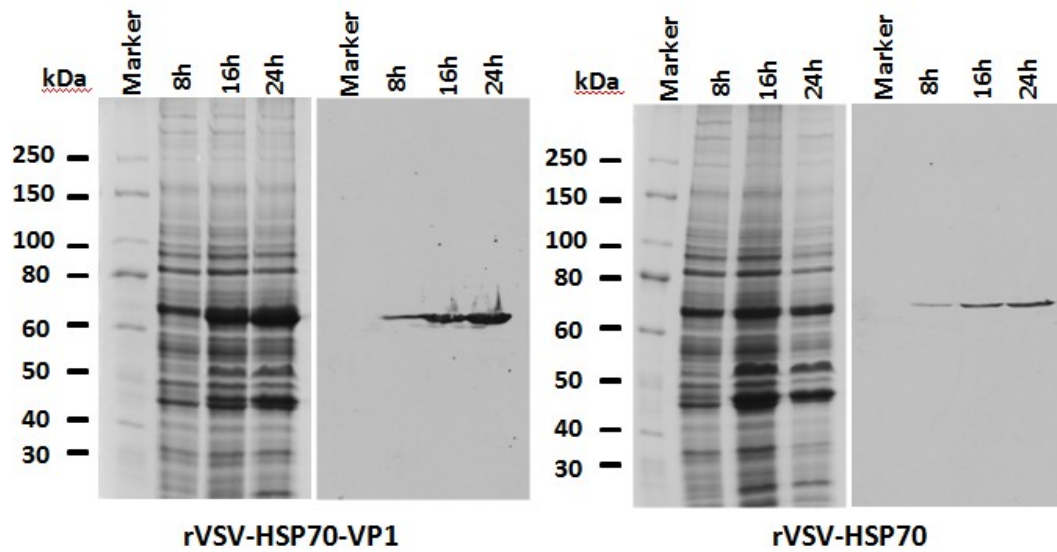


Figure 3.5. Kinetics of HSP70 expression by rVSV-HSP70 and rVSV-HSP70-VP1.

BSRT-7 cells were infected with rVSV-HSP70 or rVSV-HSP70-VP1 at MOI of 10.

Cytoplasmic extracts were harvested at indicated time points. Cells were lysed in 500 μ l of lysis buffer, and 10 μ l of lysate were analyzed by SDS-PAGE (left) and Western blot analysis (right). Identical samples from SDS-PAGE were blotted with mouse anti-HSP70 antibody for Western blot analysis.

3.4.4 Recombinant rVSV-HSP70-VP1 is more attenuated than rVSV-VP1 in a mouse model.

Recombinants rVSV-VP1, rVSV-HSP70, rVSV-HSP70-VP1, and rVSV-Luc were inoculated into mice at a dose of 10^6 PFU through a combination of intranasal and oral routes. After inoculation, animals were evaluated daily for weight loss and the presence of any clinical signs. As shown in Fig.3.6, mice inoculated with rVSV-Luc had the

greatest weight loss ($P < 0.05$) among all the recombinant viruses tested. The rVSV-Luc inoculated mice also exhibited mild clinical signs of VSV infection, such as ruffled coat, at days 4 to 10 postinoculation. Mice inoculated with rVSV-VP1 and rVSV-HSP70 also showed a moderate weight loss ($P < 0.05$) up to 6 days postinoculation. For this group, weight gain was observed after day 6 postinoculation. No significant clinical signs of VSV infection were observed in these two groups. Interestingly, the rVSV-HSP70-VP1 treatment group had significantly less weight loss compared to the rVSV-VP1 and rVSV-HSP70 treatment groups ($P < 0.05$), and the body weight of the mice in this group recovered quickly at one week postinoculation. In addition, no significant clinical signs were observed during entire experimental period. Mice inoculated with DMEM and VLPs did not have any weight loss or clinical signs of disease. This experiment indicates that all recombinant viruses were attenuated in mice, compared to wild type rVSV which causes death in the mice. However, rVSV-HSP70-VP1 was more attenuated in mice than other recombinants including rVSV-VP1, rVSV-HSP70, and rVSV-Luc.

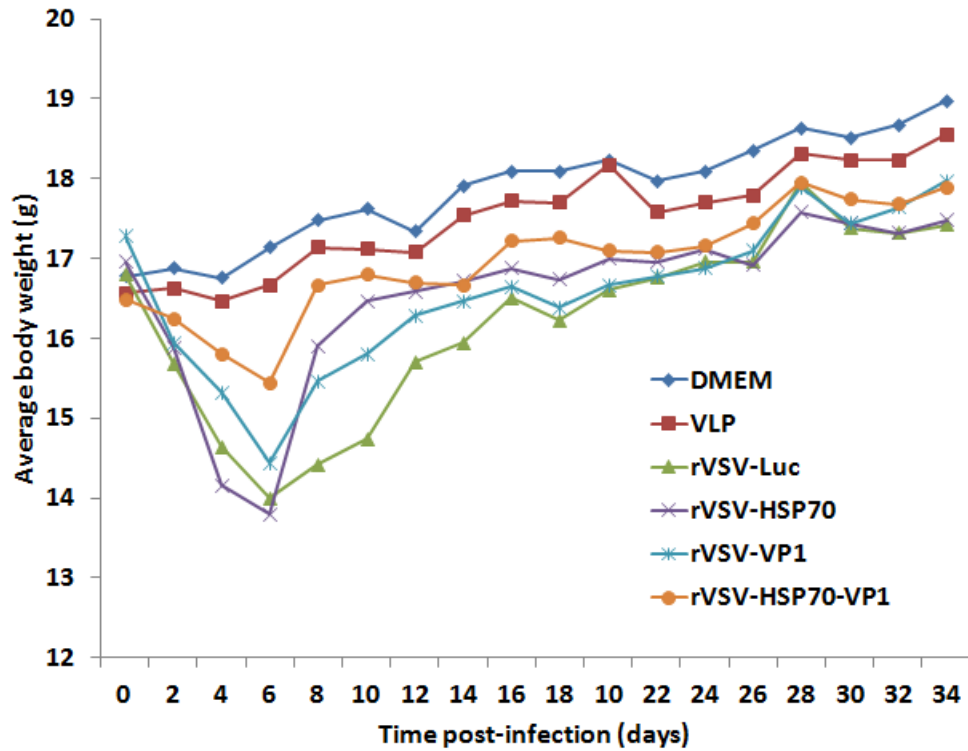


Figure 3.6. Dynamics of mouse body weight after inoculation with recombinant viruses.

Five BALB/c mice in each group were inoculated with 10^6 PFU of rVSV-Luc, rVSV-VP1, or rVSV-HSP70, or rVSV-HSP70-VP1 or 100 μ g of VLPs (purified from insect cells expressed by baculovirus) through the combination of intranasal and oral routes. Body weight for each mouse was evaluated every other day for 5 weeks. The average body weight of five mice was shown.

3.4.5 Recombinants rVSV-HSP70-VP1 and rVSV-VP1 triggered similar levels of humoral, cellular, and mucosal immunities in mice at dose of 10⁶ PFU.

To compare human NoV specific antibodies triggered by rVSV-VP1 and rVSV-HSP70-VP1, blood samples were isolated from each mouse and the serum IgG antibody response was determined by ELISA. The geometric mean titers (GMT) were calculated for each group of mice. As shown in Fig.3.7, mice inoculated with rVSV-VP1 and rVSV-HSP70-VP1 triggered significantly higher serum IgG responses than the mice that inoculated baculovirus-produced VLPs during 2-5 weeks postinoculation ($P < 0.05$). Both rVSV-VP1 and rVSV-HSP70-VP1 had a high level of antibody at one week postinoculation, and had a continuous increase in antibody titers through week 5. Mice inoculated with 100 µg of baculovirus-expressed VLPs had a similar level of human NoV-specific IgG antibodies at week 1 postinoculation. However, the IgG antibody in the VLP group had decreased by week 2 postinoculation. As controls, mice inoculated with rVSV-Luc, rVSV-HSP70, and DMEM did not have human NoV-specific serum IgG antibody responses during the experimental period. Thus, this experiment demonstrates that rVSV-VP1 and rVSV-HSP70-VP1 had a comparable IgG antibody response and had a significantly stronger antibody response than the traditional VLP-based vaccine candidate.

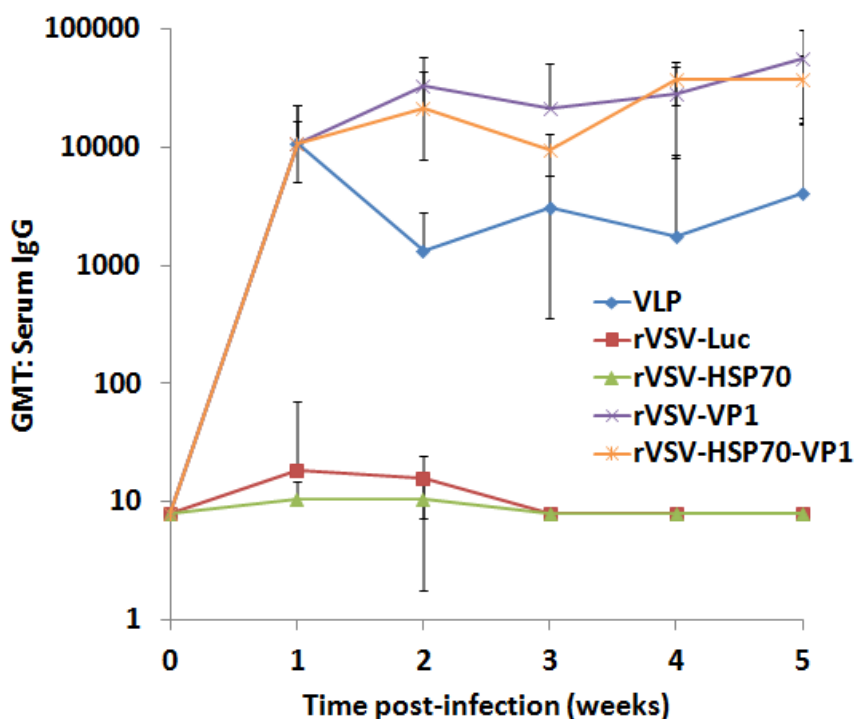


Figure 3.7. Serum IgG immune responses to VSV-based human NoV vaccines.

Groups of five BALB/c mice were inoculated with either 10^6 PFU of rVSV-VP1 or rVSV-HSP70-VP1 or 100 μ g of VLPs through the combination of intranasal and oral routes. Serum samples were collected weekly and analyzed by ELISA using human NoV-specific serum IgG antibody. Data was expressed as Geometric Mean Titers (GMT) of five mice. Error bars at each time point represent the standard deviation between mice.

To compare the cellular immune response, the spleen was isolated from each mouse at week 5 postinoculation, and the cellular immune responses were measured by a T cell proliferation assay. As shown in Fig.3.8, mice inoculated with rVSV-VP1 and rVSV-HSP70-VP1 stimulated higher human NoV-specific T cell proliferation than that

of traditional VLP-based vaccines ($P < 0.05$). However, there was no significant difference between the rVSV-VP1 and rVSV-HSP70-VP1 groups ($P > 0.05$). It should be emphasized that all mice in the rVSV-VP1 and rVSV-HSP70-VP1 groups had strong human NoV-specific T cell responses, with an average stimulation index of 9.6 and 12.0, respectively. In contrast, only three out of the five mice in the VLP group had a T cell immune response, with an average stimulation index of 4.8. As controls, mice inoculated with rVSV-Luc, rVSV-HSP70, and DMEM had background levels of T cell immune responses. Therefore, this data demonstrates that rVSV-VP1 and rVSV-HSP70-VP1 stimulate similar levels of T cell immune response, but were significantly stronger than the VLP-based vaccine candidate.

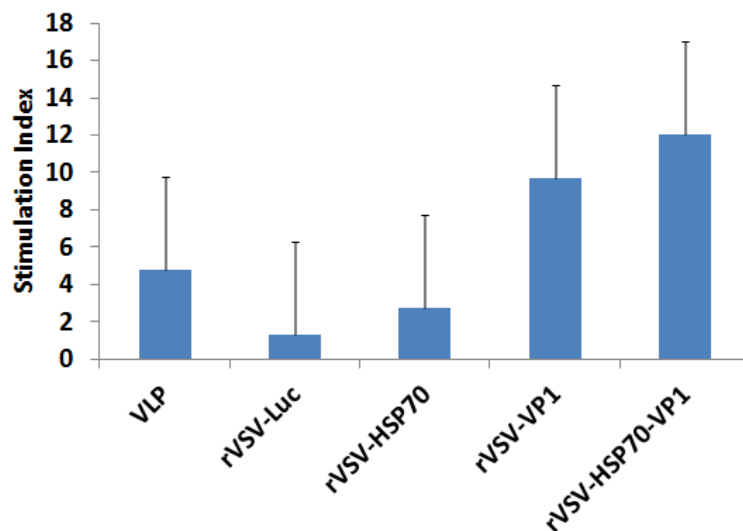


Figure 3.8. T cell proliferative responses to VSV-based human NoV vaccines.

Spleen cells were harvested from all mice in each group at week 5 post-inoculation, and stimulated with human NoV VLPs. T cell proliferation was measured by [^3H]thymidine

incorporation. The stimulation index (SI) was calculated as the mean of the following ratio: proliferation of human NoV VLP-stimulated cells/proliferation of cells in medium in cpm. Data was expressed as the mean of five mice \pm the standard deviation.

To compare the mucosal immune response, human NoV-specific and total IgA in fecal and vaginal extracts were determined by ELISA as described in Materials and Methods. The level of IgA response was expressed as the ratio between human NoV-specific IgA and total IgA. Prior to antigen inoculation, there was no human NoV-specific IgA in either fecal or vaginal samples in any mice. Figure 3.9 shows the fecal IgA antibody response at week 5 postinoculation. Only two out of five mice had an IgA response in the VLP vaccination groups. All mice in rVSV-VP1 group developed human NoV-specific IgA, while three out of five mice in the rVSV-HSP70-VP1 group exhibited an IgA response. Figure 3.10 shows the vaginal IgA antibody response at week 5 postinoculation. All mice in VLP, rVSV-VP1, and rVSV-HSP70-VP1 groups had a high level of human NoV-specific vaginal IgA antibody. In addition, rVSV-HSP70-VP1 stimulated much higher human NoV-specific IgA level in mice compare to VLP and rVSV-VP1 ($P < 0.05$). None of the mice in the rVSV-Luc, rVSV-HSP70, and DMEM groups showed human NoV-specific fecal and vaginal IgA antibody over the entire experimental period. Therefore, HSP70 enhances vaginal mucosal immunity against human NoV at dose of 10^6 PFU/mouse.

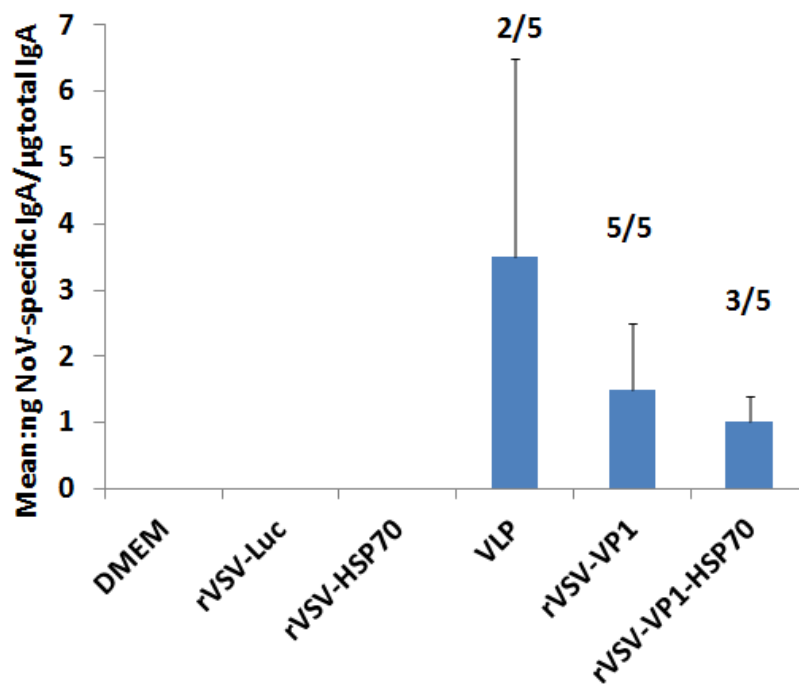


Figure 3.9. Fecal IgA responses to VSV-based human NoV vaccines.

Fecal samples were collected from all mice at week 5 post-inoculation. Samples were diluted in PBS, vortexed, and clarified by centrifugation. Human NoV-specific and total IgA antibody were detected by ELISA. The ratio between human NoV-specific IgA and total IgA was calculated for each mouse. Data was expressed as average titer of IgA-positive mice \pm standard deviation.

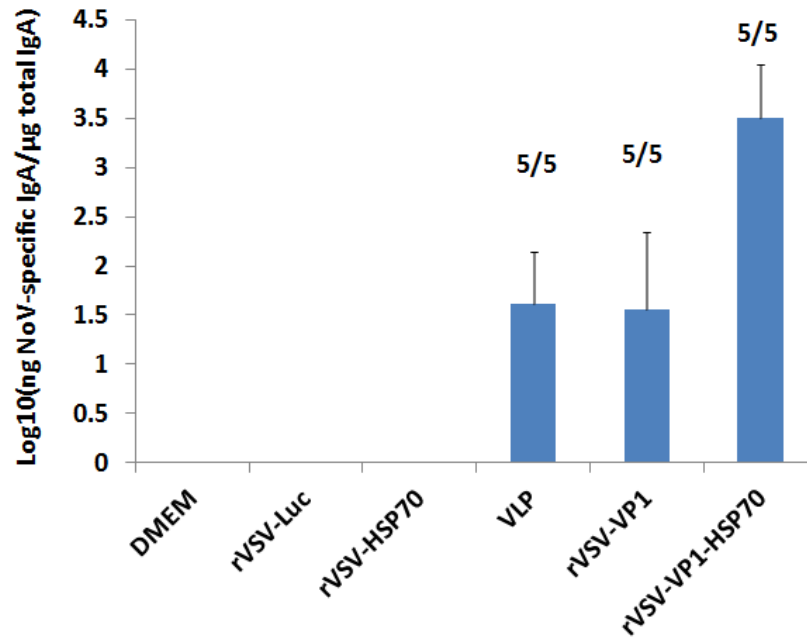


Figure 3.10. Vaginal IgA responses to VSV-based human NoV vaccines.

Vaginal samples were collected at week 5 post-inoculation from each mouse, and human NoV-specific and total IgA antibody were determined by ELISA. The level of vaginal IgA was shown as log 10 (ratio between human NoV-specific IgA and total IgA). Data was expressed as Geometric Mean Titer (GMT) of IgA-positive mice \pm standard deviation.

3.4.6 Recombinant rVSV-HSP70-VP1 stimulated higher T cell and mucosal immune responses than rVSV-VP1 at dose of 5×10^6 PFU.

The above experiments clearly demonstrated that rVSV-HSP70-VP1 and rVSV-VP1 stimulated similar levels of humoral, T cell, and fecal mucosal immunity in mice despite the fact that the VP1 protein (or VLPs) produced by rVSV-HSP70-VP1 was approximately 5 time less than that of rVSV-VP1, suggesting that HSP70 may play a role in regulating the immune response triggered by VP1 protein. To further characterize the role of HSP70, we increased the vaccination dosage to 5×10^6 PFU per mouse, the safety, serum IgG, T cell, and mucosal immune responses were determined as described above. As shown in Fig.3.11, a high dose (5×10^6 PFU) of rVSV-VP1 caused significant more weight losses compared to a low dose (10^6 PFU) of rVSV-VP1 ($P < 0.05$). However, within rVSV-HSP70-VP1, there is no significant weight difference between two doses ($P > 0.05$). Overall, mice received 5×10^6 PFU of rVSV-VP1 had more severe weight losses compared to 5×10^6 PFU of rVSV-HSP70-VP1 ($P < 0.05$), suggesting that rVSV-HSP70-VP1 was more attenuated than rVSV-VP1. Furthermore, mice inoculated with 5×10^6 PFU of rVSV-HSP70-VP1 did not exhibit any clinical signs of VSV infection whereas mice inoculated with 5×10^6 PFU of rVSV-VP1 exhibited mild clinical signs such as ruffled coat. As shown in Fig.3.12, mice inoculated with 5×10^6 and 10^6 PFU of rVSV-HSP70-VP1 and rVSV-VP1 stimulated similar levels of serum IgG antibody ($P > 0.05$), suggesting an increase in vaccination dose did not significantly enhance serum antibody responses. Interestingly, mice inoculated with 5×10^6 PFU of rVSV-HSP70-VP1 had significantly ($P < 0.05$) enhanced T cell proliferation as compared to all other

vaccination groups including 5×10^6 PFU of rVSV-VP1, 10^6 PFU of rVSV-VP1, and 10^6 PFU of rVSV-HSP70-VP1 (Fig.3.13). However, there was no significant difference ($P > 0.05$) in T cell immune response in mice vaccinated with 5×10^6 PFU of rVSV-VP1, 10^6 PFU of rVSV-VP1, and 10^6 PFU of rVSV-HSP70-VP1. Finally, fecal and vaginal IgA antibody responses were also determined. As shown in Fig.3.14, mice inoculated with 5×10^6 PFU of rVSV-HSP70-VP1 stimulated significantly higher fecal IgA antibody responses as compared to all other vaccination groups ($P < 0.05$). In addition, vaginal IgA in 5×10^6 PFU of rVSV-VP1, 5×10^6 PFU of rVSV-VP1-HSP70, and 10^6 PFU of rVSV-HSP70-VP1 was significantly higher than 10^6 PFU of rVSV-VP1 ($P < 0.05$) (Fig. 3.15). As controls, mice inoculated with DMEM and rVSV-HSP70 had background levels of serum IgG antibody, T cell proliferation, or fecal and vaginal IgA antibody responses. Thus, these data demonstrated that HSP70 enhanced T cell and mucosal immunities but not humoral antibody response at inoculation dose of 5×10^6 PFU per mouse.

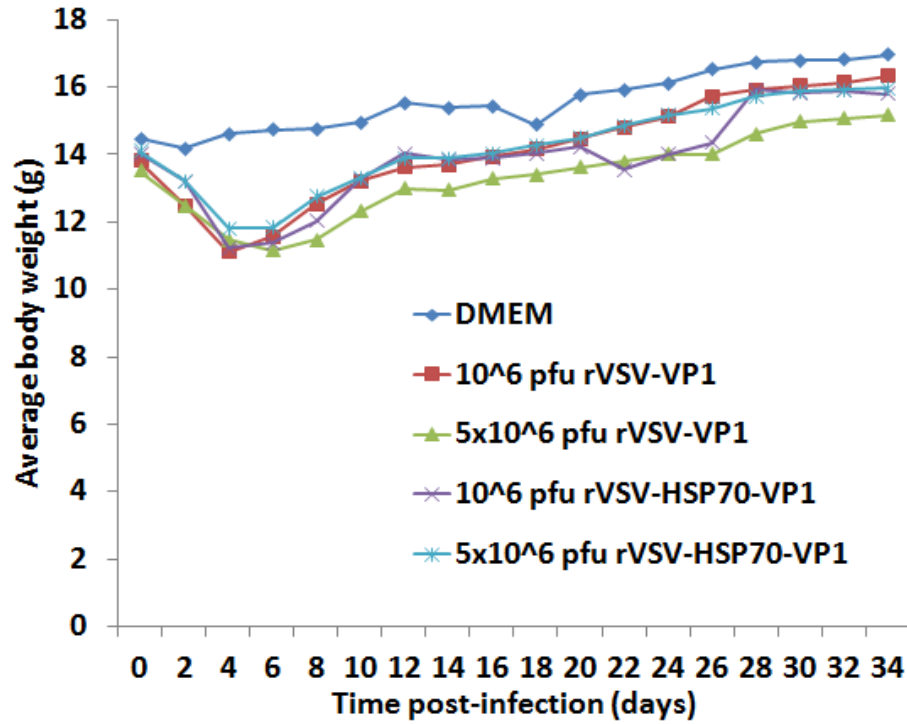


Figure 3.11. Dynamics of mouse body weight after inoculation with recombinant viruses.

Five BALB/c mice in each group were inoculated with either 10^6 PFU of rVSV-VP1, or 10^6 PFU of rVSV-HSP70-VP1, or 5×10^6 PFU of rVSV-VP1, or 5×10^6 PFU of rVSV-HSP70-VP1. Body weight for each mouse was measured every other day for 5 weeks. The average body weight of five mice was shown.

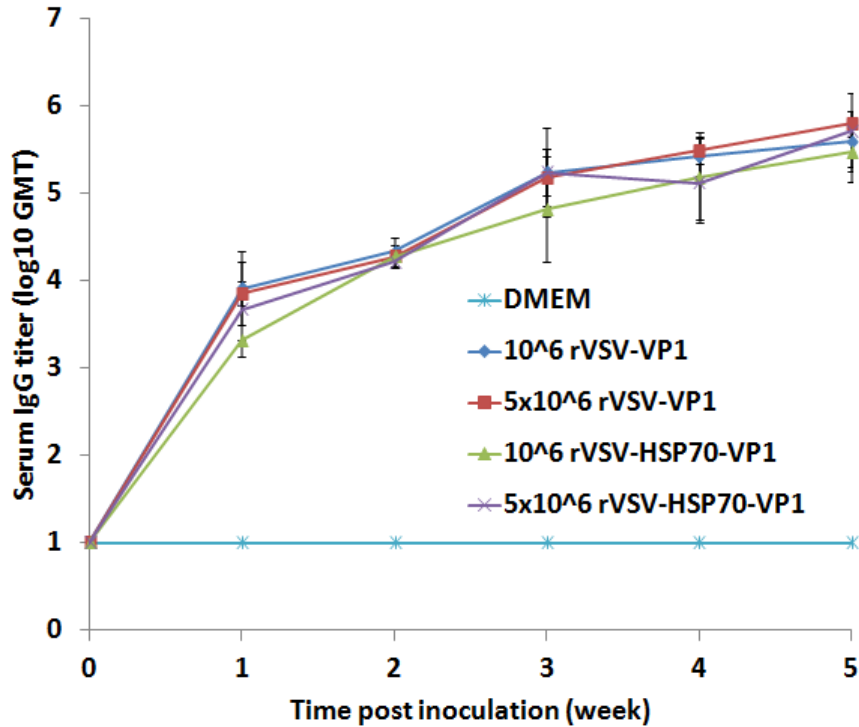


Figure 3.12. Serum IgG immune responses to VSV-based human NoV vaccines.

Groups of five BALB/c mice were inoculated with either 10⁶ PFU of rVSV-VP1, 10⁶ PFU of rVSV-HSP70-VP1, 5×10⁶ PFU of rVSV-VP1, or 5×10⁶ PFU of rVSV-HSP70-VP1. Serum samples were collected weekly and analyzed by ELISA using human NoV-specific serum IgG antibody. Data was expressed by Geometric Mean Titers (GMT) of five mice. Error bars at each time point represent the standard deviation between mice.

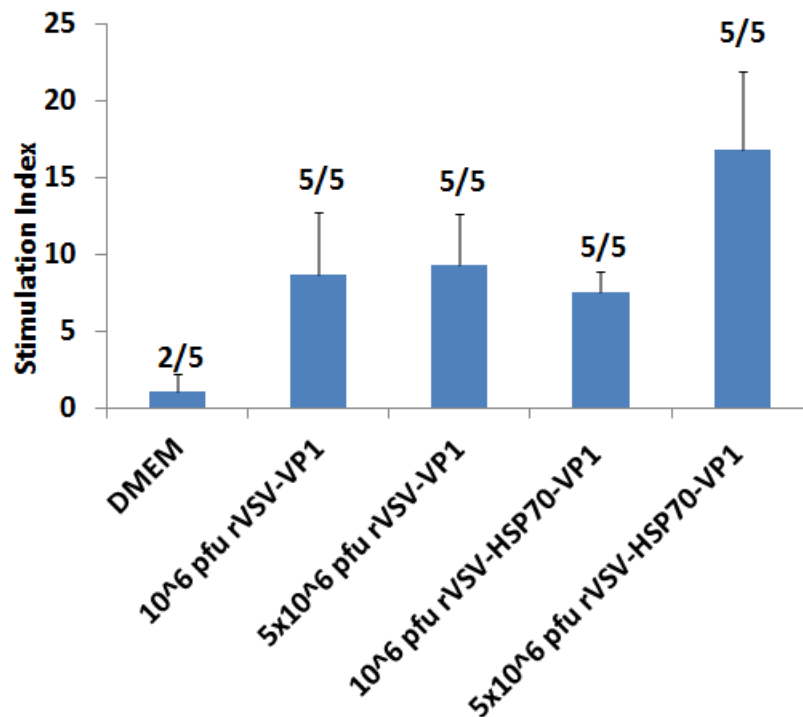


Figure 3.13. T cell proliferative responses to VSV-based human NoV vaccines.

Spleen cells were harvested from all mice in each group at week 5 post-inoculation, and stimulated with human NoV VLPs. T cell proliferation was measured by [³H]thymidine incorporation. The stimulation index (SI) was calculated as the mean of the following ratio: proliferation of human NoV VLP-stimulated cells/proliferation of cells in medium in cpm. Data was expressed as the mean of five mice ± the standard deviation.

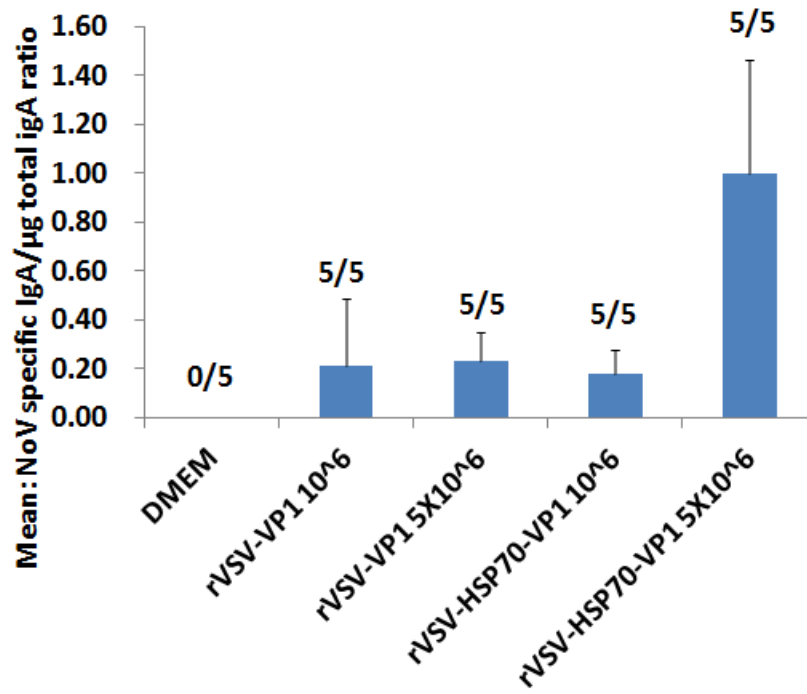


Figure 3.14. Fecal IgA responses to VSV-based human NoV vaccines.

Fecal samples were collected from all mice at week 5 post-inoculation. Samples were diluted in PBS, vortexed, clarified by centrifugation, and human NoV-specific and total IgA antibody were determined by ELISA. The ratio between human NoV-specific IgA and total IgA was calculated for each mouse. Data was expressed as average titer of IgA-positive mice \pm standard deviation.

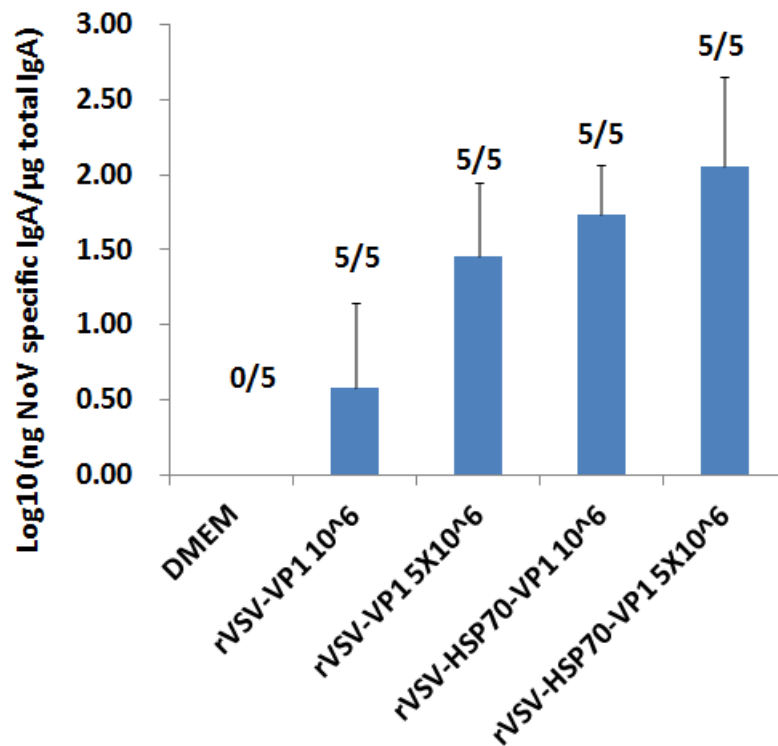


Figure 3.15. Vaginal IgA responses to VSV-based human NoV vaccines.

Vaginal samples were collected at week 5 post-inoculation from each mouse, and human NoV-specific and total IgA antibody were determined by ELISA. The level of vaginal IgA was shown as log 10 (ratio between human NoV-specific IgA and total IgA). Data was expressed as Geometric Mean Titer (GMT) of IgA-positive mice \pm standard deviation.

3.4.7 Enhanced mucosal immune responses by combination of rVSV-VP1 and rVSV-HSP70 vaccination.

If HSP70 indeed enhances the immune response triggered by the VSV-based human NoV vaccine, we expect that similar enhancement effects may be observed by administering a combined vaccination of rVSV-HSP70 and rVSV-VP1. Interestingly, mice received a combination of 10^6 PFU of rVSV-HSP70 and 10^6 PFU of rVSV-VP1 had significantly less weight loss compared to mice received 10^6 PFU of rVSV-VP1 alone ($P < 0.05$) (Fig. 3.16). As shown in Fig. 3.17, mice receiving the combination vaccination stimulated similar levels of serum IgG antibody compared to rVSV-VP1 vaccination alone. However, the combination vaccination triggered significantly higher intestinal (Fig. 3.18) and vaginal IgA (Fig. 3.19) antibody responses than single vaccination. As controls, mice inoculated with DMEM had background levels of immune responses. Therefore, this data demonstrated that combined vaccination of rVSV-HSP70 and rVSV-VP1 (at ratio of 1:1) enhanced human NoV specific mucosal immunity.

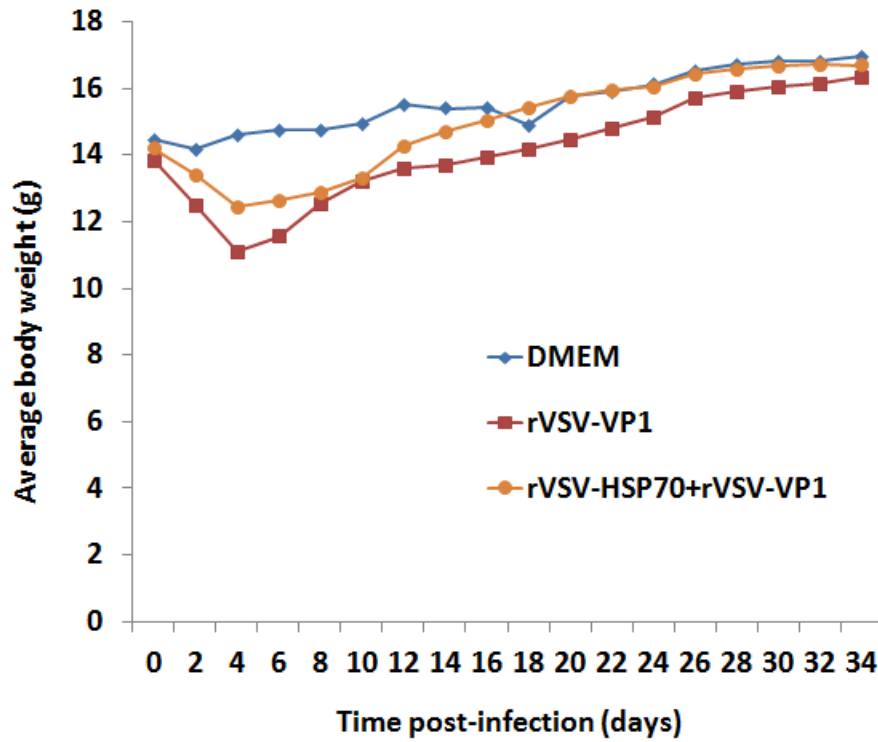


Figure 3.16. Dynamics of mouse body weight after inoculation with recombinant viruses for animal study 3.

Five BALB/c mice in each group were inoculated with either 10^6 PFU of rVSV-VP1, or the combination of 10^6 PFU of rVSV-VP1 and 10^6 PFU of rVSV-HSP70. Body weight for each mouse was evaluated every other day for 5 weeks. The average body weight of five mice was shown.

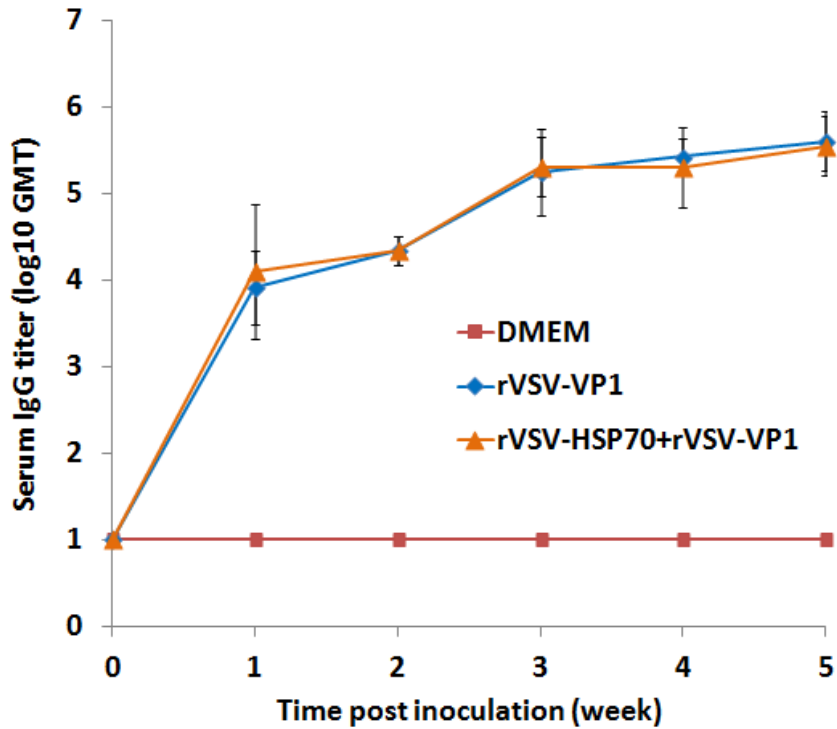


Figure 3.17. Serum IgG immune responses to VSV-based human NoV vaccines.

Groups of five BALB/c mice were inoculated with either 10^6 PFU of rVSV-VP1, or the combination of 10^6 PFU of rVSV-VP1 and 10^6 PFU of rVSV-HSP70. Serum samples were collected weekly and analyzed by ELISA using human NoV-specific serum IgG antibody. Data was expressed by Geometric Mean Titers (GMT) of five mice. Error bars at each time point represent the standard deviation between mice.

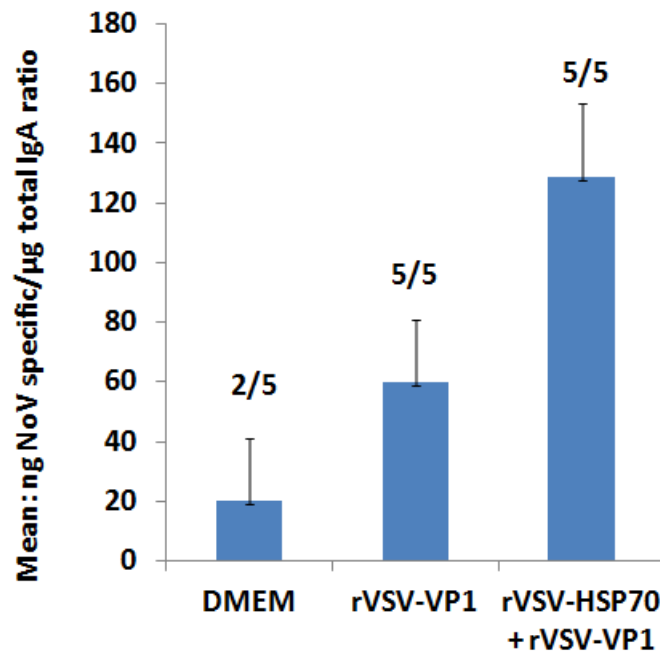


Figure 3.18. Fecal IgA responses to VSV-based human NoV vaccines.

Fecal samples were collected from all mice at week 5 post-inoculation. Samples were diluted in PBS, vortexed, and clarified by centrifugation. Human NoV-specific and total IgA antibody were detected by ELISA. The ratio between human NoV-specific IgA and total IgA was calculated for each mouse. Data was expressed as average titer of IgA-positive mice \pm standard deviation.

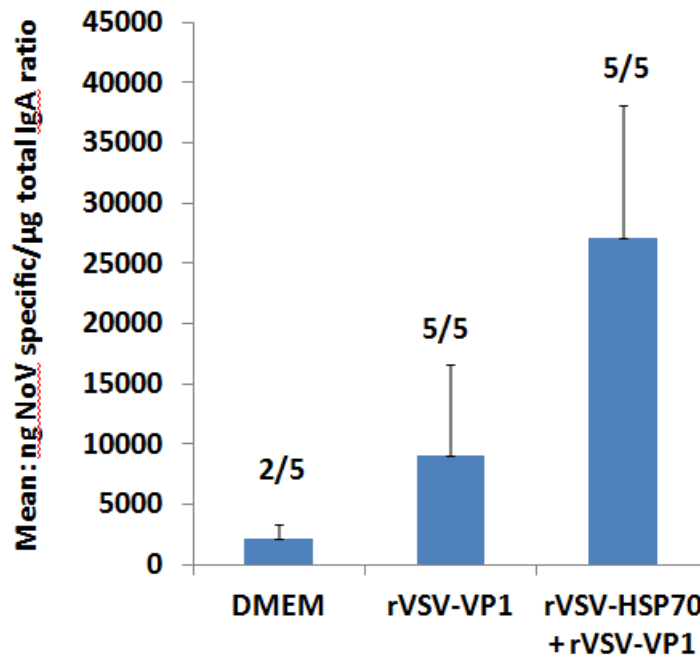


Figure 3.19. Vaginal IgA responses to VSV-based human NoV vaccines.

Vaginal samples were collected at week 5 post-inoculation from each mouse, and human NoV-specific and total IgA antibody were determined by ELISA. The level of vaginal IgA was shown as ratio between human NoV-specific IgA and total IgA. Data was expressed as Geometric Mean Titer (GMT) of IgA-positive mice \pm standard deviation.

3.5 Discussion

3.5.1 HSP70 enhances the safety of VSV-based human NoV vaccine.

One of the major concerns of VSV-based vaccines is safety, particularly since VSV is neurotropic. VSV infects a wide range of wild and domestic animals such as cattle, horses, deer and pigs, and produced vesicular lesions in the mouth, tongue, lips, gums, teats, and feet. Although VSV does not cause vesicular diseases in mice, the mouse is an

excellent small animal surrogate model to understand VSV pathogenesis because VSV causes systemic infection and fatal encephalitis. After intranasal inoculation, VSV infects olfactory neurons in the nasal mucosa and subsequently enters the central nervous system (CNS) through the olfactory nerves (Reiss et al., 1998). The virus is then disseminated to other areas in the brain through retrograde and possibly anterograde trans-neuronal transport, ultimately causing an acute brain infection (Cornish et al., 2001). The mortality, pathology, and viral burden in lung and brain tissues are dependent on the age and species of the mice.

A variety of approaches have been employed to attenuate VSV, including gene rearrangement (Wertz et al., 1998), M gene mutation (Ahmed et al., 2008), G protein cytoplasmic tail truncations (Fang et al., 2012), G protein deletions (Schnell et al., 1997), and combinations thereof. These approaches decreased viral replication in cell culture as well as virulence in mice. In this study, it was found that double insertion of HSP70 and VP1 into VSV vector resulted in further attenuation of VSV in cell culture as well as in mice. Recombinant rVSV-HSP70-VP1 formed much smaller plaques, replicated less efficiently, and synthesized less VSV proteins in cell culture compared to rVSV-VP1. In mice, rVSV-HSP70-VP1 had less body weight loss and did not exhibit clinical signs of VSV infection. Thus, insertion of multiple genes in the VSV genome backbone can serve an additional approach to further attenuate VSV vector. Presumably, HSP70 enhances the safety of VSV vector by two potential mechanisms. First, insertion of HSP70 gene at 3' end of VSV genome decreases transcription of downstream genes which in turn impairs viral replication in vitro and in vivo. This is consistent with the mechanism of VSV gene

expression in which transcription of the VSV genome results in a gradient of mRNA synthesis and protein expression. Second, expression of HSP70 from VSV vector may enhance virus clearance. Previously, it has been shown that HSP70 enhanced viral clearance of measles virus and canine distemper virus in mice (Oglesbee et al., 2002). Co-delivery of HSP70 and measles virus to mice significantly reduced virus titer and viral RNA burden in brain and lungs. However, it was also shown that HSP70 interacts with N protein of measles virus and enhances viral replication. It is not known how HSP70 modulates the balance between viral replication and viral clearance. In this study, it was found that mice co-administration of 10^6 PFU of rVSV-VP1 and rVSV-HSP70 to mice resulted in significant less weight loss compared to mice received 10^6 PFU of rVSV-VP1 alone ($P < 0.05$), suggesting that HSP70 may enhance clearance of VSV.

3.5.2 HSP70 enhances the immunogenicity of the viral vaccine.

HSP70 has been shown a strong adjuvant for a number of viral vaccines including porcine reproductive and respiratory syndrome virus (PRRSV) (Li et al., 2009a), Japanese encephalitis (JE) virus (Fei-fei et al., 2008; Ge et al., 2007), Hantaan virus (Li et al., 2008a), respiratory syncytial virus (RSV) (Zeng et al., 2008), measles virus (Oglesbee et al., 2002), and canine distemper virus (Oglesbee et al., 1996). PRRSV causes immunosuppression in pigs. It was found that recombinant adenoviruses expressing GP3/GP5 of highly pathogenic PRRSV and HSP70 stimulated stronger humoral immunity and cytokine responses (IFN-gamma and IL-4) and provided protection against virulent PRRSV challenge in pigs. However, adenoviruses expressing GP3/GP5 alone is

insufficient to induce protective immune responses in pigs. Co-delivery of HSP70 with a RSV subunit vaccine (G1F/M2) induced significant higher levels of neutralizing antibodies and CTL activity than unadjuvanted G1F/M2. Fusion of HSP70 to the nucleocapsid protein (NP) of Hantaan virus (HSP70-NP) or co-delivery of HSP70 and NP proteins (HSP70+NP) elicited significantly higher NP-specific antibody titers, and higher frequencies of IFN-gamma-producing cells and cytotoxic T lymphocyte (CTL) activities in vivo than conventional NP vaccination alone (Li et al., 2008a). HSP70 also enhanced T lymphocyte proliferation and interferon (IFN)-gamma and interleukin (IL)-4 secretion, and produced virus-specific memory B cells and long-lasting antibodies when fused with the envelope (E) protein of JE virus (Fei-fei et al., 2008).

In this study, we found that HSP70 enhanced the immunogenicity of human NoV vaccine when co-expressed from a VSV vector. At the same inoculation dose (1×10^6 PFU), rVSV-HSP70-VP1 and rVSV-VP1 triggered similar levels of specific humoral, mucosal, and cellular immunity in spite of the fact that VP1 expression by rVSV-HSP70-VP1 was approximately five-fold less than that of rVSV-VP1. This suggests that HSP70 play a role in modulating the VSV-based human NoV vaccine. To compensate for reduced VP1 expression levels of rVSV-HSP70-VP1, we increased the inoculation dose of rVSV-HSP70-VP1 five-fold to 5×10^6 PFU/mouse. We found that mice immunized with 5×10^6 PFU of rVSV-HSP70-VP1 generated significantly higher mucosal and T cell immunity than those immunized with rVSV-VP1 ($P < 0.05$). In addition, co-administration of rVSV-HSP70 and rVSV-VP1 triggered a stronger mucosal immunity than rVSV-VP1 alone. These results demonstrated that HSP70 is an adjuvant for human NoV vaccine. In

the future, it will be of great interest to investigate the mechanisms by which HSP70 enhances human NoV specific immunity.

3.5.3 VSV as a vector to delivery viral vaccines.

In the last decade, VSV has been proved to be an excellent vector to deliver foreign antigens as live vaccines, oncolytic therapy, and gene delivery (Majid et al., 2006b; Roberts et al., 1999a; Rose et al., 2001). VSV is suitable to deliver vaccines against following three viral pathogens: viruses that cause persistent infection such as HIV (Rose et al., 2001; Tan et al., 2005) and HCV (Buonocore et al., 2002); viruses that are highly lethal such as SARS (Faber et al., 2005; Kapadia et al., 2005), Ebola, and Marburg viruses (Geisbert et al., 2008a); and viruses that cannot be grown in cell culture such as human NoV. The drawback for VSV vector is that there is little experience with VSV administration in humans. However, at least three independent phase I human clinical trials are currently being carried out to test the safety, immune response, and effectiveness of the VSV-based vaccine and oncolytic therapy in human. Two VSV-based HIV vaccines (VSV-Indiana HIV gag vaccine, and HIV DNA vaccine followed by VSV-gag vaccine boost) are currently recruiting healthy, HIV-uninfected adults for the phase I clinical trials. Recombinant VSV expressing interferon beta has been approved for phase I clinical trials to treat patient with cancer. It seems clear that detailed information on safety, replication, pathogenesis, and immunogenicity of VSV-based vaccines in humans will be forthcoming.

In summary, it was found that (i) insertion of HSP70 into VSV vector further attenuates the VSV-based vaccine in cell culture in the mice model, and (ii) HSP70 enhances the human NoV-specific immunity triggered by VSV-based human NoV vaccine.

Chapter 4 : A vesicular stomatitis virus (VSV)-based human norovirus vaccine provides protection against norovirus challenge in a gnotobiotic pig model

4.1 Abstract

Human norovirus (NoV) is a major causative agent of acute gastroenteritis worldwide. It is difficult to work with this viral group as they cannot be propagated *in vitro* and lack a small animal model. Currently, there are no vaccines or effective therapeutic interventions for human NoV infection. Previously, it was demonstrated that a recombinant vesicular stomatitis virus (rVSV)-based vaccine candidate stimulated strong humoral, mucosal, and T cell immune responses against human NoV in mice. However, whether this vaccine candidate can confer protection from human NoV challenge is not known. In this study, we developed a human NoV challenge gnotobiotic pig model to examine the pathogenesis of human NoV and to test the immunogenicity of the rVSV-based vaccine. We demonstrated that newborn gnotobiotic piglets vaccinated intranasally with 2×10^7 PFU of rVSV-based vaccine induced high levels of human NoV-specific serum IgG and fecal and vaginal IgA antibody levels; mock-infected or unvaccinated control groups remained antibody-negative. Three weeks after vaccination, piglets were orally challenged with human NoV GII.4 strain 7I. Protective effects were measured by viral shedding in stools and histologic changes in the intestines. All three piglets in the

unvaccinated challenged group developed histopathologic lesions typical of human NoV infection including villous atrophy, segmented epithelial cell necrosis, and increased mononuclear inflammatory cell infiltrates including syncytial giant cells in the lamina propria of the duodenum and proximal jejunum by post-challenge day 5. In contrast, only one of five vaccinated piglets exhibited focal epithelial necrosis and villous atrophy in the duodenum. As well, one of five piglets had mild edema in jejunal lamina propria. Taken together, these results demonstrate that the rVSV-based human NoV vaccine triggered strong immunity in swine and protected gnotobiotic pigs from challenge by human NoV.

4.2 Introduction

Human norovirus (NoV) is the leading causative agent of acute nonbacterial gastroenteritis worldwide. Despite the significant health and economic impact caused by human NoV, no vaccines are currently available for this virus. Two major challenges have been encountered in the development of an effective vaccine against human NoV. First, human NoV cannot be propagated in cell culture. Therefore, we must rely on human clinical specimens to prepare a large pool of human NoV stock that can be used for challenge studies. Second, there are no small animal models for human NoV. Thus, it has been highly challenging to explore whether a vaccine candidate is able to protect hosts from clinical symptoms such as gastroenteritis, intestinal histologic changes, and viral shedding. To date, human NoV virus-like particles (VLPs) (Ball et al., 1998), P particle (Tan et al., 2011), and alphavirus-based human NoV vaccine (LoBue et al., 2009)

candidates have been shown to trigger variable immune responses in rodent models. However, mice cannot be used as an animal challenge model because they are not permissive for human NoV infection. Therefore, little is known whether these vaccine candidates are actually protective, even though they have been shown to be immunogenic. To date, limited information about the efficacy of human NoV vaccine candidates is available and is based on the study of human volunteer subjects. Although human volunteer studies are valuable, the susceptibility of an individual to human NoV depends on their preexisting immunity, blood type, and age. Moreover, based on safety concerns, human volunteer studies should be limited. Therefore, the development of an animal model to understand the pathogenesis and immunology of human NoV is urgently needed.

Gnotobiotic pigs are immunocompetent at birth, lacking maternal antibodies and any exposure to microbial antigens. They are delivered by C Section and protected from the environment and contamination with commensals and other infectious pathogens by physical barriers provided by isolation units. The similarities between human and pig gastrointestinal structure, physiology, and immunology are increasingly being utilized for infectious disease studies, with pigs mimicking many aspects of human physiology and recognized as significantly more predictive of therapeutic efficacy than rodent models. Thus, the gnotobiotic pig is an ideal model to study the primary immune response of a specific pathogen. To date, the gnotobiotic pig has been used as an animal model to study the pathogenesis and immunogenicity of human enteric viruses, such as

rotavirus (Yuan et al., 1996) and human NoV (Cheetham et al., 2006); human bacterial pathogens such as *Helicobacter pylori* (Krakowka et al., 1991), and porcine pathogens such as porcine circovirus 1 and 2, porcine parvovirus, porcine reproductive and respiratory virus (Krakowka et al., 2000), and porcine torque teno virus (Krakowka and Ellis, 2008). Previously, it has been shown that pigs infected with human NoV GII.4 strain HS66 showed mild diarrhea, virus shedding, seroconversion, and lesions in the intestines, suggesting that human NoV is able to replicate in gnotobiotic pigs (Cheetham et al., 2006). In addition, a VLPs-based vaccine candidate induced norovirus-specific immune responses in gnotobiotic pigs and protected pigs from viral shedding and diarrhea (Souza et al., 2007b).

In Chapters 2 and 3, it was demonstrated that a recombinant vesicular stomatitis virus (rVSV)-based human NoV vaccine candidate triggered strong humoral, cellular, and mucosal immunity in BALB/c mice. Although these results are promising, it is not known whether the VSV-based human NoV vaccine candidate can protect the host from challenge with human NoV. Therefore, the objectives of this chapter are to identify human NoV clinical isolates from recent outbreaks, to examine the pathogenesis of these human NoV clinical strains in gnotobiotic pigs, and finally to determine whether the VSV-based human NoV vaccine candidate can protect pigs from virulent human NoV challenge.

4.3 Materials and Methods

4.3.1 Characterization of three human norovirus GII.4 strains.

Human NoV clinical isolates 5M, 7I, and 7G were originally isolated from an outbreak of acute gastroenteritis in Ohio. Stool samples were diluted 1:10 in PBS, shaken vigorously for 1 min and centrifuged for 30 min at 3,500×g. The sample was filtered through 0.8 µm and 0.22 µm filters, aliquoted and stored at -80 °C until use. Viral RNA was extracted from specimens using an RNeasy Kit (Qiagen) and first strand cDNA was synthesized by SuperScriptase III (Invitrogen). The entire genomic cDNA of these human NoV strains was amplified by RT-PCR using five to six overlapping fragments. The sequence of the primers and their locations in viral genome are summarized in Table 1 and Figure 1, respectively. The fragments were then amplified by Platinum PCR Supermix (Invitrogen, MD), with a denaturation step at 94 °C for 30s, an annealing step at 55 °C for 30s, and an elongation step at 72 °C for 2min. The PCR products were then purified and cloned into a pGEM-T-easy vector (Promega), and sequenced at the Plant Microbe Genetics Facility at The Ohio State University. The genomic RNA was then quantified by real-time RT-PCR. To confirm that other enteric viruses, such as human sapovirus and rotaviruses, were not present, two sets of primers were designed to amplify human sapovirus and rotavirus-specific genes.

Table 4.1. Primers for cloning and sequencing the genome of human NoV.

Name	Sequence (5' to 3')
NoV(+)-1-22	GTGAATGAAGATGGCGTCTAAC
NoV(-)-1920-1899	GCGTTCTTCCACATGTCAGGTT
NoV(+)-1832-1855	CGCATCGATTTCTCGTGTATGCA
NoV(-)-3702-3682	GCTGGTTCATAGGTGCCAGGT
NoV(+)-3595-3614	CTGTGGTGCACCAATCCTAG
NoV(-)-5304-5284	CACCTGGAGCGTTTCTAGG
NoV VP1 up	ATGAAGATGGCGTCGAATGAC
NoV VP1 down	TTATAATACACGTCTGCGCCC
NoV(+)-5199-5219	GCACCTGTAGCGGGCCAACAA
NoV(-)-7096-7076	GCGGCCTGCATTGTATGTTGT
NoV(+)-7001-7023	CAATCAACGCCCCCATGACAAA
NoV(-)-7558-7536	AAAGACACTAAAGAAGAGAAAGA

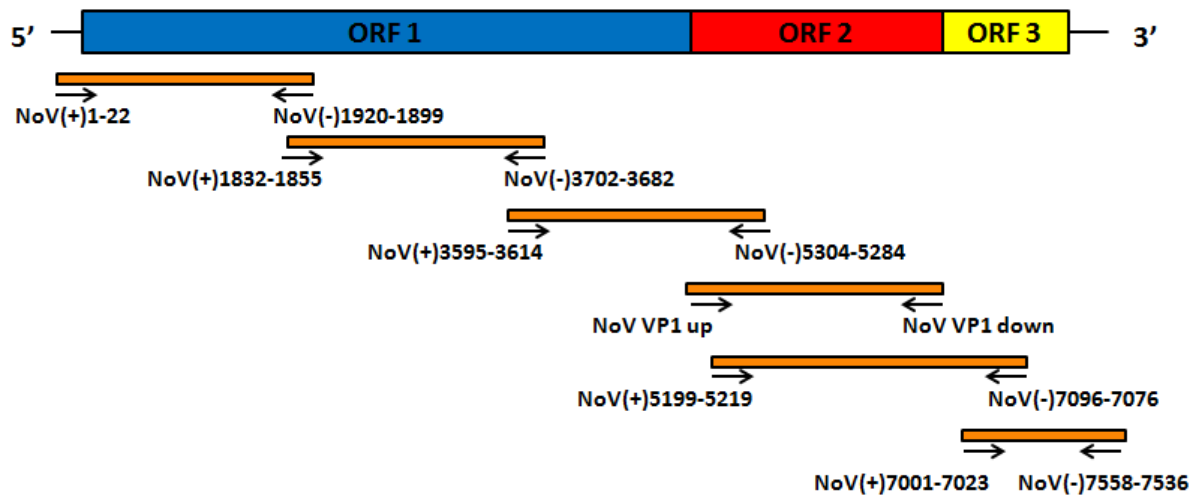


Figure 4.1. Primers for cloning and sequencing the genome of human NoV.

Schematic representation of the human NoV genome is shown. The blue, red, and yellow boxes indicate open reading frames (ORF) 1, 2, and 3 respectively. Arrows indicate the positions and directions of the primers that were used for amplifying and sequencing the human NoV genome. Orange boxes represent the PCR products amplified by the corresponding primers. The detailed sequences of the primers are shown in Table 4.1.

4.3.2 Quantification of viral RNA by real-time RT-PCR.

Since human NoV cannot be grown in cell culture, real-time RT-PCR was used to quantify viral genomic RNA copies. Briefly, total RNA was extracted from samples using an RNeasy Kit (Qiagen), followed by reverse transcription and real-time PCR. First strand cDNA was synthesized by SuperScriptase III (Invitrogen) using the primer VP1-P1 (5'- TTATAATACACGTCTGCGCCC-3'), which targets the VP1 gene of human

NoV. The VP1 gene was then quantified by real-time PCR using custom Taqman primers and probes (Forward primer, 5'-CACCGCCGGGAAAATCA-3') (Reverse primer: 5'-GCCTTCAGTTGGGAAATTTGG-3') (Reporter: 5'-FAM-ATTTGCAGCAGTCCC-NFQ-3') on a StepOne real-time PCR machine (Applied Biosystems, Foster City, CA). PCR reaction and cycling parameters followed the manufacturer's protocol (Invitrogen). Briefly, TaqMan Fast Universal Master Mix was used for all reactions. For cycling parameters, a holding stage at 95°C was maintained for 2 minutes prior to cycling, followed by 40 cycles of 94°C for 15 seconds for denaturation, 55°C for 30 seconds for annealing, and 72°C for 15 seconds for extension. Standard curves and StepOne Software v2.1 were used to quantify genomic RNA copies. Viral RNA was expressed as mean log₁₀ genomic RNA copies/ml ± standard deviation.

4.3.3 Delivery of gnotobiotic piglets.

All animal protocols used in this study were approved by the Institutional Laboratory Animal Care and Use Committee. Date-mated pregnant adult multiparous sows were purchased from a commercial pork production unit (Shoup Brothers, Smithville, OH) and transported to the Goss Laboratory at The Ohio State University for Caesarian delivery of gnotobiotic piglet litters using previously described methods (Eaton et al., 1996). The surgery (Caesarian section) was performed on or near the 112th day of gestation. Piglets were then maintained in sterile isolator units. The average size of litters ranged from 10-16 piglets.

4.3.4 Pathogenesis of human NoV in gnotobiotic piglets.

Experimental design was depicted in Figure 2A. Fourteen two-day-old gnotobiotic piglets from one litter were randomly divided into three groups (five pigs per group for virus challenge, and 4 pigs per group for mock infected control). Prior to virus inoculation, all the piglets received 8 ml of 100 mM sodium bicarbonate orally to neutralize stomach acids. Piglets in group 1 were inoculated orally with 5 ml of DMEM and served as normal controls. Piglets in groups 2 and 3 were inoculated with 10^8 genomic RNA copies of human NoV isolates 5M and 7I, respectively. After virus challenge, rectal swabs were collected, and diarrhea scores were recorded (0, normal; 1, pasty; 2, semiliquid; 3, watery). The diarrhea cumulative score of each pig represents the sum of daily rectal swab scores. The mean cumulative score of each group was calculated using the following formula: The sum of each pig's diarrhea cumulative score divided by the number of pigs. Fecal samples were also used for the determination of viral shedding by real time RT-PCR. All the piglets were sacrificed at day 7 post-inoculation. After termination, segments of intestines (duodenum, jejunum, ileum, and terminal colon), intestinal contents, spleen, kidney, and liver were collected for the examination of gross pathological and histopathological changes, and the detection of viruses.

4.3.5 Immunogenicity of VSV-based human NoV vaccine (rVSV-VP1) in gnotobiotic piglets.

Experimental design was depicted in Figure 2B. Eleven two-day-old gnotobiotic piglets from one litter were randomly divided into three groups. The 5 piglets in group 1 were

vaccinated intranasally with 2×10^7 PFU of recombinant VSV expressing the human NoV capsid protein (rVSV-VP1). The 3 piglets in group 2 were inoculated intranasally with 2×10^7 PFU of recombinant VSV expressing luciferase (rVSV-Luc). The 3 piglets in group 3 received 500 μ l of DMEM intranasally. After inoculation, piglets were observed twice a day to evaluate clinical symptoms of VSV infection including fever, body weight reduction, and vesicular lesions. Blood samples were collected weekly for determination of serum IgG. At week 4 post-vaccination, fecal, nasal, and vaginal swab samples were collected for determination of mucosal IgA antibodies. At week 4 post-vaccination, piglets in groups 1 and 2 were challenged with 10^8 genomic RNA copies of human NoV GII.4 strain 7I, piglets in group 3 were inoculated with 5ml MEM. Prior to challenge, all the piglets received 8 ml of 100 mM sodium bicarbonate orally to neutralize stomach acids. After virus challenge, rectal swabs were collected, and diarrhea scores were recorded daily. Fecal samples were also used for the determination of viral shedding. All the piglets were sacrificed at day 5 post-challenge. After termination, segments of intestines (duodenum, jejunum, ileum, and terminal colon), intestinal contents, spleen, kidney, and liver were collected for the examination of gross pathological and histopathological changes, and the detection of viruses.

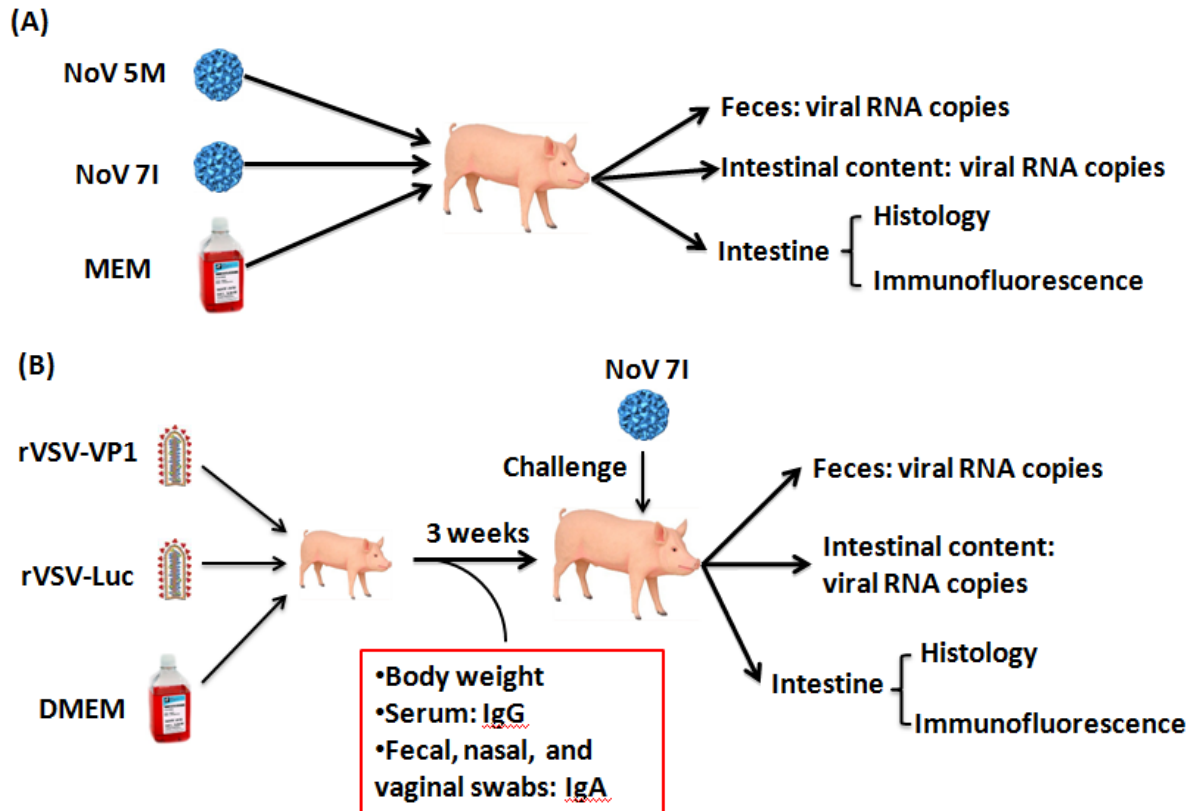


Figure 4.2. Flow diagrams of experimental design.

(A) Pathogenesis of human NoV strains 7I and 5M in gnotobiotic piglets. (B)

Immunogenicity of VSV-based human NoV vaccine (rVSV-VP1) in gnotobiotic piglets.

4.3.6 Detection of human NoV in feces, intestinal contents, intestinal tissues by real-time RT-PCR.

Fecal samples from rectal swabs were eluted in 300 μ l MEM at a dilution of 1:5. Intestinal contents from different sections of intestines (duodenum, jejunum, ileum, and terminal colon) were diluted in 80 μ l MEM at a dilution of 1:5. All samples were centrifuged at 6,000 g for 5 min, and supernatants were collected for RNA extraction using an RNeasy Mini kit (Qiagen, Valencia, CA). Twenty mg of intestinal tissues were

homogenized in liquid N₂ and used for total RNA extraction. The presence of human NoV RNA was detected by real-time RT-PCR using the procedure described above. Negative controls (rectal swabs, intestinal contents, and intestinal tissues from mock-inoculated pigs) for RNA extraction and real-time RT-PCR were included in each assay.

4.3.7 Indirect immunofluorescence on whole intestinal tissue mounts.

After euthanasia, segments of duodenum, jejunum, ileum, and terminal colon from inoculated pigs or samples from mock-inoculated pigs were collected. Indirect immunofluorescence was performed on whole-mount intestinal tissues. The intestinal tissues were fixed with 4% paraformaldehyde-0.2% glutaraldehyde in 0.1 M potassium phosphate buffer (PPB) (pH 7.4) for 2 h at RT. The fixed samples were washed four times with PPB, and quenched with PPB containing 50 mM glycine for 1 h at RT. After permeabilization with 0.1% Triton X-100 in PBS for 1 h, tissues were washed with PBS, blocked with PBS containing 2% bovine serum albumin and 5% goat serum for 30 min at RT. The samples were incubated with guinea pig anti-human NoV (1:5,000 dilution) overnight at 4°C in the incubation buffer containing 10 mM potassium phosphate buffer (PPB) [pH 7.4], 150 mM NaCl, 10 mM sodium azide, and 0.2% bovine serum albumin. After washing with PBS six times, the samples were incubated with the secondary antibody, goat anti-guinea pig IgG (Invitrogen; A11075) labeled with AlexaFluor488 [Ex (nm) 499, Em (nm) 519] which produces green color at a dilution of 1:1,200. Samples were stained with the nuclear stain SYTOX orange (Invitrogen; S11368) [Ex (nm) 547, Em (nm) 570] for 15 min, giving a red color, and the actin stain AlexaFluor633-labeled

phalloidin (Invitrogen; A222884) [Ex (nm) 632, Em (nm) 648] for 30min, producing a blue color. Samples were examined using a laser scanning confocal microscope (Olympus FV-1000, Germany).

4.3.8 Serum IgG ELISA.

Ninety-six-well plates were coated with 50 µl of highly purified human NoV VLPs (7.5 µg/ml) in 50 mM NaCO₃ buffer (pH 9.6) at 4°C overnight. Individual serum samples were tested for human NoV-specific IgG on VLP-coated plates. Briefly, serum samples were 2-fold-serially diluted and added to VLP-coated wells. After incubation at room temperature for 1 h, the plates were washed five times with PBS-Tween (0.05%), followed by incubation with 50 µl of goat anti-mouse IgG horseradish peroxidase-conjugated secondary antibody (Sigma) at a dilution of 1:80,000 for 1 h. Plates were washed and developed with 75 µl of 3'3',5'5'-tetramethylbenzidine (TMB), and the optical density (OD) at 450 nm was determined using an enzyme-linked immunosorbent assay (ELISA) plate reader. End point titer values were determined as the reciprocal of the highest dilution that had an absorbance value greater than background level (DMEM control).

4.3.9 Fecal IgA ELISA.

For each stool sample, human NoV-specific and total fecal IgA were determined as described previously. Fecal pellets were diluted 1:2 (wt/vol) in PBS containing 0.1%

Tween and a Complete EDTA-free proteinase inhibitor cocktail tablet (Roche). Samples were vortexed twice for 30 s and clarified twice by centrifugation at $10,000 \times g$ for 10 min. Ninety-six-well plates were coated with 50 μ l of highly purified human NoV VLPs (1 μ g/ml) in 50 mM NaCO₃ buffer (pH 9.6) at 4°C overnight for detection of human NoV-specific IgA, while total fecal IgA was determined by capturing all fecal extract IgA molecules with 1 μ g/ml sheep anti-mouse IgA (Sigma). To block nonspecific protein binding, the plates were incubated for 4 h at 4°C with 10% (wt/vol) dry milk in PBS (10% BLOTTO). The level of IgA was calculated from a standard curve that was determined by the absorbance values of the mouse IgA standard (Sigma). The human NoV-specific IgA level was expressed in nanograms per milliliter, and each corresponding total IgA level was expressed in micrograms per milliliter.

4.3.10 Vaginal and nasal human NoV-specific IgA ELISA.

Ninety-six-well plates were coated with human NoV VLPs in selected columns as described above. After an overnight blocking at 4°C with 5% BLOTTO, 100 μ l of vaginal or nasal extracts at 1:15 dilution was added to each well, the sample was serially diluted 2-fold down the plate and incubated for 2 h at 37°C. The remaining protocol was identical as described above for the human NoV-specific fecal IgA ELISA or the serum IgG ELISA.

4.3.11 Histologic examination.

Segments of the intestinal tissues, pieces of lungs, kidneys, livers, spleens, and mesenteric lymph nodes were preserved in 10% (v/v) phosphate-buffered formalin. Fixed tissues were embedded in paraffin, sectioned at 5 microns, and stained with hematoxylin-eosin (HE) for the examination of histological changes by light microscopy. The severity of intestinal histological change was scored based on the following criteria: grade 3 (severe), grade 2 (moderate), grade 1 (mild), and grade 0 (no lesions).

4.3.12 Sequence alignment and analysis.

Sequence alignment was performed by using the Megalign program in Lasergene (DNASTAR). The human NoV strains used in sequence analysis are summarized in Table 2.

4.3.13 Statistical analyses.

Statistical analysis was performed by one-way multiple comparisons using Minitab 16 statistical analysis software (Minitab Inc., State College, PA). A *P* value of <0.05 was considered statistically significant.

4.4 Results

4.4.1 Characterization of three human NoV GII.4 strains from Ohio.

Human fecal specimens, designated 5M, 7I, and 7G, were collected from outbreaks of acute gastroenteritis in Ohio. The fecal samples were processed and filtered as described in Materials and Methods. Total RNA was extracted from each sample and RT-PCR was performed using two primers targeting the conserved region of the human NoV VP1 gene. It was found that all three samples were human NoV-positive. To exclude the presence of other enteric viruses such as human sapovirus, and rotaviruses, primers targeting human sapovirus and rotavirus-specific genes were used in qPCR. All clinical specimens were negative of human sapovirus and rotavirus. Subsequently, the genomic RNA was then quantified by real-time RT-PCR. Human NoV isolates 5M, 7I, and 7G were found to have 6.7×10^6 , 1.5×10^7 , and 3×10^7 genomic RNA copies/ml, respectively.

To further characterize these human NoV strains, the entire genomic cDNA of these human NoV strains was amplified by RT-PCR using five to six overlapping fragments. The genome of each specimen was cloned to pGEM-T-easy vector and sequenced. The full-length genome of the viral isolates 5M, 7I, and 7G was 7558, 7558, and 7559 nt in length, and has been deposited into GeneBank at accession numbers JQ798158, JX126912, and JX126913, respectively. The genome encodes three ORFs, nonstructural (NS) genes, VP1, and VP2. No recombination or gene deletion was found in any of the three strains. At the nucleotide level, the genomic sequence of strains 5M, 7I, and 7G share 97.8-99.6% identity. At the amino acid level, NS, VP1, and VP2 proteins share

98.6-99.5%, 97.8-98.7%, and 98.1-98.9% homology with each other. Phylogenetic analyses were performed using the amino acid sequence of the VP1 gene. As shown in Fig. 4.3, all three human NoV strains share the highest homology with known GII.4 strains Hu/MD145-12/87/US and Hu/Farmington Hills/02/US, confirming that these isolates belong to the norovirus genotype GII.4, the most prevalent genotype circulating in the human population worldwide. The classification and GenBank accession numbers of norovirus strains that were used for sequence analysis are listed in Table 4.2.

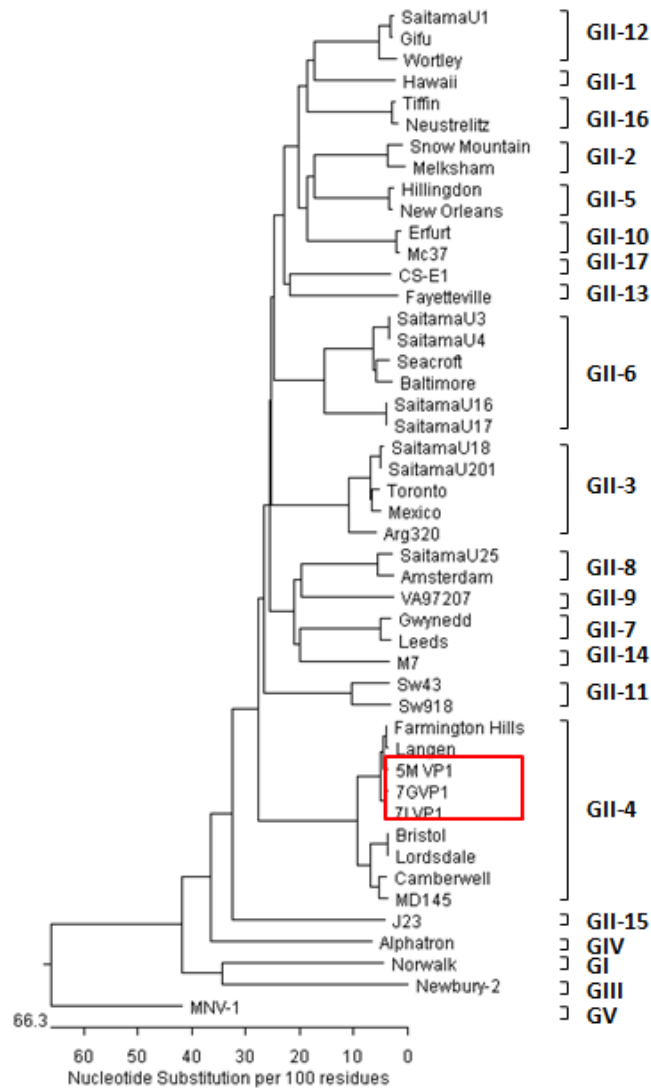


Figure 4.3. Phylogenetic tree of genogroup II NoVs based on the capsid protein VP1 sequences.

The phylogenetic tree was constructed by MegAlign (DNASar) using the Neighbor-Joining method. The three human NoV GII.4 strains, 5M, 7G, and 7I, are indicated by a red box. Genogroups (G) and genotypes (numbers after G) are indicated. The human NoV GI-1/Norwalk, GIII/Newbury-2, GIV/Alphatron, and GV/MNV-1 strains were used as outgroup controls.

Table 4.2. Classification and GenBank accession numbers of norovirus strains used for sequence analysis.

Strain	Genus/genogroup-genotype	Abbreviation	GenBank
Hu/Norwalk/68/US	NoV/GI-1	Norwalk	M87661
Hu/NLV/Hawaii virus/1971/US	NoV/ GII-1	Hawaii	U07611
Hu/Melksham/89/UK	NoV/ GII-2	Melksham	X81879
Hu/Snow Mountain/76/US	NoV/GII-2*	Snow Mountain	AY134748
Hu/Mexico/89/MX	NoV/GII-3	Mexico	U22498
Hu/Toronto/91/CA	NoV/GII-3	Toronto	U02030
Hu/SaitamaU18/97-99/JP	NoV/GII-3	SaitamaU18	AB039781
Hu/SaitamaU201/98/JP	NoV/GII-3	SaitamaU201	AB039782
Hu/Arg320/ARG	NoV/GII-3 *	Arg320	AF190817
Hu/Camberwell/101922/94/AUS	NoV/GII-4	Camberwell	AF145896
Hu/Lordsdale/93/UK	NoV/GII-4	Lordsdale	X86557
Hu/Bristol/93/UK	NoV/GII-4	Bristol	X76716
Hu/MD145-12/87/US	NoV/GII-4	MD145	AY032605
Hu/Farmington Hills/02/US	NoV/GII-4	Farmington	AY502023
Hu/Langen1061/02/DE	NoV/GII-4	Langen	AY485642
Hu/Hillingdon/93/UK	NoV/GII-5	Hillingdon	AJ277607
Hu/New Orleans 306/94/US	NoV/GII-5	New Orleans	AF414422
Hu/Baltimore/274/1993/US	NoV/GII-6	Baltimore	AF414408
Hu/SaitamaU3/97/JP	NoV/GII-6	SaitamaU3	AB039776
Hu/SaitamaU4/97/JP	NoV/GII-6	SaitamaU4	AB039777
Hu/SaitamaU16/97/JP	NoV/GII-6	SaitamaU16	AB039778
Hu/SaitamaU17/97/JP	NoV/GII-6	SaitamaU17	AB039779
Hu/Seacroft/90/UK	NoV/GII-6 *	Seacroft	AJ277620
Hu/Leeds/90/UK	NoV/GII-7	Leeds	AJ277608
Hu/Gwynedd/273/94/US	NoV/GII-7	Gwynedd	AF414409
Hu/Amsterdam/98-18/98/NET	NoV/GII-8	Amsterdam	AF195848
Hu/SaitamaU25/97-99/JP	NoV/GII-8	SaitamaU25	AB039780
Hu/VA97207/97/US	NoV/GII-9 *	VA97207	AY038599
Hu/NLV/Erfurt/546/00/DE	NoV/GII-10	Erfurt	AF427118
Hu/Mc37/00-01/THA	NoV/GII-10	Mc37	AY237415
Po/Sw43/97/JP	NoV/GII-11	Sw43	AB074892
Po/Sw918/97/JP	NoV/GII-11	Sw918	AB074893
Hu/Gifu/96/JP	NoV/GII-12	Gifu	AB045603
Hu/Wortley/90/UK	NoV/GII-12	Wortley	AJ277618
Hu/SaitamaU1/97-99/JP	NoV/GII-12	SaitamaU1	AB039775
Hu/Fayetteville/98/US	NoV/GII-13	Fayetteville	AY113106
Hu/M7/99/US	NoV/GII-14	M7	AY130761
Hu/J23/99/US	NoV/GII-15	J23	AY130762
Hu/Tiffin/99/US	NoV/GII-16	Tiffin	AY502010
Hu/Meustrelitz260/00/DE	NoV/GII-16	Neustrelitz	AY772730
Hu/CS-E1/02/US	NoV/GII-17	CS-E1	AY502009
Bo/Newbury-2/76/UK	NoV/GIII-2	Newbury-2	AF097917
Hu/Alphatron/98-2/98/NET	NoV/GIV	Alphatron	AF195847
Mu/MNV-1/03/US	NoV/GV	MNV-1	AY228235

* Previously reported recombinants.

4.4.2 Pathogenesis of human NoV strains 7I and 5M in gnotobiotic piglets.

The pathogenesis of human NoV strains 7I and 5M was determined in newborn gnotobiotic piglets. Previously, it was reported that human NoV GII.4 strain HS66 caused diarrhea in gnotobiotic piglets (Cheetham et al., 2006). However, in the current study, neither 7I nor 5M infected piglets developed significant diarrhea during the 7 day time period. In addition, piglets infected by 7I and 5M did not show other physiological changes such as body weight drop and fever. At day 7 post-inoculation, all piglets were sacrificed, and viral shedding in fecal samples was determined by real-time RT-PCR. As shown in Fig. 4.4, human NoV was detected in fecal samples from days 2 to 6 post-inoculation for piglets infected with 5M. The piglets inoculated with 7I had shorter virus shedding time, from days 3 to 5 post-inoculation. For both groups, fecal viral shedding reached a peak, approximately 10^5 genomic copies /g, at day 1-2 post-inoculation. At day 5 post-challenge, 4 out of 5 pigs had fecal viral shedding in 7I and 5M groups with an average titer of 8896 and 2342 RNA copies/ml respectively.

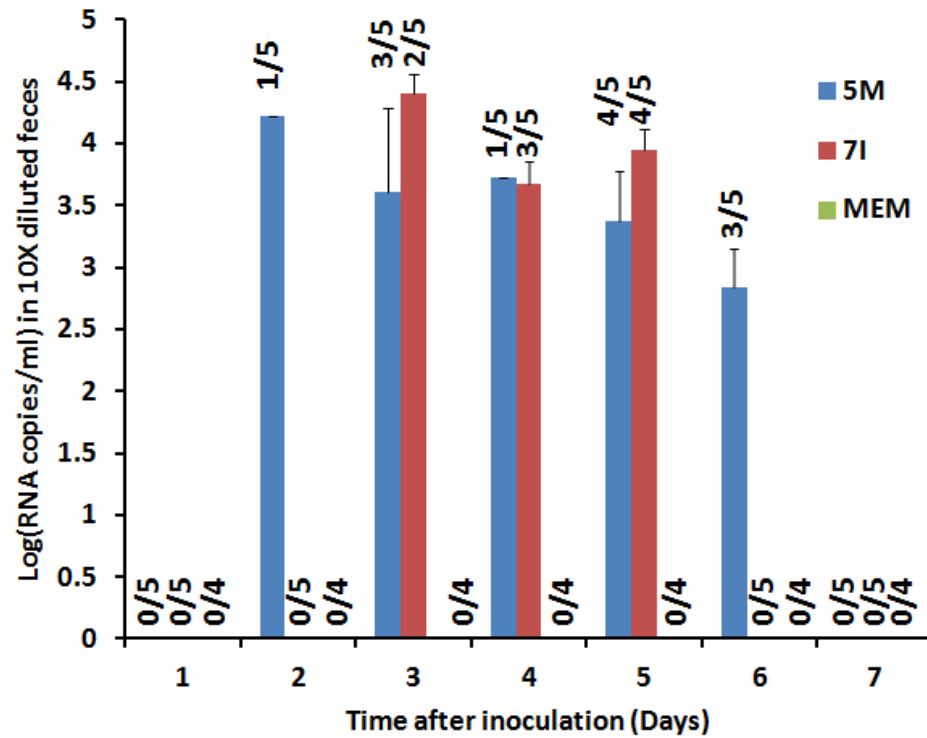


Figure 4.4. Fecal viral shedding detected by real time RT-PCR after human NoV infection.

Fecal samples were collected from all piglets in each group daily. Samples were diluted in MEM, vortexed, clarified by centrifugation, and total RNA was extracted from supernatants. The human NoV RNA was detected by real-time RT-PCR. The data was shown as log₁₀ (RNA copies/ml) in 10 times diluted samples. Data was expressed as average fecal viral titer of NoV-positive pig ± the standard deviation.

After termination, intestines, intestinal contents, spleen, kidney, and liver were collected for the examination of gross pathological and histopathological changes, and the detection of viruses. No significant gross pathologic change was found in intestines, spleen, kidney, and liver. Viral RNAs were not detected in spleen, kidney, or liver tissues. Histopathological changes were observed in the duodenum and jejunum samples from strain 7I-infected piglets (Fig. 4.5). Intestinal epithelium of the jejunum from the 7I group showed epithelial loss (presumed necrosis or apoptosis) of villous tips with resultant conversion of normal absorptive to flattened and squamoid epithelium. The related changes associated with epithelial loss had a variable degree of villous shortening (villous atrophy) and associated edema of the lamina propria variably within the duodenum (3/5 piglets) and jejunum (1/5) (Table 4.3). 5M did not cause significant histological changes in the intestines. To determine viral antigen distribution following human NoV challenge, an indirect immunofluorescent assay was performed on whole intestinal tissue mounts using human NoV antibody against VP1 protein. As shown in Fig. 4.6, a large number of norovirus antigen-containing cells were detected in jejunum from 7I group, although fewer antigen positive cells were detectable in duodenum and ileum segments in 7I group. Antigen positive cells were not detected in the terminal colon. In contrast, gnotobiotic pigs infected by 5M had detectable antigens only in duodenum but not jejunum, ileum, or terminal colon segments. In addition, the number of antigen positive cells detected in the 5M group was significantly less than the 7I group. As controls, all intestinal samples from mock-inoculated pigs were negative for norovirus antigen. Collectively, it was concluded that (i) both 7I and 5M had viral shedding in

stools although no significant diarrhea was observed; (ii) 7I, but not 5M, caused significant histological changes in duodenum and jejunum; (iii) different human NoV strains may have different pathogenesis in gnotobiotic pigs, and (iv) gnotobiotic pigs may serve as an animal model for human NoV challenge studies.

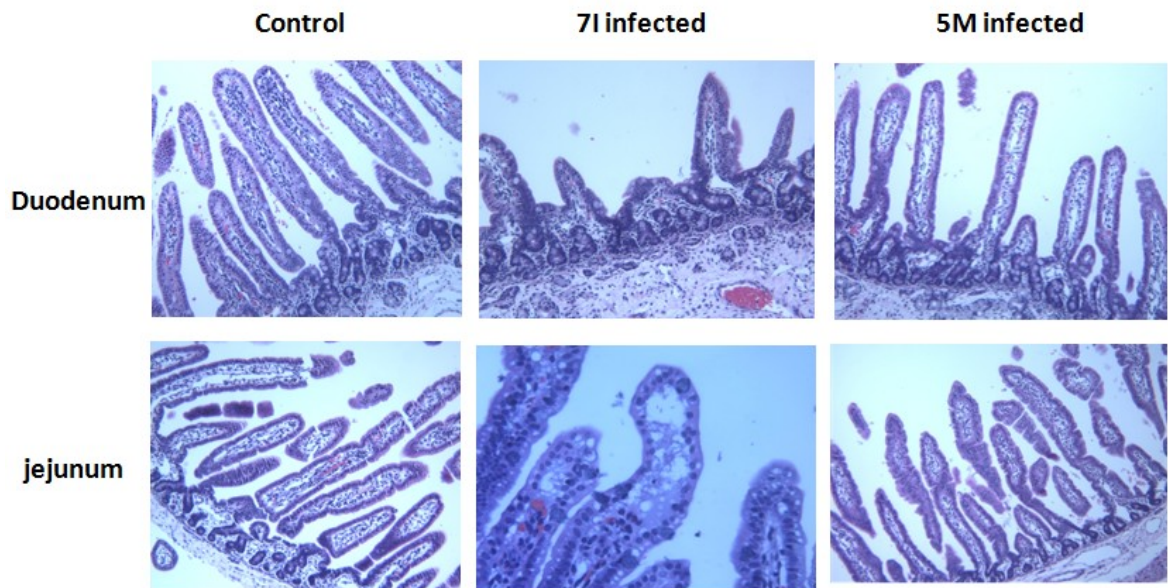


Figure 4.5. Histological changes in the small intestines of gnotobiotic pigs infected by human NoV.

Sections of small intestines were embedded in paraffin, sectioned at 5 microns, and stained with hematoxylin-eosin (HE) for the examination of histological changes by light microscopy. Upper panels show duodenum sections, and lower panels show jejunum sections. Villous atrophy and epithelial villous tip damage were observed in duodenum and jejunum sections from 7I-infected pigs.

Table 4.3. Histological changes in the small intestines of gnotobiotic pigs infected by human NoV.

Group	Pigs	Number of pigs with histological	
		changes in duodenum	changes in jejunum
NoV 5M	5	0/5	0/5
NoV 7I	5	3/5	1/5
MEM	4	0/4	0/4

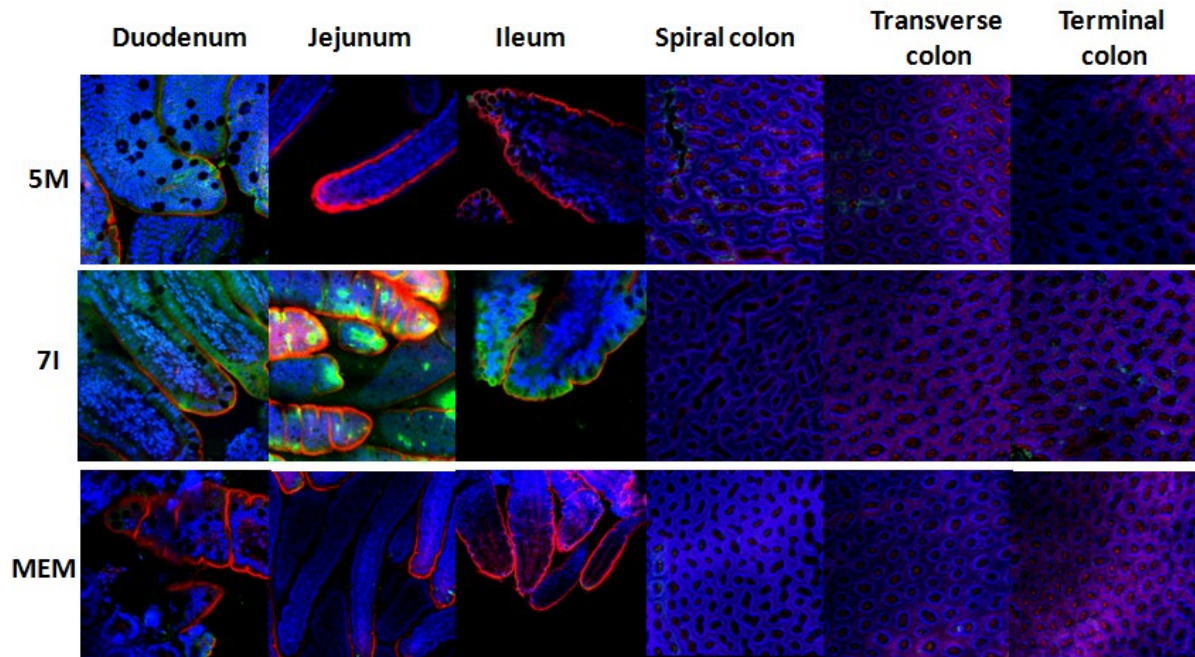


Figure 4.6. Localization of the human NoV capsid protein in whole-mount small intestinal tissues by an indirect immunofluorescent assay.

The intestinal tissues were fixed and incubated with guinea pig anti-human NoV antibody, followed by incubation with goat anti-guinea pig IgG labeled with AlexaFluor488 (green). Nuclei were stained with SYTOX orange (blue). Actin was stained with phallotoxin Alexa633 (red). Columns from left to right show duodenum, jejunum, ileum, spiral colon, transverse colon, and terminal colon. Upper, middle, and lower panels show intestinal sections from 5M, 7I, and mock (MEM)-infected pigs, respectively.

4.4.3 The safety of rVSV-VP1 in gnotobiotic piglets.

Swine are known to be one of the natural hosts of VSV. It has been shown that pigs infected with wild type VSV Indiana serotype exhibited typical symptoms of VSV infection such as fever, weight loss, and vesicular lesions in the mouth, tongue, lips, gums, teats, and feet (Letchworth et al., 1999). However, piglets vaccinated with rVSV-VP1 and rVSV-Luc did not show signs of VSV infection or weight loss or vesicle lesion during the three week experimental period. This evidence suggests that both rVSV-VP1 and rVSV-Luc were significantly attenuated in its natural host, the pig.

4.4.4 Immunogenicity of rVSV-VP1 in gnotobiotic piglets.

After vaccination, blood samples were collected weekly and serum IgG antibody against human NoV was determined by ELISA. As shown in Fig.4.7, piglets vaccinated with rVSV-VP1 developed a high level of human NoV-specific IgG. At 1 week post-inoculation, all the piglets in rVSV-VP1 group developed human NoV-specific IgG. The IgG antibody levels gradually increased at week 2 post-inoculation, with a GMT of 1088. At week 3 post vaccination the GMT reached 7782. No human NoV-specific IgG antibody was detected in the rVSV-Luc and unvaccinated control groups during entire experimental period.

To determine the mucosal immunity, fecal, nasal, and vaginal (if female) swabs were collected at week 4 post-vaccination. Total IgA and human NoV-specific IgA antibodies in these samples were determined by ELISA. The level of IgA response was expressed as

the ratio between human NoV-specific IgA and total IgA. As shown in Fig. 4.8, all the piglets vaccinated with rVSV-VP1 developed human NoV-specific IgA responses in fecal, nasal, and vaginal samples. Interestingly, human NoV-specific IgA in nasal swabs was significantly higher than fecal and vaginal samples ($P < 0.05$). None of the piglets in the rVSV-Luc and DMEM groups showed human NoV-specific fecal, nasal, and vaginal IgA antibody over the entire experimental period. Therefore, these results demonstrated that rVSV-VP1 triggered mucosal immunity in piglets.

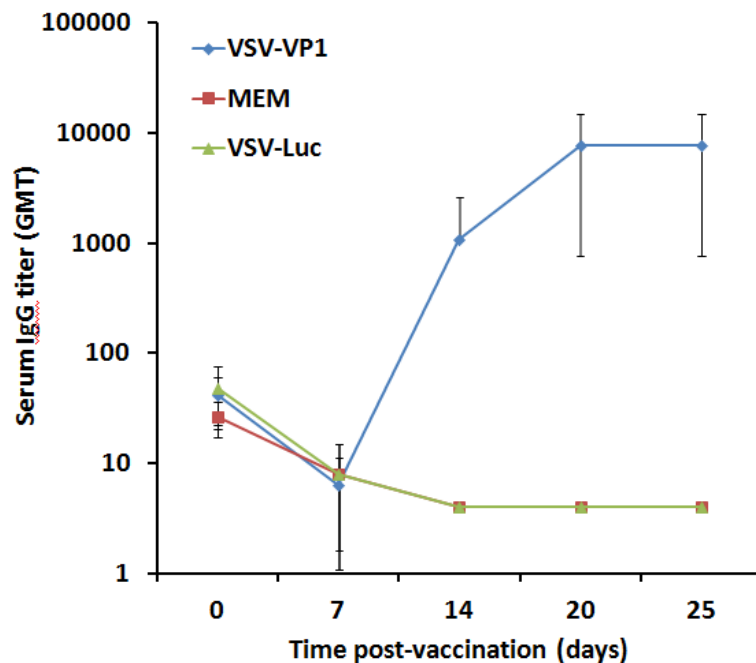


Figure 4.7. VSV-based human NoV vaccine stimulates a high level of serum IgG immune response in gnotobiotic pigs.

Gnotobiotic piglets were inoculated intranasally with 2×10^7 PFU of rVSV-VP1 or rVSV-Luc. Serum samples were collected weekly and analyzed by ELISA for human NoV-

specific serum IgG antibody. Data was expressed by Geometric Mean Titers (GMT) of all the piglets in each group. Error bars at each time point represent the standard deviation between piglets.

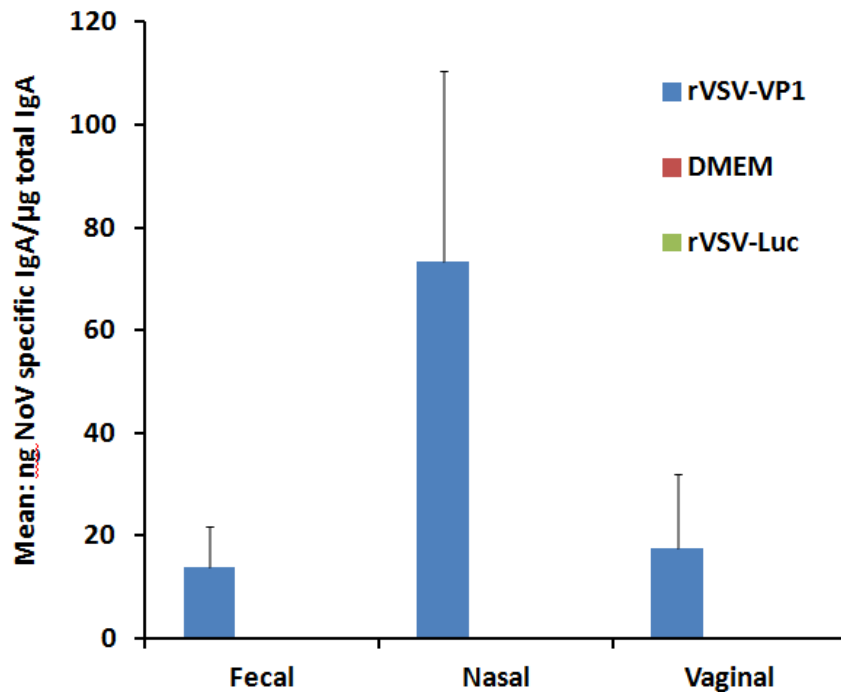


Figure 4.8. VSV-based human NoV vaccine stimulates a high level of mucosal IgA immune response in gnotobiotic pigs.

Fecal samples were collected at week 4 post-vaccination. Samples were diluted in MEM, vortexed, clarified by centrifugation, and human NoV-specific and total IgA antibodies were determined by ELISA. Human NoV-specific antibody was detected in all pigs vaccinated with rVSV-VP1, whereas the pigs inoculated with rVSV-Luc and DMEM were negative. The ratio between human NoV-specific IgA and total IgA was calculated

for each pig. Data was expressed as average titer of IgA-positive pigs \pm the standard deviation.

At week 4 post-vaccination, piglets were challenged with human NoV strain 7I, and diarrhea score, viral shedding in feces, intestine histology, and antigen distribution were determined. Consistent with the pathogenesis study, no significant diarrhea was observed in rVSV-VP1, rVSV-Luc, or challenge control groups. Thus, diarrhea was not used as the criteria for the evaluation of protection efficacy. As shown in Fig. 4.9, piglets inoculated with rVSV-VP1 and rVSV-Luc had similar levels of viral shedding at days 3 and 4 post-challenge. However, at day 5 post-challenge, less viral shedding was detected in the rVSV-VP1 group compared to the rVSV-Luc group. As shown in Fig. 4.10, piglets inoculated with rVSV-VP1 and rVSV-Luc had similar viral titers in all the intestinal contents samples. Although rVSV-VP1 group and rVSV-Luc group showed similar NoV titer, fewer pigs in rVSV-VP1 group were positive in NoV compared to the rVSV-Luc group. Importantly, piglets vaccinated with rVSV-VP1 were protected from intestinal histologic changes caused by 7I. Piglets inoculated with rVSV-Luc developed significant histologic lesions in the duodenum and jejunum after challenge with 7I (Table 4.4 and Table 4.5). Specifically, two out of three piglets in rVSV-Luc group showed syncytial giant cells and villous atrophy in the lamina propria of duodenum, and all three piglets showed villous atrophy in the jejunum. In contrast, only one out of five piglets in rVSV-VP1 group had mild epithelial loss and villous atrophy in the duodenum samples and only one out of five piglets had mild edema in lamina propria in the jejunum samples.

Finally, all tissue samples were stained with human NoV polyclonal antibody, followed by an indirect immunofluorescence assay. As shown in Fig. 4.11, a large amount of human NoV antigens were detected in duodenum, jejunum, and ileum of the pig intestines in the rVSV-Luc group. Piglets vaccinated with rVSV-VP1 had significantly less human NoV antigen in both the duodenum and jejunum sections. No antigen was detected in the mock-infected control samples. Taken together, these results demonstrated that the VSV-based human NoV vaccine triggered strong humoral and mucosal immunities, and protected gnotobiotic pigs from histological changes in intestine after the challenge of human NoV.

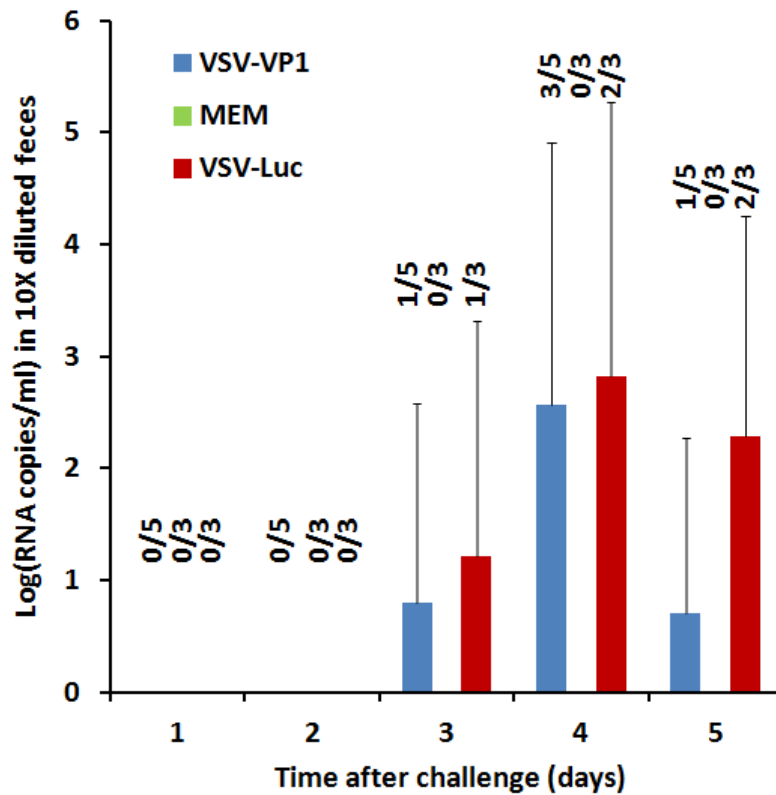


Figure 4.9. Fecal viral shedding of human NoV detected by real time RT-PCR after human NoV challenge.

Fecal samples were collected from all piglets in each group daily after challenge with human NoV 7I. Samples were diluted in MEM, vortexed, clarified by centrifugation, and RNA was extracted from supernatants. The human NoV RNA was detected by real-time RT-PCR. The data was shown as log₁₀ (RNA copies/ml) in 10 times diluted samples. Data was expressed as average fecal viral titer of NoV-positive pig ± the standard deviation.

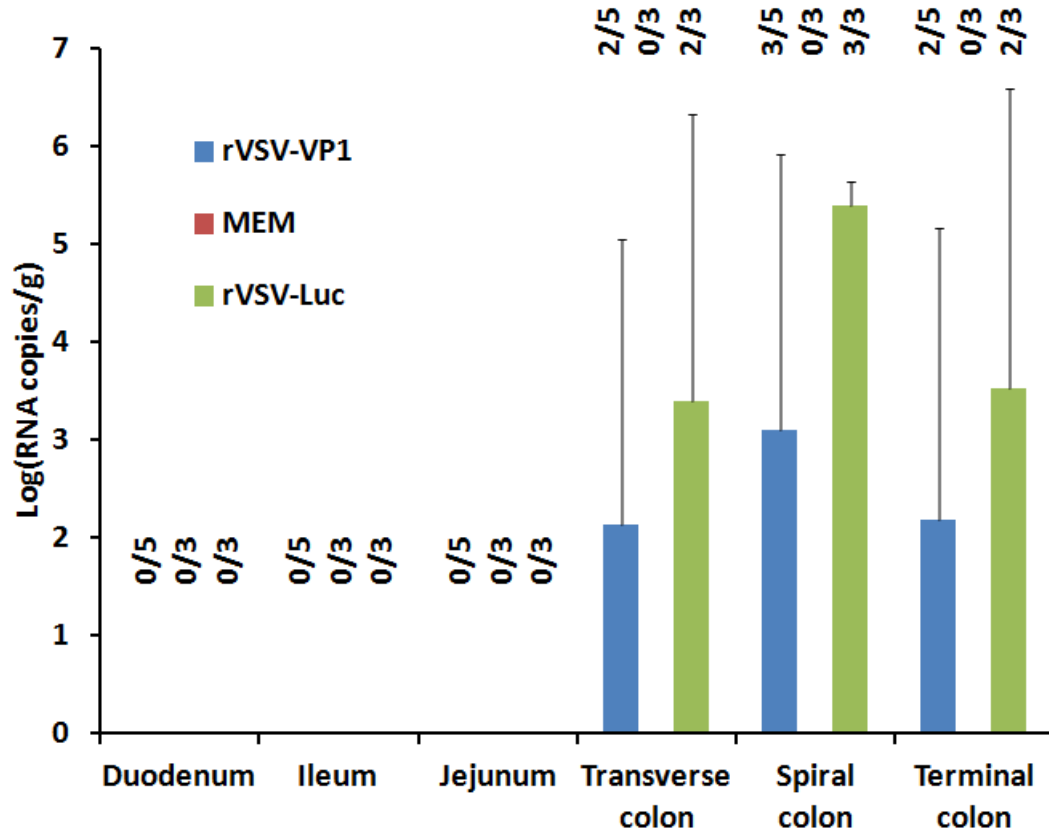


Figure 4.10. Detection of human NoV RNA in intestinal contents by real-time RT-PCR.

After termination, intestinal contents were collected from all piglets in each group. Samples were diluted in MEM, vortexed, clarified by centrifugation, and RNA was extracted from supernatants. The human NoV RNA was detected by real-time RT-PCR. The data was shown as log₁₀ (RNA copies/g). Data was expressed as average viral titer of NoV-positive pig ± the standard deviation.

Table 4.4. Histological changes in the small intestines of gnotobiotic pigs challenged by human NoV after vaccination.

Group	Pigs	Number of pigs with histological changes in duodenum	Number of pigs with histological changes in jejunum	Number of pigs with histological changes in ileum
No challenge control (MEM)	3	0/3	0/3	0/3
Challenge control (rVSV-Luc)	3	2/3	3/3	1/3
Vaccination and challenge (rVSV-VP1)	5	1/5	1/5	0/5

Table 4.5. Histological changes in the small intestines of gnotobiotic pigs challenged by human NoV after vaccination in detail.

Group	Duodenum					Jejunum					Ileum				
	SGC	lp ed	lp inf	epith necro	VASGC	SGC	lp ed	lp inf	epith necro	VASGC	SGC	lp ed	lp inf	epith necro	VA
No challenge control (MEM)	0	0	0	0	0	0	0	0	0	0	0	0	0	0	0
Challenge control (rVSV-Luc)	2/3	2/3	2/3	1/3	2/3	0	2/3	0	1/3	3/3	0	0	0	0	1/3
Vaccination and challenge (rVSV-VP1)	0	0	0	1/5	1/5	0	1/5	0	0	0	0	0	0	0	0

lp = lamina propria; epith = intestinal epithelia (enterocyte); SGC = syncytial giant cells; ed = edema; inf = inflammatory cell infiltrates (PMN); VA = villous atrophy

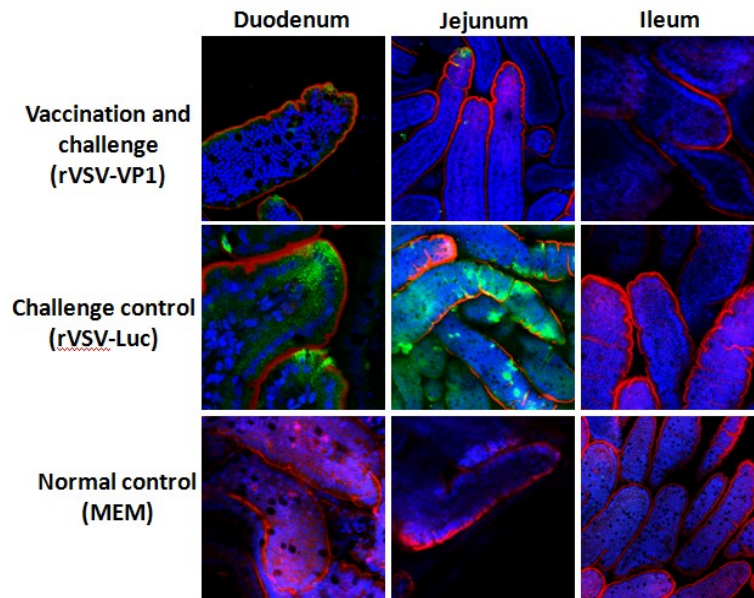


Figure 4.11. Detection of the human NoV capsid protein in whole-mount small intestinal tissues by an indirect immunofluorescence assay.

Piglets were inoculated intranasally with 2×10^7 PFU of rVSV-VP1 or rVSV-Luc. At 4 weeks post vaccination, piglets in rVSV-VP1 and rVSV-Luc groups were challenged with human NoV 7I. The intestinal tissues were fixed and incubated with guinea pig anti-human NoV antibody, followed by incubation with goat anti-guinea pig IgG labeled with AlexaFluor488 (green). Nuclei were stained with SYTOX orange (blue). Actin was stained with phalloxin Alexa633 (red). Columns from left to right show duodenum, jejunum, and ileum. Upper, middle, and lower panels show intestinal sections from rVSV-VP1, rVSV-Luc, and normal control groups respectively. For rVSV-VP1 vaccinated group, a small amounts of human NoV capsid protein were detected at the tip of duodenum and jejunum. For rVSV-Lucgroup, a large number of NoV antigen positive cells were detected in the duodenum and jejunum. All sections from normal control and all ileum sections were negative for NoV antigen.

4.5 Discussion

To date, there is no FDA approved vaccine for human NoV. One of the most challenging hurdles in human NoV vaccine development is the lack of a small animal model. Although several human NoV vaccine candidates, such as VLP-based subunit vaccine, have been shown to be safe and immunogenic in mice, it is not known whether they can protect hosts from virulent challenge (Ball et al., 1998). In this study, it was found that the gnotobiotic pig is a permissive animal model for human NoV. However, two GII.4 human NoV strains exhibited different pathogenesis in gnotobiotic pigs. Specifically, human NoV strain 7I caused viral shedding and histologic lesions in intestines whereas human NoV strain 5M caused viral shedding without detectable histologic lesions. Using a gnotobiotic pig as the challenge model, it was found that the VSV-based human NoV vaccine (rVSV-VP1) not only triggered high levels of serum IgG and mucosal IgA antibody responses, but also protected pigs from intestinal pathological changes after challenge with human NoV strain 7I. To our knowledge, this is the first report of a live vectored vaccine that is protective against norovirus challenge.

4.5.1 Pathogenesis of human NoV in animal models.

It has been a challenge to develop an animal model for human NoV. Soon after the discovery of human NoV in 1972, Wyatt et al., (1978) found that chimpanzees were permissive for asymptomatic norovirus infection (Wyatt et al., 1978). Challenge of other nonhuman primates, such as rhesus macaques and newborn pigtail macaques, with human NoV strains resulted in only sporadic asymptomatic infections (Rockx et al.,

2005; Subekti et al., 2002). Most recently, Bok et al., (2011) re-evaluated the infectivity of human NoV in the chimpanzee model (Bok et al., 2011). It was found that norovirus seronegative chimpanzees inoculated intravenously with the human NoV strain Norwalk virus did not show clinical signs of gastroenteritis, but the onset and duration of virus shedding in stool and serum antibody responses were similar to that observed in humans. However, the use of chimpanzees will likely be prohibited in the future biomedical research according to a report released on December 15, 2011 from the Institute of Medicine of the National Academies and National Research Council. Therefore, there is critical need to develop an alternative animal model for human NoV.

Gnotobiotic pigs have been shown to be a good animal model to study several enteric pathogens including rotavirus. The pathogenesis of human NoV in gnotobiotic pigs was first reported by Cheetham et al. (2006). It was found that gnotobiotic pigs infected by human NoV GII.4 strain HS66 developed mild diarrhea and had viral shedding in feces from postinoculation days 1 to 4. However, only 1 out of 7 pigs had mild histopathologic lesions in the proximal small intestine. In addition, 18 of 31 human NoV-inoculated pigs had detectable norovirus antigens in duodenal and jejunal enterocytes as determined by immunofluorescent assay using a monoclonal antibody against the human NoV capsid. In contrast to the findings of Cheetham et al., (2006), none of pigs challenged 7I and 5M developed diarrhea in our study. Interestingly, the two GII.4 strains 7I and 5M showed distinct pathotypes in gnotobiotic pigs. Pigs challenged with 5M had viral shedding from days 2 to 6, whereas pigs challenged with 7I had viral shedding from days 3 to 5. Most

importantly, duodenum and jejunum segments from pigs infected by 7I had significant histologic lesions characterized by epithelial loss of villous tips, villous shortening, atrophy, and edema of the lamina propria. In contrast, no significant histologic changes were found in pigs infected by 5M. Consistent with the histologic data, the amount of antigen detected in duodenum, jejunum, and ileum segments from the 7I group was significantly increased compared to the 5M group. In combination with the observations from HS66 strain (Cheetham et al., 2006), it appears that different human NoV strains have variable pathogenesis in gnotobiotic pigs despite the fact that all three strains belong to the GII.4 genotype. It is known that human NoV utilizes histo-blood group antigen (HBGAs) as their functional receptors (Tan and Jiang, 2005a). Sequence analysis found that the receptor binding pockets in VP1 of HS66, 7I, and 5M are highly conserved, suggesting that all three strains bind to the same HBGAs. It is possible that genetic variability, particularly, the amount of HBGAs in intestinal cells among individual pigs may affect pathogenesis. Another possibility associated with pathotypes is the differences in nucleotide sequence in non-coding region of the genome and/or amino acid sequence in viral proteins. In fact, HS66, 7I, and 5M share 98.6% amino acid identity in VP1 protein, and 7I and 5M share 97.8% nucleotide sequence identity. It will be of interest to determine the specific amino acids, nucleotides, or elements accounting for these differences between strains and how they contribute to the differences in viral pathogenesis. However, such studies cannot be conducted until the development of a cell culture system that can grow human NoV and a reverse genetics system that will allow for genetic manipulation of the viral genome.

4.5.2 Protection efficacy of human NoV vaccine candidates.

Currently, little is known about the protection efficacy of human NoV vaccine candidates. Souza et al., (2007) first reported the protection of VLP-based subunit vaccine candidate in gnotobiotic pigs. It was found that gnotobiotic pigs inoculated orally/intranasally with human NoV GII.4 HS66 strain VLP formulated with immunostimulating complexes (ISCOM) or mutant *E. coli* LT toxin (mLT) triggered a variable level of intestinal and systemic antibody and cytokine responses, and induced increased protection rates against viral shedding and diarrhea (75–100%) compared to controls (57% of controls had viral shedding). Most recently, it was reported that chimpanzees vaccinated intramuscularly with Norwalk virus (genogroup I, GI) VLPs were protected from homologous Norwalk virus infection when challenged 2 and 18 months after vaccination, whereas chimpanzees that received VLPs derived from MD145 (genogroup II, GII) were not protected against heterologous Norwalk virus infection.

In this study, we demonstrated that the VSV-based human NoV vaccine candidate is safe, immunogenic, and protective in gnotobiotic pigs. Gnotobiotic pigs vaccinated with rVSV-VP1 did not exhibit any clinical signs of VSV infection, suggesting that rVSV-VP1 is highly attenuated in swine, one of the natural hosts of VSV. It was found that gnotobiotic pigs vaccinated with rVSV-VP1 generated a high level of serum human NoV specific IgG at week 2 post-vaccination and the antibody levels gradually increased at weeks 3 and 4. At week 4 post-vaccination, all pigs vaccinated with rVSV-VP1 had high

levels of fecal, nasal, and vaginal human NoV specific IgA antibodies. Most importantly, gnotobiotic pigs vaccinated with rVSV-VP1 were protected from intestinal histologic lesions after challenge with 7I. In addition, viral antigen expression was significantly reduced in duodenum, jejunum, and ileum in the rVSV-VP1 vaccinated group. Pigs vaccinated with rVSV-VP1 had lower viral shedding at day 5 post-challenge compared to the rVSV-Luc group, although both rVSV-VP1 and rVSV-Luc had similar levels of viral RNA present at days 3 and 4. This data demonstrated that rVSV-VP1 vaccination can protect pigs from norovirus-induced pathological changes and inhibit viral replication in the intestine. In the future, it will be interesting to determine whether rVSV-VP1 vaccination can protect humans from norovirus infection.

Soon after the discovery of VLPs, human clinical trials using a recombinant baculovirus expressing human NoV VLPs was initiated by Ball et al., (Ball et al., 1999a) . It was shown that VLPs were safe and immunogenic when delivered by the oral route. Subsequently, a transgenic potato-based VLP vaccine was also tested in human volunteers (Tacket et al., 2000; Tacket et al., 2003). 19 out of 20 subjects who ingested transgenic potato developed measurable human NoV antibody-secreting cells. However, only 20% of subjects produced serum anti-human NoV IgG, and 30% produced fecal anti-human NoV IgA. Recently, a human vaccination trial followed by a human NoV challenge study was conducted (Atmar et al., 2011). Within 50 human subjects vaccinated with two doses of Norwalk virus VLPs (with chitosan and monophosphoryl lipid A as adjuvants), 70% of them developed Norwalk virus-specific IgA seroresponse.

After challenge with homologous virus, it was found that vaccination significantly reduced the frequency of Norwalk virus gastroenteritis (occurring in 69% of placebo recipients vs. 37% of vaccine recipients) and Norwalk virus infection (82% of placebo recipients vs. 61% of vaccine recipients). Although these results are highly promising, the efficacy of these vaccine candidates needs to be further improved.

4.5.3 The need to explore new vaccine candidates against human NoV.

Recent epidemiological studies found that severe clinical outcomes including death are often associated with high risk populations such as the elderly, children, and immunocompromised individuals. The CDC estimates that 900,000 clinic visits by children in the developed world occur annually as a result of norovirus infections, leading to an estimated 64,000 hospitalizations (Patel et al., 2008). From 1999-2007 norovirus caused, on average, 797 deaths per year in the U.S., surging up 50% during epidemic seasons. The burden of human NoV is much greater in the developing world, where the CDC estimates that norovirus causes the death of 200,000 children under the age of 5 every year (Hall et al., 2011). This data indicates that there is an urgent need to develop an efficacious vaccine for human NoV. Although a VLP-based vaccine candidate is currently in human clinical trials, it requires a high dose of VLPs, multiple booster immunizations, and does not provide cross protection against heterologous norovirus infection. In addition, the duration of immune responses and the protection efficacy is limited. In general, live attenuated virus vaccines stimulate strong systemic immunity and provide durable protection. In fact, live attenuated rotavirus vaccines have been

successful in preventing rotavirus infection in children. However, a live attenuated vaccine is impossible for human NoV since it cannot be grown in cell culture. As an alternative strategy, a live vectored vaccine may be suitable. In this study, it was demonstrated that a VSV vectored vaccine candidate (rVSV-VP1) is capable of generating high levels of systemic and mucosal immunities and protecting an animal model from virulent challenge. Noroviruses are highly diverse, both antigenically and genetically. One of the important advantages of using VSV as a vector, is that VSV can accommodate and express multiple antigens. Insertion of multiple VP1, P domain, or conserved epitopes into a single VSV vector will likely result in a multivalent human NoV vaccine candidate, which may provide broad cross-protection against different human NoV strains. Such a vaccine would greatly reduce the burden of human NoV infection. Coupled with the fact that several VSV-vectored HIV vaccines (Spearman, 2003) and VSV-based oncolytic agents are currently in human clinical trials, the safety and efficacy of VSV-based vaccine and therapy will be forthcoming. From this prospective, VSV-vectored human NoV is a highly promising vaccine candidate that may have important applications in the future.

In summary, the VSV-based human NoV vaccine candidate (rVSV-VP1) is not only safe in gnotobiotic pigs, but also triggered strong humoral and mucosal immunities and protected piglets from human NoV infection.

Chapter 5 : Future directions

5.1 Determine whether the VSV-based human NoV vaccine can provide cross-protection against different human NoV strains.

Noroviruses are very diverse, both antigenically and genetically (Zheng et al., 2006). To date, thousands of norovirus strains have been identified worldwide. Five genogroups of noroviruses, GI, GII, GIII, GIV, and GV, have been assigned. Noroviruses that infect humans are mainly from three genogroups, GI, GII, and GIV. Within a genogroup, noroviruses are further divided into genotypes. Currently, there are at least 33 norovirus genotypes. Ideally, an effective vaccine should provide cross-protection against different genogroups and genotypes of human NoV. However, recent experiments have shown that a VLP-based subunit vaccine failed to provide sufficient cross-protection against heterogeneous human NoV strains.

In this study, recombinant rVSV expressing the VP1 gene of human NoV GII.4 strain HS66 can provide protective immune responses against a different human NoV GII.4 strain, 7I. Based on the VP1 amino acid sequence, 7I and HS66 share 98% homology. This data suggests that rVSV-VP1 can provide sufficient protection against different strains of human NoV within the GII.4 genotype. Important future research

should focus on whether rVSV-VP1 can provide cross protection against different genogroups of human NoV such as the GI.1 genogroup, to which Norwalk virus belongs.

Another advantage of using VSV as a vector is that it can harbor multiple foreign genes. In the future, it will be of great interest to generate recombinant VSV expressing multiple VP1 genes or P domains of different human NoV strains (Fig. 5.1 A and B). Such a multivalent live vaccine candidate will likely generate specific immunity that can provide sufficient protection against different genogroups of human NoV.

Recently, it was found that a foreign antigen can be efficiently expressed when it is inserted in the loop region of the P domain of human NoV VP1 gene (Tan and Jiang, 2012). For example, a P particle of human NoV carrying rotavirus antigenic peptides on the surface loop was found to induce immune response against both norovirus and rotavirus in mice (Tan and Jiang, 2012). Similarly, VSV may be used to produce norovirus P particles carrying other viral antigens, generating a multivalent vaccine against norovirus and other viruses (Fig. 5.1C).

Additionally, experimental evidence indicates that one role of the norovirus minor capsid protein (VP2) is to increase the expression of the major capsid protein (VP1) and to stabilize the VLPs from disassembly and protease degradation (Bertolotti-Ciarlet et al., 2003). Thus, co-expressing human NoV VP1 and VP2 in the VSV vector may produce more stable VLPs, and further enhance the vaccine efficacy (Fig. 5.1D).

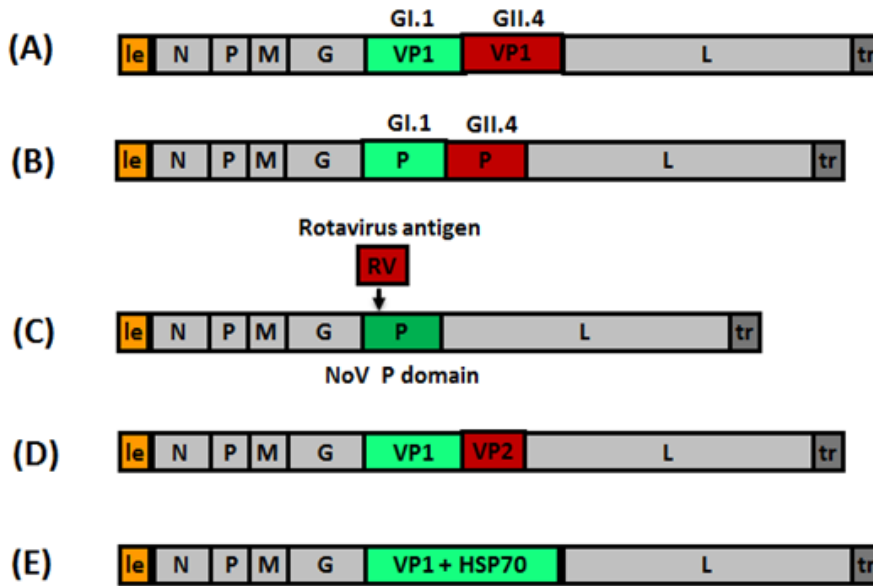


Figure 5.1. Strategies to improve the efficacy of VSV-based human NoV vaccine

5.1.1 Improve the adjuvant effect of HSP70.

In this study, it was found that co-expression of HSP70 and VP1 located in different positions in the VSV genome enhanced T cell and mucosal immunity against human NoV. An alternative strategy is to fuse VP1 and HSP70 as a single insertion in the VSV genome, which may further improve the binding to antigen-presenting cells (APCs) and enhance the T- and B-mediated adaptive immunity (Fig. 5.1E).

In addition, the mechanism by which HSP70 enhances the immune response against human NoV is not known. Such mechanistic studies will validate the adjuvant function of HSP70 for the VSV-based vaccine. Previously, it was shown that HSP70 interacts with the N protein of measles virus and enhances viral replication. Conversely, HSP70 also activates innate and adaptive immunity that enhance viral clearance. It is not

known how HSP70 modulates the balance between viral replication and viral clearance. Similar to measles virus infection, HSP70 may increase VSV replication by binding to VSV proteins. The mechanism of HSP70 activation of the innate and adaptive immune responses in VSV infected BALB/c mice remains unclear. The signaling pathways of HSP70 in macrophage cells also remain to be elucidated.

Other heat shock proteins, such as HSP60, may also be used as an adjuvant for the VSV-based vaccine. The host protein HSP60 was found to bind to the VSV transcriptase complex tightly (Qanungo et al., 2004). It is possible that HSP60 plays an important role during VSV transcription and replication.

HSP40 was found to promote high affinity binding between the measles virus N protein tail and HSP70 through stimulation of HSP70 ATPase activity (Couturier et al., 2010). If HSP70 binds to VSV proteins, co-expression of HSP40 together with HSP70 may enhance the adjuvant effect of HSP70 for the VSV based vaccine.

5.1.2 Facilitate the clinical trials of the VSV-based human NoV vaccine candidate.

In this study, it was demonstrated that the VSV-based human NoV vaccine not only triggered high levels of human NoV-specific humoral, cellular, and mucosal immunity, but also protected gnotobiotic piglets from virulent challenge. Clearly, rVSV-VP1 and rVSV-HSP70-VP1 are promising vaccine candidates for human NoV. These studies will facilitate future clinical trials of the VSV-based vaccine candidates in non-human primates and humans. It has been proven that VSV is an excellent vector for vaccines, oncolytic therapy, and gene delivery. In fact, VSV-vectored HIV vaccines and

VSV-based oncolytic agents are currently in human clinical trials. It will be interesting to determine whether the VSV-based human NoV vaccine can protect non-human primates and humans from norovirus infection.

References

(2011). Statement by NIH Director Dr. Francis Collins on the Institute of Medicine report addressing the scientific need for the use of chimpanzees in research.(Brief article). National Institutes of Health: News and Events, NA.

Abraham, G., and Banerjee, A.K. (1976). Sequential transcription of the genes of vesicular stomatitis virus. *Proc Natl Acad Sci U S A* 73, 1504-1508.

Abraham, G., Rhodes, D.P., and Banerjee, A.K. (1975). Novel initiation of RNA synthesis in vitro by vesicular stomatitis virus. *Nature* 255, 37-40.

Ahmed, M., Marino, T.R., Puckett, S., Kock, N.D., and Lyles, D.S. (2008). Immune response in the absence of neurovirulence in mice infected with m protein mutant vesicular stomatitis virus. *J Virol* 82, 9273-9277.

Arias, C.F., Isa, P., Guerrero, C.A., Mendez, E., Zarate, S., Lopez, T., Espinosa, R., Romero, P., and Lopez, S. (2002). Molecular biology of rotavirus cell entry. *Arch Med Res* 33, 356-361.

Asea, A., Rehli, M., Kabingu, E., Boch, J.A., Bare, O., Auron, P.E., Stevenson, M.A., and Calderwood, S.K. (2002). Novel signal transduction pathway utilized by extracellular HSP70: role of toll-like receptor (TLR) 2 and TLR4. *J Biol Chem* 277, 15028-15034.

Atmar, R.L., Bernstein, D.I., Harro, C.D., Al-Ibrahim, M.S., Chen, W.H., Ferreira, J., Estes, M.K., Graham, D.Y., Opekun, A.R., Richardson, C., *et al.* (2011). Norovirus vaccine against experimental human Norwalk Virus illness. *N Engl J Med* 365, 2178-2187.

Atmar, R.L., Opekun, A.R., Gilger, M.A., Estes, M.K., Crawford, S.E., Neill, F.H., and Graham, D.Y. (2008). Norwalk virus shedding after experimental human infection. *Emerg Infect Dis* 14, 1553-1557.

Bailey, D., Thackray, L.B., and Goodfellow, I.G. (2008). A single amino acid substitution in the murine norovirus capsid protein is sufficient for attenuation in vivo. *J Virol* 82, 7725-7728.

- Ball, J.M., Graham, D.Y., Opekun, A.R., Gilger, M.A., Guerrero, R.A., and Estes, M.K. (1999a). Recombinant Norwalk virus-like particles given orally to volunteers: phase I study. *Gastroenterology* 117, 40-48.
- Ball, J.M., Hardy, M.E., Atmar, R.L., Conner, M.E., and Estes, M.K. (1998). Oral immunization with recombinant Norwalk virus-like particles induces a systemic and mucosal immune response in mice. *J Virol* 72, 1345.
- Ball, L.A. (1977). Transcriptional mapping of vesicular stomatitis virus in vivo. *J Virol* 21, 411-414.
- Ball, L.A., Pringle, C.R., Flanagan, B., Perepelitsa, V.P., and Wertz, G.W. (1999b). Phenotypic consequences of rearranging the P, M, and G genes of vesicular stomatitis virus. *J Virol* 73, 4705-4712.
- Ball, L.A., and White, C.N. (1976). Order of transcription of genes of vesicular stomatitis virus. *Proc Natl Acad Sci U S A* 73, 442-446.
- Baric, R.S., Yount, B., Lindesmith, L., Harrington, P.R., Greene, S.R., Tseng, F.C., Davis, N., Johnston, R.E., Klapper, D.G., and Moe, C.L. (2002). Expression and self-assembly of Norwalk virus capsid protein from Venezuelan equine encephalitis virus replicons. *J Virol* 76, 3023-3030.
- Barr, J.N., Whelan, S.P., and Wertz, G.W. (1997). cis-Acting signals involved in termination of vesicular stomatitis virus mRNA synthesis include the conserved AUAC and the U7 signal for polyadenylation. *J Virol* 71, 8718-8725.
- Becker, K.M., Moe, C.L., Southwick, K.L., and MacCormack, J.N. (2000). Transmission of Norwalk virus during football game. *N Engl J Med* 343, 1223-1227.
- Belliot, G., Sosnovtsev, S.V., Mitra, T., Hammer, C., Garfield, M., and Green, K.Y. (2003). In vitro proteolytic processing of the MD145 norovirus ORF1 nonstructural polyprotein yields stable precursors and products similar to those detected in calicivirus-infected cells. *J Virol* 77, 10957-10974.
- Bertolotti-Ciarlet, A., Crawford, S.E., Hutson, A.M., and Estes, M.K. (2003). The 3' end of Norwalk virus mRNA contains determinants that regulate the expression and stability of the viral capsid protein VP1: a novel function for the VP2 protein. *J Virol* 77, 11603-11615.
- Bertolotti-Ciarlet, A., White, L.J., Chen, R., Prasad, B.V., and Estes, M.K. (2002). Structural requirements for the assembly of Norwalk virus-like particles. *J Virol* 76, 4044.
- Blanchard, E., Brand, D., and Roingard, P. (2003). Endogenous virus and hepatitis C virus-like particle budding in BHK-21 cells. *J Virol* 77, 3888-3889.

- Blumberg, B.M., Giorgi, C., and Kolakofsky, D. (1983). N protein of Vesicular Stomatitis Virus selectively encapsidates Leader RNA in vitro. *Cell* 32, 559-567.
- Bok, K., Parra, G.I., Mitra, T., Abente, E., Shaver, C.K., Boon, D., Engle, R., Yu, C., Kapikian, A.Z., Sosnovtsev, S.V., *et al.* (2011). Chimpanzees as an animal model for human norovirus infection and vaccine development. *Proc Natl Acad Sci U S A* 108, 325-330.
- Bourhis, J.M., Canard, B., and Longhi, S. (2006). Structural disorder within the replicative complex of measles virus: functional implications. *Virology* 344, 94-110.
- Braxton, C.L., Puckett, S.H., Lyles, D.S., and Mizel, S.B. (2010). Protection against lethal vaccinia virus challenge by using an attenuated matrix protein mutant vesicular stomatitis virus vaccine vector expressing poxvirus antigens. *J Virol* 84, 3552.
- Buonocore, L., Blight, K.J., Rice, C.M., and Rose, J.K. (2002). Characterization of vesicular stomatitis virus recombinants that express and incorporate high levels of hepatitis C virus glycoproteins. *J Virol* 76, 6865.
- Burch, A.D., and Weller, S.K. (2004). Nuclear sequestration of cellular chaperone and proteasomal machinery during herpes simplex virus type 1 infection. *J Virol* 78, 7175-7185.
- Burroughs, J.N., and Brown, F. (1978). Presence of a covalently linked protein on calicivirus RNA. *J Gen Virol* 41, 443-446.
- Carleton, M., and Brown, D.T. (1996). Events in the endoplasmic reticulum abrogate the temperature sensitivity of Sindbis virus mutant ts23. *J Virol* 70, 952-959.
- Carsillo, T., Carsillo, M., Niewiesk, S., Vasconcelos, D., and Oglesbee, M. (2004). Hyperthermic pre-conditioning promotes measles virus clearance from brain in a mouse model of persistent infection. *Brain Res* 1004, 73-82.
- Carsillo, T., Carsillo, M., Traylor, Z., Niewiesk, S., Oglesbee, M., Rajala-Schultz, P., and Popovich, P. (2009). Major histocompatibility complex haplotype determines hsp70-dependent protection against measles virus neurovirulence. *J Virol* 83, 5544.
- Carsillo, T., Traylor, Z., Choi, C., Niewiesk, S., and Oglesbee, M. (2006a). hsp72, a host determinant of measles virus neurovirulence. *J Virol* 80, 11031-11039.
- Carsillo, T., Zhang, X., Vasconcelos, D., Niewiesk, S., and Oglesbee, M. (2006b). A single codon in the nucleocapsid protein C terminus contributes to in vitro and in vivo fitness of Edmonston measles virus. *J Virol* 80, 2904-2912.

- Chan, M.C., Wong, Y.P., and Leung, W.K. (2007). Cell culture assay for human noroviruses. *Emerg Infect Dis* *13*, 1117; author reply 1117-1118.
- Cheetham, S., Souza, M., Meulia, T., Grimes, S., Han, M.G., and Saif, L.J. (2006). Pathogenesis of a genogroup II human norovirus in gnotobiotic pigs. *J Virol* *80*, 10372.
- Chen, R., Neill, J.D., Estes, M.K., and Prasad, B.V.V. (2006). X-Ray Structure of a Native Calicivirus: Structural Insights into Antigenic Diversity and Host Specificity. *Proc Natl Acad Sci USA* *103*, 8048.
- Chen, W., Lin, Y., Liao, C., and Hsieh, S. (2000). Modulatory effects of the human heat shock protein 70 on DNA vaccination. *J Biomed Sci* *7*, 412-419.
- Choi, J.M., Hutson, A.M., Estes, M.K., and Prasad, B.V. (2008). Atomic resolution structural characterization of recognition of histo-blood group antigens by Norwalk virus. *Proc Natl Acad Sci U S A* *105*, 9175-9180.
- Ciupitu, A.M., Petersson, M., O'Donnell, C.L., Williams, K., Jindal, S., Kiessling, R., and Welsh, R.M. (1998). Immunization with a lymphocytic choriomeningitis virus peptide mixed with heat shock protein 70 results in protective antiviral immunity and specific cytotoxic T lymphocytes. *J Exp Med* *187*, 685-691.
- Clements, J.D., Hartzog, N.M., and Lyon, F.L. (1988). Adjuvant activity of escherichia-coli heat-labile entero-toxin and effect on the induction of oral tolerance in mice to unrelated protein antigens. *Vaccine* *6*, 269-277.
- Cornish, T.E., Stallknecht, D.E., Brown, C.C., Seal, B.S., and Howerth, E.W. (2001). Pathogenesis of experimental vesicular stomatitis virus (New Jersey serotype) infection in the deer mouse (*Peromyscus maniculatus*). *Vet Pathol* *38*, 396-406.
- Couturier, M., Buccellato, M., Costanzo, S., Bourhis, J.M., Shu, Y., Nicaise, M., Desmadril, M., Flaudrops, C., Longhi, S., and Oglesbee, M. (2010). High affinity binding between Hsp70 and the C-terminal domain of the measles virus nucleoprotein requires an Hsp40 co-chaperone. *Journal of molecular recognition : JMR* *23*, 301-315.
- D'Souza, D.H., Sair, A., Williams, K., Papafragkou, E., Jean, J., Moore, C., and Jaykus, L. (2006). Persistence of caliciviruses on environmental surfaces and their transfer to food. *Int J Food Microbiol* *108*, 84-91.
- Daughenbaugh, K.F., Fraser, C.S., Hershey, J.W., and Hardy, M.E. (2003). The genome-linked protein VPg of the Norwalk virus binds eIF3, suggesting its role in translation initiation complex recruitment. *EMBO J* *22*, 2852-2859.

- de Jong, P.R., Schadenberg, A.W., Jansen, N.J., and Prakken, B.J. (2009). Hsp70 and cardiac surgery: molecular chaperone and inflammatory regulator with compartmentalized effects. *Cell Stress Chaperones* *14*, 117-131.
- de Silva, A.M., Balch, W.E., and Helenius, A. (1990). Quality control in the endoplasmic reticulum: folding and misfolding of vesicular stomatitis virus G protein in cells and in vitro. *J Cell Biol* *111*, 857-866.
- Donaldson, E.F., Lindesmith, L.C., Lobue, A.D., and Baric, R.S. (2008). Norovirus pathogenesis: mechanisms of persistence and immune evasion in human populations. *ImmunolRev* *225*, 190.
- Donaldson, E.F., Lindesmith, L.C., Lobue, A.D., and Baric, R.S. (2010). Viral shape-shifting: norovirus evasion of the human immune system. *Nat Rev Microbiol* *8*, 231-241.
- Doultree, J.C., Druce, J.D., Birch, C.J., Bowden, D.S., and Marshall, J.A. (1999). Inactivation of feline calicivirus, a Norwalk virus surrogate. *J Hosp Infect* *41*, 51-57.
- Duizer, E., Bijkerk, P., Rockx, B., De Groot, A., Twisk, F., and Koopmans, M. (2004a). Inactivation of caliciviruses. *Appl Environ Microbiol* *70*, 4538-4543.
- Duizer, E., Schwab, K.J., Neill, F.H., Atmar, R.L., Koopmans, M.P., and Estes, M.K. (2004b). Laboratory efforts to cultivate noroviruses. *JGenVirol* *85*, 79.
- Earl, P.L., Moss, B., and Doms, R.W. (1991). Folding, interaction with GRP78-BiP, assembly, and transport of the human immunodeficiency virus type 1 envelope protein. *J Virol* *65*, 2047-2055.
- Emerson, S.U., and Wagner, R.R. (1972). Dissociation and reconstitution of the transcriptase and template activities of vesicular stomatitis B and T virions. *JVirol* *10*, 297-309.
- Emerson, S.U., and Yu, Y. (1975). Both NS and L proteins are required for in vitro RNA synthesis by vesicular stomatitis virus. *JVirol* *15*, 1348-1356.
- Estes, M.K., Ball, J.M., Guerrero, R.A., Opekun, A.R., Gilger, M.A., Pacheco, S.S., and Graham, D.Y. (2000). Norwalk virus vaccines: challenges and progress. *JInfectDis* *181*, 367.
- Estes, M.K., Prasad, B.V., and Atmar, R.L. (2006). Noroviruses everywhere: has something changed? *CurrOpinInfectDis* *19*, 467.
- Ettayebi, K., and Hardy, M.E. (2003). Norwalk virus nonstructural protein p48 forms a complex with the SNARE regulator VAP-A and prevents cell surface expression of vesicular stomatitis virus G protein. *J Virol* *77*, 11790-11797.

- Ezelle, H.J., Markovic, D., and Barber, G.N. (2002). Generation of hepatitis C virus-like particles by use of a recombinant vesicular stomatitis virus vector. *J Virol* 76, 12325.
- Faber, M., Lamirande, E.W., Roberts, A., Rice, A.B., Koprowski, H., Dietzschold, B., and Schnell, M.J. (2005). A single immunization with a rhabdovirus-based vector expressing severe acute respiratory syndrome coronavirus (SARS-CoV) S protein results in the production of high levels of SARS-CoV-neutralizing antibodies. *J Gen Virol* 86, 1435.
- Fang, X., Zhang, S., Sun, X., Li, J., and Sun, T. (2012). Evaluation of attenuated VSVs with mutated M or/and G proteins as vaccine vectors. *Vaccine* 30, 1313-1321.
- Farkas, T., Cross, R.W., Hargitt, E., 3rd, Lerche, N.W., Morrow, A.L., and Sestak, K. (2010). Genetic diversity and histo-blood group antigen interactions of rhesus enteric caliciviruses. *J Virol* 84, 8617-8625.
- Farkas, T., Sestak, K., Wei, C., and Jiang, X. (2008). Characterization of a rhesus monkey calicivirus representing a new genus of Caliciviridae. *J Virol* 82, 5408-5416.
- Fei-fei, G., Jian, W., Feng, X., Li-ping, S., Quan-yun, S., Jin-ping, Z., Pu-yan, C., and Pei-hong, L. (2008). Japanese encephalitis protein vaccine candidates expressing neutralizing epitope and M.T hsp70 induce virus-specific memory B cells and long-lasting antibodies in swine. *Vaccine* 26, 5590-5594.
- Fellowes, O.N., Dimopoulos, G.T., and Callis, J.J. (1955). Isolation of vesicular stomatitis virus from an infected laboratory worker. *American Journal of Veterinary Research* 16, 623-626.
- Fernandez-Vega, V., Sosnovtsev, S.V., Belliot, G., King, A.D., Mitra, T., Gorbalenya, A., and Green, K.Y. (2004). Norwalk Virus N-Terminal Nonstructural Protein Is Associated with Disassembly of the Golgi Complex in Transfected Cells. *J Virol* 78, 4827-4837.
- Fields, B.N., Knipe, D.M., and Howley, P.M. (2007). *Fields virology* (Philadelphia, Wolters Kluwer Health/Lippincott Williams & Wilkins).
- Follett, E.A., Pringle, C.R., Wunner, W.H., and Skehel, J.J. (1974). Virus replication in enucleate cells: vesicular stomatitis virus and influenza virus. *J Virol* 13, 394-399.
- Garbutt, M., Liebscher, R., Wahl-Jensen, V., Jones, S., Moller, P., Wagner, R., Volchkov, V., Klenk, H.D., Feldmann, H., and Stroher, U. (2004). Properties of replication-competent vesicular stomatitis virus vectors expressing glycoproteins of filoviruses and arenaviruses. *J Virol* 78, 5458-5465.

- Ge, F.F., Qiu, Y.F., Yang, Y.W., and Chen, P.Y. (2007). An hsp70 fusion protein vaccine potentiates the immune response against Japanese encephalitis virus. *Arch Virol* 152, 125-135.
- Geisbert, T.W., Daddario-DiCaprio, K.M., Geisbert, J.B., Reed, D.S., Feldmann, F., Grolla, A., Stroehrer, U., Fritz, E.A., Hensley, L.E., Jones, S.M., *et al.* (2008). Vesicular stomatitis virus-based vaccines protect nonhuman primates against aerosol challenge with Ebola and Marburg viruses. *Vaccine* 26, 6894-6900.
- Glass, P.J., White, L.J., Ball, J.M., Leparac-Goffart, I., Hardy, M.E., and Estes, M.K. (2000). Norwalk virus open reading frame 3 encodes a minor structural protein. *J Virol* 74, 6581.
- Goodgame, R. (2006). Norovirus gastroenteritis. *Curr Gastroenterol Rep* 8, 401-408.
- Guerrero, R.A., Ball, J.M., Krater, S.S., Pacheco, S.E., Clements, J.D., and Estes, M.K. (2001). Recombinant Norwalk virus-like particles administered intranasally to mice induce systemic and mucosal (fecal and vaginal) immune responses. *J Virol* 75, 9713-9722.
- Guo, L., Zhou, H., Wang, M., Song, J., Han, B., Shu, Y., Ren, L., Si, H., Qu, J., Zhao, Z., *et al.* (2009). A recombinant adenovirus prime-virus-like particle boost regimen elicits effective and specific immunities against norovirus in mice. *Vaccine* 27, 5233-5238.
- Gurer, C., Cimorelli, A., and Luban, J. (2002). Specific incorporation of heat shock protein 70 family members into primate lentiviral virions. *J Virol* 76, 4666-4670.
- Haglund, K., Leiner, I., Kerksiek, K., Buonocore, L., Pamer, E., and Rose, J.K. (2002). High-level primary CD8(+) T-cell response to human immunodeficiency virus type 1 gag and env generated by vaccination with recombinant vesicular stomatitis viruses. *J Virol* 76, 2730-2738.
- Hall, A.J., Centers for Disease Control and Prevention (U.S.), and National Center for Immunization and Respiratory Diseases (U.S.) (2011). Updated norovirus outbreak management and disease prevention guidelines (Atlanta, GA, U.S. Dept. of Health and Human Services, Centers for Disease Control and Prevention).
- Hammond, C., and Helenius, A. (1994). Folding of VSV G protein: sequential interaction with BiP and calnexin. *Science* 266, 456-458.
- Hanson, R.P., Rasmussen, A.F., Brandly, C.A., and Brown, J.W. (1950). Human infection with the virus of vesicular stomatitis. *Journal of Laboratory and Clinical Medicine* 36, 754-758.

- Hardy, M.E. (2005). Norovirus protein structure and function. *FEMS Microbiol Lett* 253, 1-8.
- Hardy, M.E., White, L.J., Ball, J.M., and Estes, M.K. (1995). Specific proteolytic cleavage of recombinant norwalk virus capsid protein. *J Virol* 69, 1693-1698.
- Harrington, P.R., Yount, B., Johnston, R.E., Davis, N., Moe, C., and Baric, R.S. (2002). Systemic, Mucosal, and Heterotypic Immune Induction in Mice Inoculated with Venezuelan Equine Encephalitis Replicons Expressing Norwalk Virus-Like Particles. *The Journal of Virology* 76, 730.
- Harris, J.P., Edmunds, W.J., Pebody, R., Brown, D.W., and Lopman, B.A. (2008). Deaths from norovirus among the elderly, England and Wales. *Emerging Infectious Diseases* 14, 1546-1552.
- Hsu, C.C., Wobus, C.E., Steffen, E.K., Riley, L.K., and Livingston, R.S. (2005). Development of a microsphere-based serologic multiplexed fluorescent immunoassay and a reverse transcriptase PCR assay to detect murine norovirus 1 infection in mice. *Clin Diagn Lab Immunol* 12, 1145-1151.
- Hutson, A.M., Airaud, F., LePendou, J., Estes, M.K., and Atmar, R.L. (2005). Norwalk virus infection associates with secretor status genotyped from sera. *J Med Virol* 77, 116-120.
- Hutson, A.M., Atmar, R.L., and Estes, M.K. (2004). Norovirus disease: changing epidemiology and host susceptibility factors. *Trends Microbiol* 12, 279-287.
- Hutson, A.M., Atmar, R.L., Graham, D.Y., and Estes, M.K. (2002). Norwalk virus infection and disease is associated with ABO histo-blood group type. *J Infect Dis* 185, 1335-1337.
- Hutson, A.M., Atmar, R.L., Marcus, D.M., and Estes, M.K. (2003). Norwalk virus-like particle hemagglutination by binding to h histo-blood group antigens. *J Virol* 77, 405-415.
- Hwang, L.N., Englund, N., and Pattnaik, A.K. (1998). Polyadenylation of vesicular stomatitis virus mRNA dictates efficient transcription termination at the intercistronic gene junctions. *J Virol* 72, 1805-1813.
- Iverson, L.E., and Rose, J.K. (1981). Localized attenuation and discontinuous synthesis during Vesicular Stomatitis-Virus Transcription. *Cell* 23, 477-484.
- Jayakar, H.R., Jeetendra, E., and Whitt, M.A. (2004). Rhabdovirus assembly and budding. *Virus research* 106, 117-132.

- Jiang, X., Graham, D.Y., Wang, K., and Estes, M.K. (1990). Norwalk virus genome cloning and characterization. *Science (Washington D C)* *250*, 1580-1583.
- Jiang, X., Wang, M., Graham, D.Y., and Estes, M.K. (1992). Expression, self-assembly, and antigenicity of the Norwalk virus capsid protein. *J Virol* *66*, 6527.
- Jiang, X., Wang, M., Wang, K., and Estes, M.K. (1993). Sequence and genomic organization of Norwalk virus. *Virology* *195*, 51-61.
- Johnson, J.E., Schnell, M.J., Buonocore, L., and Rose, J.K. (1997). Specific targeting to CD4+ cells of recombinant vesicular stomatitis viruses encoding human immunodeficiency virus envelope proteins. *J Virol* *71*, 5060-5068.
- Johnson, P.C., Mathewson, J.J., DuPont, H.L., and Greenberg, H.B. (1990). Multiple-challenge study of host susceptibility to Norwalk gastroenteritis in US adults. *J Infect Dis* *161*, 18-21.
- Jones, S.M., Feldmann, H., Stroher, U., Geisbert, J.B., Fernando, L., Grolla, A., Klenk, H.D., Sullivan, N.J., Volchkov, V.E., Fritz, E.A., *et al.* (2005). Live attenuated recombinant vaccine protects nonhuman primates against Ebola and Marburg viruses. *Nature medicine* *11*, 786-790.
- Kahn, J.S., Roberts, A., Weibel, C., Buonocore, L., and Rose, J.K. (2001). Replication-competent or attenuated, nonpropagating vesicular stomatitis viruses expressing respiratory syncytial virus (RSV) antigens protect mice against RSV challenge. *J Virol* *75*, 11079.
- Kapadia, S.U., Rose, J.K., Lamirande, E., Vogel, L., Subbarao, K., and Roberts, A. (2005). Long-term protection from SARS coronavirus infection conferred by a single immunization with an attenuated VSV-based vaccine. *Virology* *340*, 174.
- Kapikian, A.Z., Wyatt, R.G., Dolin, R., Thornhill, Ts, Kalica, A.R., and Chanock, R.M. (1972). Visualization by immune electron-microscopy of a 27-nm particle associated with acute infectious nonbacterial gastroenteritis. *J Virol* *10*, 1075-1081.
- Karst, S.M., Wobus, C.E., Lay, M., Davidson, J., and Virgin, H.W.t. (2003). STAT1-dependent innate immunity to a Norwalk-like virus. *Science* *299*, 1575-1578.
- Kitamoto, N., Tanaka, T., Natori, K., Takeda, N., Nakata, S., Jiang, X., and Estes, M.K. (2002). Cross-reactivity among several recombinant calicivirus virus-like particles (VLPs) with monoclonal antibodies obtained from mice immunized orally with one type of VLP. *J Clin Microbiol* *40*, 2459-2465.
- Koopmans, M. (2008). Progress in understanding norovirus epidemiology. *Current opinion in infectious diseases* *21*, 544.

- Koopmans, M., and Duizer, E. (2004). Foodborne viruses: an emerging problem. *Int J Food Microbiol* 90, 23-41.
- Krakovka, S., Eaton, K.A., Rings, D.M., and Morgan, D.R. (1991). Gastritis induced by *Helicobacter pylori* in gnotobiotic piglets. *Rev Infect Dis* 13 *Suppl* 8, S681-685.
- Krakovka, S., and Ellis, J.A. (2008). Evaluation of the effects of porcine genogroup 1 torque teno virus in gnotobiotic swine. *Am J Vet Res* 69, 1623-1629.
- Krakovka, S., Ellis, J.A., Meehan, B., Kennedy, S., McNeilly, F., and Allan, G. (2000). Viral wasting syndrome of swine: experimental reproduction of postweaning multisystemic wasting syndrome in gnotobiotic swine by coinfection with porcine circovirus 2 and porcine parvovirus. *Vet Pathol* 37, 254-263.
- Kumaraguru, U., Gierynska, M., Norman, S., Bruce, B.D., and Rouse, B.T. (2002). Immunization with chaperone-peptide complex induces low-avidity cytotoxic T lymphocytes providing transient protection against herpes simplex virus infection. *J Virol* 76, 136-141.
- Kuyumcu-Martinez, M., Belliot, G., Sosnovtsev, S.V., Chang, K.O., Green, K.Y., and Lloyd, R.E. (2004). Calicivirus 3C-like proteinase inhibits cellular translation by cleavage of poly(A)-binding protein. *J Virol* 78, 8172-8182.
- Lawson, N.D., Stillman, E.A., Whitt, M.A., and Rose, J.K. (1995). Recombinant Vesicular Stomatitis Viruses from DNA. *Proc Natl Acad Sci USA* 92, 4477.
- Lay, M.K., Atmar, R.L., Guix, S., Bharadwaj, U., He, H., Neill, F.H., Sastry, K.J., Yao, Q., and Estes, M.K. (2010). Norwalk virus does not replicate in human macrophages or dendritic cells derived from the peripheral blood of susceptible humans. *Virology* 406, 1-11.
- Letchworth, G.J., Rodriguez, L.L., and Del carrera, J. (1999). Vesicular stomatitis. *Vet J* 157, 239-260.
- Leung, W.K., Chan, P.K., Lee, N.L., and Sung, J.J. (2010). Development of an in vitro cell culture model for human noroviruses and its clinical application. *Hong Kong Med J* 16, 18-21.
- Li, J., Jiang, P., Li, Y., Wang, X., Cao, J., and Zeshan, B. (2009a). HSP70 fused with GP3 and GP5 of porcine reproductive and respiratory syndrome virus enhanced the immune responses and protective efficacy against virulent PRRSV challenge in pigs. *Vaccine* 27, 825-832.
- Li, J., Li, K.N., Gao, J., Cui, J.H., Liu, Y.F., and Yang, S.J. (2008a). Heat shock protein 70 fused to or complexed with hantavirus nucleocapsid protein significantly enhances

specific humoral and cellular immune responses in C57BL/6 mice. *Vaccine* 26, 3175-3187.

Li, J., Rahmeh, A., Brusica, V., and Whelan, S.P. (2009b). Opposing effects of inhibiting cap addition and cap methylation on polyadenylation during vesicular stomatitis virus mRNA synthesis. *J Virol* 83, 1930-1940.

Li, J., Rahmeh, A., Morelli, M., and Whelan, S.P. (2008b). A conserved motif in region v of the large polymerase proteins of nonsegmented negative-sense RNA viruses that is essential for mRNA capping. *J Virol* 82, 775-784.

Li, J., Wang, J.T., and Whelan, S.P. (2006). A unique strategy for mRNA cap methylation used by vesicular stomatitis virus. *Proc Natl Acad Sci U S A* 103, 8493-8498.

Li, J.R., Fontaine-Rodriguez, E.C., and Whelan, S.P.J. (2005). Amino acid residues within conserved domain VI of the vesicular stomatitis virus large polymerase protein essential for mRNA cap methyltransferase activity. *J Virol* 79, 13373-13384.

Lichty, B.D., Power, A.T., Stojdl, D.F., and Bell, J.C. (2004). Vesicular stomatitis virus: re-inventing the bullet. *Trends in molecular medicine* 10, 210-216.

Lin, B.Y., Makhov, A.M., Griffith, J.D., Broker, T.R., and Chow, L.T. (2002). Chaperone proteins abrogate inhibition of the human papillomavirus (HPV) E1 replicative helicase by the HPV E2 protein. *Mol Cell Biol* 22, 6592-6604.

Lindesmith, L., Moe, C., Marionneau, S., Ruvoen, N., Jiang, X., Lindblad, L., Stewart, P., LePendu, J., and Baric, R. (2003). Human susceptibility and resistance to Norwalk virus infection. *Nat Med* 9, 548-553.

Liu, J.S., Kuo, S.R., Makhov, A.M., Cyr, D.M., Griffith, J.D., Broker, T.R., and Chow, L.T. (1998). Human Hsp70 and Hsp40 chaperone proteins facilitate human papillomavirus-11 E1 protein binding to the origin and stimulate cell-free DNA replication. *J Biol Chem* 273, 30704-30712.

LoBue, A.D., Lindesmith, L.C., and Baric, R.S. (2010). Identification of Cross-Reactive Norovirus CD4(+) T Cell Epitopes. *J Virol* 84, 8530-8538.

LoBue, A.D., Thompson, J.M., Lindesmith, L., Johnston, R.E., and Baric, R.S. (2009). Alphavirus-adjuvanted norovirus-like particle vaccines: heterologous, humoral, and mucosal immune responses protect against murine norovirus challenge. *J Virol* 83, 3212-3227.

- Lopman, B.A., Adak, G.K., Reacher, M.H., and Brown, D.W. (2003). Two epidemiologic patterns of norovirus outbreaks: surveillance in England and Wales, 1992-2000. *Emerg Infect Dis* 9, 71-77.
- Majid, A.M., Ezelle, H., Shah, S., and Barber, G.N. (2006). Evaluating replication-defective vesicular stomatitis virus as a vaccine vehicle. *J Virol* 80, 6993-7008.
- Marks, P.J., Vipond, I.B., Carlisle, D., Deakin, D., Fey, R.E., and Caul, E.O. (2000). Evidence for airborne transmission of Norwalk-like virus (NLV) in a hotel restaurant. *Epidemiol Infect* 124, 481-487.
- Marks, P.J., Vipond, I.B., Regan, F.M., Wedgwood, K., Fey, R.E., and Caul, E.O. (2003). A school outbreak of Norwalk-like virus: evidence for airborne transmission. *Epidemiol Infect* 131, 727-736.
- Matlin, K.S., Reggio, H., Helenius, A., and Simons, K. (1982). Pathway of vesicular stomatitis virus entry leading to infection. *J Mol Biol* 156, 609-631.
- Mead, P.S., Slutsker, L., Dietz, V., McCaig, L.F., Bresee, J.S., Shapiro, C., Griffin, P.M., and Tauxe, R.V. (1999). Food-related illness and death in the United States. *Emerging Infectious Diseases* 5, 607-625.
- Milani, V., Noessner, E., Ghose, S., Kuppner, M., Ahrens, B., Scharner, A., Gastpar, R., and Issels, R.D. (2002). Heat shock protein 70: role in antigen presentation and immune stimulation. *Int J Hyperthermia* 18, 563-575.
- Millar, D.G., Garza, K.M., Odermatt, B., Elford, A.R., Ono, N., Li, Z., and Ohashi, P.S. (2003). Hsp70 promotes antigen-presenting cell function and converts T-cell tolerance to autoimmunity in vivo. *Nat Med* 9, 1469-1476.
- Multhoff, G. (2002). Activation of natural killer cells by heat shock protein 70. *Int J Hyperthermia* 18, 576-585.
- Mumphrey, S.M., Changotra, H., Moore, T.N., Heimann-Nichols, E.R., Wobus, C.E., Reilly, M.J., Moghadamfalahi, M., Shukla, D., and Karst, S.M. (2007). Murine norovirus 1 infection is associated with histopathological changes in immunocompetent hosts, but clinical disease is prevented by STAT1-dependent interferon responses. *J Virol* 81, 3251-3263.
- Newport, G.R. (1991). Heat shock proteins as vaccine candidates. *Semin Immunol* 3, 17-24.
- Ng, H.H., Robert, F., Young, R.A., and Struhl, K. (2002a). Genome-wide location and regulated recruitment of the RSC nucleosome-remodeling complex. *Genes Dev* 16, 806-819.

- Ng, K.K., Cherney, M.M., Vazquez, A.L., Machin, A., Alonso, J.M., Parra, F., and James, M.N. (2002b). Crystal structures of active and inactive conformations of a caliciviral RNA-dependent RNA polymerase. *J Biol Chem* 277, 1381-1387.
- O'Keeffe, B., Fong, Y., Chen, D., Zhou, S., and Zhou, Q. (2000). Requirement for a kinase-specific chaperone pathway in the production of a Cdk9/cyclin T1 heterodimer responsible for P-TEFb-mediated tat stimulation of HIV-1 transcription. *J Biol Chem* 275, 279-287.
- Ogino, T., and Banerjee, A.K. (2007). Unconventional mechanism of mRNA capping by the RNA-dependent RNA polymerase of vesicular stomatitis virus. *Mol Cell* 25, 85-97.
- Oglesbee, M., and Niewiesk, S. (2011). Measles virus neurovirulence and host immunity. *Future Virol* 6, 85-99.
- Oglesbee, M., Pratt, M., and Carsillo, T. (2002). Role for Heat Shock Proteins in the Immune Response to Measles Virus Infection. *Viral Immunol* 15, 399.
- Oglesbee, M., Ringler, S., and Krakowka, S. (1990). Interaction of canine distemper virus nucleocapsid variants with 70K heat-shock proteins. *J Gen Virol* 71 (Pt 7), 1585-1590.
- Oglesbee, M.J., Liu, Z., Kenney, H., and Brooks, C.L. (1996). The highly inducible member of the 70 kDa family of heat shock proteins increases canine distemper virus polymerase activity. *JGenVirol* 77 (Pt 9), 2125.
- Parrino, T.A., Schreiber, D.S., Trier, J.S., Kapikian, A.Z., and Blacklow, N.R. (1977). Clinical immunity in acute gastroenteritis caused by Norwalk agent. *N Engl J Med* 297, 86-89.
- Patel, M.M., Widdowson, M.A., Glass, R.I., Akazawa, K., Vinje, J., and Parashar, U.D. (2008). Systematic literature review of role of noroviruses in sporadic gastroenteritis. *Emerg Infect Dis* 14, 1224-1231.
- Petrovsky, N., and Aguilar, J.C. (2004). Vaccine adjuvants: Current state and future trends. *Immunology and Cell Biology* 82, 488-496.
- Pfister, T., and Wimmer, E. (2001). Polypeptide p41 of a Norwalk-like virus is a nucleic acid-independent nucleoside triphosphatase. *J Virol* 75, 1611-1619.
- Prasad, B.V., Hardy, M.E., Dokland, T., Bella, J., Rossmann, M.G., and Estes, M.K. (1999). X-ray crystallographic structure of the Norwalk virus capsid. *Science (New York, NY)* 286, 287.
- Prasad, B.V.V., and Hardy, M.E. (1999). X-ray Crystallographic Structure of the Norwalk Virus Capsid. *Science* 286, 287.

Publicover, J., Ramsburg, E., and Rose, J.K. (2005). A single-cycle vaccine vector based on vesicular stomatitis virus can induce immune responses comparable to those generated by a replication-competent vector. *J Virol* 79, 13231-13238.

Qanungo, K.R., Shaji, D., Mathur, M., and Banerjee, A.K. (2004). Two RNA polymerase complexes from vesicular stomatitis virus-infected cells that carry out transcription and replication of genome RNA. *Proc Natl Acad Sci U S A* 101, 5952-5957.

Ravn, V., and Dabelsteen, E. (2000). Tissue distribution of histo-blood group antigens. *APMIS* 108, 1-28.

Reiss, C.S., Plakhov, I.V., and Komatsu, T. (1998). Viral replication in olfactory receptor neurons and entry into the olfactory bulb and brain. *Ann N Y Acad Sci* 855, 751-761.

Reuter, J.D., Vivas-Gonzalez, B.E., Gomez, D., Wilson, J.H., Brandsma, J.L., Greenstone, H.L., Rose, J.K., and Roberts, A. (2002). Intranasal vaccination with a recombinant vesicular stomatitis virus expressing cottontail rabbit papillomavirus L1 protein provides complete protection against papillomavirus-induced disease. *J Virol* 76, 8900.

Roberts, A., Buonocore, L., Price, R., Forman, J., and Rose, J.K. (1999). Attenuated vesicular stomatitis viruses as vaccine vectors. *J Virol* 73, 3723-3732.

Roberts, A., Kretzschmar, E., Perkins, A.S., Forman, J., Price, R., Buonocore, L., Kawaoka, Y., and Rose, J.K. (1998). Vaccination with a Recombinant Vesicular Stomatitis Virus Expressing an Influenza Virus Hemagglutinin Provides Complete Protection from Influenza Virus Challenge. *J Virol* 72, 4704.

Rockx, B., De Wit, M., Vennema, H., Vinje, J., De Bruin, E., Van Duynhoven, Y., and Koopmans, M. (2002). Natural history of human calicivirus infection: a prospective cohort study. *Clin Infect Dis* 35, 246-253.

Rockx, B.H., Bogers, W.M., Heeney, J.L., van Amerongen, G., and Koopmans, M.P. (2005). Experimental norovirus infections in non-human primates. *J Med Virol* 75, 313-320.

Rose, N.F., Marx, P.A., Luckay, A., Nixon, D.F., Moretto, W.J., Donahoe, S.M., Montefiori, D., Roberts, A., Buonocore, L., and Rose, J.K. (2001). An effective AIDS vaccine based on live attenuated vesicular stomatitis virus recombinants. *Cell* 106, 539.

Sagara, J., and Kawai, A. (1992). Identification of heat shock protein 70 in the rabies virion. *Virology* 190, 845-848.

- Saphire, A.C., Guan, T., Schirmer, E.C., Nemerow, G.R., and Gerace, L. (2000). Nuclear import of adenovirus DNA in vitro involves the nuclear protein import pathway and hsc70. *J Biol Chem* 275, 4298-4304.
- Scallan, E. (2011). Foodborne Illness Acquired in the United States—Major Pathogens. *Emerg Infect Dis* Emerging Infectious Diseases 17.
- Schnell, M.J., Buonocore, L., Kretzschmar, E., Johnson, E., and Rose, J.K. (1996). Foreign glycoproteins expressed from recombinant vesicular stomatitis viruses are incorporated efficiently into virus particles. *Proc Natl Acad Sci U S A* 93, 11359-11365.
- Schnell, M.J., Johnson, J.E., Buonocore, L., and Rose, J.K. (1997). Construction of a novel virus that targets HIV-1-infected cells and controls HIV-1 infection. *Cell* 90, 849-857.
- Seah, E.L., Gunsekere, I.C., Marshall, J.A., and Wright, P.J. (1999). Variation in ORF3 of genogroup 2 Norwalk-like viruses. *Arch Virol* 144, 1007-1014.
- Seán, P.J.W., Ball, L.A., Barr, J.N., and Wertz, G.T.W. (1995). Efficient Recovery of Infectious Vesicular Stomatitis Virus Entirely from cDNA Clones. *Proc Natl Acad Sci USA* 92, 8388-8392.
- Sekaly, R.-P. (2008). The failed HIV Merck vaccine study: A step back or a launching point for future vaccine development? *Journal of Experimental Medicine* 205, 7-12.
- Shirato, H. (2011). Norovirus and histo-blood group antigens. *Jpn J Infect Dis* 64, 95-103.
- Singh, I., Doms, R.W., Wagner, K.R., and Helenius, A. (1990). Intracellular transport of soluble and membrane-bound glycoproteins: folding, assembly and secretion of anchor-free influenza hemagglutinin. *EMBO J* 9, 631-639.
- Souza, M., Azevedo, M.S., Jung, K., Cheetham, S., and Saif, L.J. (2008). Pathogenesis and immune responses in gnotobiotic calves after infection with the genogroup II.4-HS66 strain of human norovirus. *J Virol* 82, 1777-1786.
- Souza, M., Cheetham, S.M., Azevedo, M.S., Costantini, V., and Saif, L.J. (2007a). Cytokine and antibody responses in gnotobiotic pigs after infection with human norovirus genogroup II.4 (HS66 strain). *J Virol* 81, 9183-9192.
- Souza, M., Costantini, V., Azevedo, M.S., and Saif, L.J. (2007b). A human norovirus-like particle vaccine adjuvanted with ISCOM or mLT induces cytokine and antibody responses and protection to the homologous GII.4 human norovirus in a gnotobiotic pig disease model. *Vaccine* 25, 8448-8459.

- Souza, M., Costantini, V., Azevedo, M.S.P., and Saif, L.J. (2007c). Human norovirus-like particle vaccine adjuvanted with ISCOM or mLT induces cytokine and antibody responses and protection to the homologous GII.4 human norovirus in a gnotobiotic pig disease model. *Vaccine* 25, 8448-8459.
- Spearman, P. (2003). HIV vaccine development: Lessons from the past and promise for the future. *Curr Hiv Res* 1, 101-120.
- Srivastava, P. (2002). Roles of heat-shock proteins in innate and adaptive immunity. *Nat Rev Immunol* 2, 185-194.
- Straub, T.M., Honer zu Bentrup, K., Orosz-Coghlan, P., Dohnalkova, A., Mayer, B.K., Bartholomew, R.A., Valdez, C.O., Bruckner-Lea, C.J., Gerba, C.P., Abbaszadegan, M., *et al.* (2007). In vitro cell culture infectivity assay for human noroviruses. *Emerg Infect Dis* 13, 396-403.
- Subekti, D.S., Tjaniadi, P., Lesmana, M., McArdle, J., Iskandriati, D., Budiarsa, I.N., Walujo, P., Suparto, I.H., Winoto, I., Campbell, J.R., *et al.* (2002). Experimental infection of *Macaca nemestrina* with a Toronto Norwalk-like virus of epidemic viral gastroenteritis. *J Med Virol* 66, 400-406.
- Suzue, K., and Young, R.A. (1996). Heat shock proteins as immunological carriers and vaccines. *EXS* 77, 451-465.
- Tacket, C.O., Mason, H.S., Losonsky, G., Estes, M.K., Levine, M.M., and Arntzen, C.J. (2000). Human immune responses to a novel norwalk virus vaccine delivered in transgenic potatoes. *J Infect Dis* 182, 302-305.
- Tacket, C.O., Sztein, M.B., Losonsky, G.A., Wasserman, S.S., and Estes, M.K. (2003). Humoral, mucosal, and cellular immune responses to oral Norwalk virus-like particles in volunteers. *Clin Immunol* 108, 241-247.
- Tan, G.S., McKenna, P.M., Koser, M.L., McLinden, R., Kim, J.H., McGettigan, J.P., and Schnell, M.J. (2005). Strong cellular and humoral anti-HIV Env immune responses induced by a heterologous rhabdoviral prime-boost approach. *Virology* 331, 82.
- Tan, M., Huang, P., Meller, J., Zhong, W., Farkas, T., and Jiang, X. (2003). Mutations within the P2 domain of norovirus capsid affect binding to human histo-blood group antigens: evidence for a binding pocket. *J Virol* 77, 12562-12571.
- Tan, M., Huang, P., Xia, M., Fang, P.A., Zhong, W., McNeal, M., Wei, C., Jiang, W., and Jiang, X. (2011). Norovirus P particle, a novel platform for vaccine development and antibody production. *J Virol* 85, 753-764.

- Tan, M., and Jiang, X. (2005a). Norovirus and its histo-blood group antigen receptors: an answer to a historical puzzle. *Trends Microbiol* *13*, 285-293.
- Tan, M., and Jiang, X. (2005b). The P Domain of Norovirus Capsid Protein Forms a Subviral Particle That Binds to Histo-Blood Group Antigen Receptors. *JVirol* *79*, 14017.
- Tan, M., and Jiang, X. (2012). Norovirus P particle: a subviral nanoparticle for vaccine development against norovirus, rotavirus and influenza virus. *Nanomedicine (Lond)* *7*, 889-897.
- Tan, M., Xia, M., Chen, Y., Bu, W., Hegde, R.S., Meller, J., Li, X., and Jiang, X. (2009). Conservation of Carbohydrate Binding Interfaces - Evidence of Human HBGA Selection in Norovirus Evolution. *PLoS One* *4*.
- Tan, M., Zhong, W., Song, D., Thornton, S., and Jiang, X. (2004). E. coli-expressed recombinant norovirus capsid proteins maintain authentic antigenicity and receptor binding capability. *JMedVirol* *74*, 641.
- Taube, S., Kurth, A., and Schreier, E. (2005). Generation of recombinant Norovirus-like particles (VLP) in the human endothelial kidney cell line 293T. *ArchVirol* *150*, 1425.
- Taube, S., Rubin, J.R., Katpally, U., Smith, T.J., Kendall, A., Stuckey, J.A., and Wobus, C.E. (2010). High-resolution x-ray structure and functional analysis of the murine norovirus 1 capsid protein protruding domain. *J Virol* *84*, 5695-5705.
- Todryk, S.M., Gough, M.J., and Pockley, A.G. (2003). Facets of heat shock protein 70 show immunotherapeutic potential. *Immunology* *110*, 1.
- Triantafilou, K., Fradelizi, D., Wilson, K., and Triantafilou, M. (2002). GRP78, a coreceptor for coxsackievirus A9, interacts with major histocompatibility complex class I molecules which mediate virus internalization. *J Virol* *76*, 633-643.
- Vabulas, R.M., Ahmad-Nejad, P., Ghose, S., Kirschning, C.J., Issels, R.D., and Wagner, H. (2002). HSP70 as endogenous stimulus of the Toll/interleukin-1 receptor signal pathway. *J Biol Chem* *277*, 15107-15112.
- Vasconcelos, D.Y., Cai, X.H., and Oglesbee, M.J. (1998). Constitutive overexpression of the major inducible 70 kDa heat shock protein mediates large plaque formation by measles virus. *JGenVirol* *79*, 2239.
- Wertz, G.W., Perepelitsa, V.P., and Ball, L.A. (1998). Gene rearrangement attenuates expression and lethality of a nonsegmented negative strand RNA virus. *Proc Natl Acad Sci U S A* *95*, 3501-3506.
- Whelan, S.P., Barr, J.N., and Wertz, G.W. (2004). Transcription and replication of nonsegmented negative-strand RNA viruses. *Curr Top Microbiol Immunol* *283*, 61-119.

- Whelan, S.P.J., Ball, L.A., Barr, J.N., and Wertz, G.T.W. (1995). Efficient recovery of infectious vesicular stomatitis-virus entirely from cDNA clones. *Proc Natl Acad Sci USA* *92*, 8388-8392.
- Whelan, S.P.J., and Wertz, G.W. (2002). Transcription and Replication Initiate at Separate Sites on the Vesicular Stomatitis Virus Genome. *Proc Natl Acad Sci USA* *99*, 9178-9183.
- White, L.J., Ball, J.M., Hardy, M.E., Tanaka, T.N., Kitamoto, N., and Estes, M.K. (1996). Attachment and entry of recombinant Norwalk virus capsids to cultured human and animal cell lines. *J Virol* *70*, 6589.
- Wobus, C.E., Karst, S.M., Thackray, L.B., Chang, K.O., Sosnovtsev, S.V., Belliot, G., Krug, A., Mackenzie, J.M., Green, K.Y., and Virgin, H.W. (2004). Replication of Norovirus in cell culture reveals a tropism for dendritic cells and macrophages. *PLoS Biol* *2*, e432.
- Wobus, C.E., Thackray, L.B., and Virgin, H.W. (2006). Murine norovirus: a model system to study norovirus biology and pathogenesis. *J Virol* *80*, 5104-5112.
- Wright, C.M., Seguin, S.P., Fewell, S.W., Zhang, H., Ishwad, C., Vats, A., Lingwood, C.A., Wipf, P., Fanning, E., Pipas, J.M., *et al.* (2009). Inhibition of Simian Virus 40 replication by targeting the molecular chaperone function and ATPase activity of T antigen. *Virus Res* *141*, 71-80.
- Wyatt, R.G., Greenberg, H.B., Dalgard, D.W., Allen, W.P., Sly, D.L., Thornhill, T.S., Chanock, R.M., and Kapikian, A.Z. (1978). Experimental infection of chimpanzees with the Norwalk agent of epidemic viral gastroenteritis. *J Med Virol* *2*, 89-96.
- Xia, M., Farkas, T., and Jiang, X. (2007). Norovirus capsid protein expressed in yeast forms virus-like particles and stimulates systemic and mucosal immunity in mice following an oral administration of raw yeast extracts. *J Med Virol* *79*, 74.
- Yuan, L., Ward, L.A., Rosen, B.I., To, T.L., and Saif, L.J. (1996). Systematic and intestinal antibody-secreting cell responses and correlates of protective immunity to human rotavirus in a gnotobiotic pig model of disease. *J Virol* *70*, 3075.
- Zakikhany, K., Allen, D.J., Brown, D., and Iturriza-Gomara, M. (2012). Molecular evolution of GII-4 Norovirus strains. *PLoS One* *7*, e41625.
- Zeng, R., Zhang, Z., Mei, X., Gong, W., and Wei, L. (2008). Protective effect of a RSV subunit vaccine candidate G1F/M2 was enhanced by a HSP70-Like protein in mice. *Biochem Biophys Res Commun* *377*, 495-499.

Zhang, X., Bourhis, J.-M., Longhi, S., Carsillo, T., Buccellato, M., Morin, B., Canard, B., and Oglesbee, M. (2005). Hsp72 recognizes a P binding motif in the measles virus N protein C-terminus. *Virology* 337, 162.

Zhang, X.R., Buehner, N.A., Hutson, A.M., Estes, M.K., and Mason, H.S. (2006). Tomato is a highly effective vehicle for expression and oral immunization with Norwalk virus capsid protein. *Plant Biotechnology Journal* 4, 419-432.

Zheng, D.P., Ando, T., Fankhauser, R.L., Beard, R.S., Glass, R.I., and Monroe, S.S. (2006). Norovirus classification and proposed strain nomenclature. *Virology* 346, 312-323.